

AMERICAN UNIVERSITY OF BEIRUT

ROLE OF MICROBIOTA IN DIABETES-ASSOCIATED
COLORECTAL CANCER

by

MOHAMED HUSSEIN NOURELDEIN

A thesis

submitted in partial fulfillment of the requirements
for the degree of Doctor of Philosophy (PhD) in Biomedical Sciences
to the Department of Anatomy, Cell Biology and Physiological Sciences
of the Faculty of Medicine
at the American University of Beirut

Beirut, Lebanon
November 2020

AMERICAN UNIVERSITY OF BEIRUT

ROLE OF MICROBIOTA IN DIABETES-ASSOCIATED
COLORECTAL CANCER

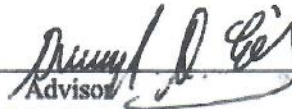
by

MOHAMED HUSSEIN NOURELDEIN

Approved by:

Dr. Assaad Eid

Department of Anatomy, Cell Biology and Physiological Sciences


Advisor

Dr. Nadine Darwiche

Department of Molecular Biology and Genetics


Chair of the Committee

Dr. Farhad Danesh

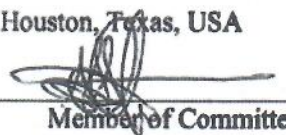
Section of Nephrology

The University of Texas MD Anderson Cancer Center, Houston, Texas, USA

 on behalf of
Member of Committee Dr. Danesh.

Dr. Assam El-Osta

Department of Diabetes, Central Clinical School
Monash University, Melbourne, Australia


Member of Committee

Dr. Alessia Fornoni

Division of Nephrology, Department of Medicine
University of Miami, Miami, FL, USA

 on behalf of
Member of Committee Dr. Fornoni

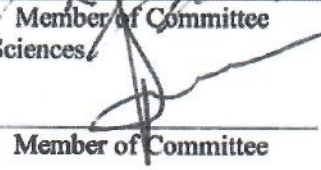
Dr. Abdo Jurjus

Department of Anatomy, Cell Biology and Physiological Sciences


Member of Committee

Dr. Ali Taher

Department of Internal Medicine


Member of Committee

Date of thesis/dissertation defense: [November 3rd, 2020]

AMERICAN UNIVERSITY OF BEIRUT

DISSERTATION RELEASE FORM

Student Name: Noureldein
Last

Mohamed
First

Hussein
Middle

Master's Thesis

Master's Project

Doctoral Dissertation

I authorize the American University of Beirut to: (a) reproduce hard or electronic copies of my thesis, dissertation, or project; (b) include such copies in the archives and digital repositories of the University; and (c) make freely available such copies to third parties for research or educational purposes.

I authorize the American University of Beirut, to: (a) reproduce hard or electronic copies of it; (b) include such copies in the archives and digital repositories of the University; and (c) make freely available such copies to third parties for research or educational purposes
after:

One ---- year from the date of submission of my thesis, dissertation, or project.

Two ---- years from the date of submission of my thesis, dissertation, or project.

Three -X- years from the date of submission of my thesis, dissertation, or project.

Mohamed Noureldein

November 6th, 2020

Signature

Date

ACKNOWLEDGMENTS

This page is the most difficult one to write in this whole long thesis. At the end of this incredible journey, I am overtaken by gratitude for many people. I will never be able to give them credit by writing a few words in this section, but I hope they feel my genuine and sincere appreciation for what they have done for me.

Praise be to God who guided me throughout this journey and gave me the strength and patience to reach this point in my career.

Many thanks are due to Dr. Nadine Darwiche, my academic advisor, chair of my PhD committee and my guardian angel. Thank you for being relentlessly supportive and helpful to me. Any problem, that I have faced during my PhD curriculum, was solved as soon as I discussed it with you. Thanks for having your door always open for me and for the reinforcement and encouragement you always provided.

I have to search for a new word for gratitude to say to Dr. Assaad Eid that can convey what I feel but I think they haven't coined such a word yet. Dr. Eid is the best supervisor and mentor anyone can wish for. His support, trust, encouragement, and kindness are beyond any description. It is hard to count the number of opportunities that he has created for me to make the best of my PhD years and to learn as much as I can through these years. He is not just a supervisor; he is a career builder. He is an exemplary mentor. I can't express how grateful I am for everything he has done for me.

I was fortunate enough to join the Eid family. I think this lab is very unique in establishing a wonderful working and social experience with its selection of amazing people. There is no space to mention everyone and I don't want to forget anyone. Special thanks to Dr. Fatima Mohsen who has been my direct mentor in the lab and who taught me many valuable techniques and ignited my passion towards the study of diabetes-associated colorectal cancer. Many thanks to Batoul Dia who has been an astonishing close friend. She was very helpful during my lab work and was a great support system for me the whole time. I am grateful to have Sara Bitar as my partner in the topic of diabetes-associated cancer. She is a great lab partner, meticulous, clever and hardworking and we had many great memories together. Finally, I owe so much to my best friend, Natalie Youssef. Thank you for always being there for me and for your kindness and support. Friends that I made in this lab will stay with me for a very long time.

This work won't have been done without the support of my family. It wasn't easy to be far from them for these few years but they always find a way to transfer their support and kind regards across any distances.

AN ABSTRACT OF THE THESIS OF

Mohamed Hussein Noureldein for PhD of Biomedical Sciences

Major: Physiology

Title: Role of Microbiota in Diabetes-Associated Colorectal Cancer

Diabetes mellitus is a complex disease that affects the whole-body metabolism and energy utilization. The disturbances of these vital functions affect body organs in different drastic ways. Not long ago, several studies have reported an association between diabetes mellitus and cancer. However, the mechanistic link between these two diseases is still speculative. Diabetes mellitus is accompanied by a chronic state of inflammation that can eventually lead to many types of cancers including colorectal cancer (CRC). Diabetes changes the gastrointestinal environment and hence the microbiota of the host, a condition known as dysbiosis. Dysbiosis have emerged to be an important contributing factor for the pathogenesis of diabetes and CRC. Throughout this PhD work, we focused on: identifying the microbial signature associated with diabetes and CRC; and identifying the signaling mechanism altered by dysbiosis and leading to the progression of CRC in diabetes. *MKR* mice that can spontaneously develop type 2 diabetes were used in our work. For CRC induction, another subset of mice was treated with azoxymethane and dextran sulfate sodium, to identify the link between both diabetes and CRC. Fecal samples were collected at different time points to detect the differences in microbiota that occur along the course of the diseases. In parallel experiments, a subset of control mice was depleted of their endogenous microbiota after weaning, then mice were inoculated with fecal microbial transplant from diabetic mice and mice with CRC. After 5 weeks of transplantation, all groups of mice were treated with azoxymethane and dextran sulfate sodium. Further, and to verify if dysbiosis is playing a role in the observed pathogenesis, a subset of the diabetic mice and diabetic mice with CRC were treated with probiotics or butyrate to determine the beneficial effect of probiotics on the progression of these chronic conditions. At the end of the treatment, 16S rRNA sequencing was performed to identify different microbial communities in the fecal samples. Besides, at sacrifice, blood was collected, and colons were harvested for molecular, anatomical, histological, and biochemical analysis. Our analysis focused on inflammatory, and reactive oxygen species (ROS) production pathways. Our results show that diabetes is associated with a defined microbial signature that is characterized by reduction of butyrate-forming bacteria. This dysbiosis is associated with gastrointestinal complications reflected by a reduction in colon lengths. These changes are reversed upon treatment with probiotics or butyrate, which rectified the observed dysbiosis. Inoculation of control mice with diabetic microbiota and cancer microbiota resulted in the development of more aggressive CRC and higher number of polyps after chemical induction of CRC. Diabetes-associated dysbiosis resulted in less production of beneficial butyrate in both cecal and fecal contents, which consequently led to over-activation of histone deacetylase (HDAC)3 enzymes. Our data also show that the downstream effectors of HDAC3, namely inflammatory cytokines (mainly interleukin (IL)-1 β) and NADPH oxidase (NOX)4 are over-expressed in diabetic mice as a result of activation of HDAC3 in colon tissue. Collectively our data suggest that diabetes is associated with dysbiosis characterized by lower abundance of butyrate-forming bacteria leading to less butyrate production and activation of HDAC3 resulting in over-expression of inflammatory cytokines and NOX4 leading to gastrointestinal complications and CRC.

CONTENTS

ACKNOWLEDGMENTS	V
AN ABSTRACT OF THE THESIS OF	VI
CONTENTS.....	VII
ILLUSTRATIONS	X
TABLES	XIII
LIST OF ABBREVIATIONS.....	XIV
CHAPTER 1	1
INTRODUCTION	1
1.1. Diabetes Mellitus Epidemiology	1
1.2. Diabetes and Colorectal Cancer	2
1.3. Diabetes Mellitus, Colorectal Cancer and Dysbiosis	5
1.4. Bacterial Metabolites.....	10
1.5. Histone Deacetylase (HDAC) in Diabetes	13
1.6. Dysbiosis and Immunity.....	13
1.7. Reactive Oxygen Species (ROS) in Diabetes and Cancer.....	16
1.8. Probiotics in Diabetes and CRC	18
CHAPTER 2	23
AIMS	23
CHAPTER 3	25
MATERIALS AND METHODS.....	25
3.1. Animal Studies	25
3.1.1. Assessment of the effect of butyrate on <i>MKR</i> mice	25
3.1.2. Establishing if dysbiosis play a key role in diabetes-associated CRC	26

3.1.3. Microbiota depletion and fecal microbial transplant.....	28
3.1.4. Probiotics treatment.....	29
3.2. 16S rRNA sequencing	31
3.3. Oral Glucose Tolerance Test.....	35
3.4. Sacrifice and Organ Harvesting.....	35
3.5. Determination of Random Blood Glucose and Circulatory Cytokines.....	35
3.6. Determination of glycated hemoglobin (HbA _{1c})	36
3.7. Isolation of fecal DNA and Microbial Gene Analysis	36
3.8. Real Time PCR.....	38
3.9. Determination of Fecal and Cecal Butyrate Content.....	38
3.10. Determination of Histone acetylase and histone deacetylase 3 activities	39
3.11. Detection of reactive oxygen species production in colon tissues using HPLC ...	39
3.12. Primary Culture	39
3.13. Western Blot.....	40
3.14. Statistical Analysis	41

CHAPTER 442

RESULTS42

4.1. <i>MKR</i> mice develop type 2 diabetes without obesity and suffer from gastrointestinal dysfunction	42
4.2. <i>MKR</i> mice have impaired glucose utilization.....	43
4.3. Diabetes results in more aggressive colorectal cancer phenotype.....	44
4.4. Fecal microbial transplant of diabetic and cancer microbiota results in more aggressive colorectal cancer phenotype.	45
4.5. Diabetic mice microbiota contains less <i>Bacteroid fragilis</i> and butyrate-forming bacteria	47
4.6. Quality control of 16S rRNA sequencing data.....	49
4.7. 16S rRNA microbiota sequencing results	51
4.7.1. Alpha diversity	51
4.7.2. Taxonomy.....	54
4.7.3. Beta diversity.....	59
4.7.4. Microbiota composition in control, diabetic and colorectal cancer mice.....	64
4.7.5. Tests of significances	68
4.7.6. Analysis of composition of microbiome (ANCOM).....	69
4.7.7. Significantly characteristic bacteria in each group.....	71
4.8. Diabetes is coupled to a decrease in Cecal and fecal butyrate content, a higher activity of the colon HDAC3 and alteration of inflammatory cytokines	76
4.9. Diabetes causes alteration of inflammatory cytokines and increases expression of IL-1 β	77
4.10. Butyrate treatment reverse diabetes-induced ROS production and NADPH oxidase 4 protein expression.....	79
4.11. Diabetes and colorectal cancer increase the expression of IL-1 β and NOX4.....	80
4.12. Effect of FMT on the expression of IL-1 β and NOX4.....	81
4.13. NADPH oxidase 4 protein expression is under control of HDAC 3	83

4.14. Butyrate reverses GI disturbance and molecular changes observed in diabetes ...	84
4.15. Probiotics reverses GI disturbance and molecular changes observed in diabetes.	86
CHAPTER 5	89
DISCUSSION	89
CHAPTER 6	104
CONCLUSION	104
BIBLIOGRAPHY	105
APPENDIX 1	136
Publications related to the thesis	136
Conferences	137
APPENDIX 2	138
Analysis of microbiota using mothur	138
Analysis of microbiota using qiime2	142
APPENDIX 3	148
Supplementary Figures	148

ILLUSTRATIONS

Figure	Page
1. Epidemiology of Diabetes Mellitus in the Middle East-North Africa region (IDF, 2019).....	2
2. Compositional and functional alterations in the healthy gut microbiota versus the obese-diabetic microbiota (Patterson <i>et al.</i> , 2015).	7
3. Interplay between diabetes, obesity and microbiota in the development of diabetic complications. Adapted from (Gonzalez <i>et al.</i> , 2017).....	9
4. Proposed mechanisms of butyrate in the pathogenesis of diabetes (Khan <i>et al.</i> , 2015).....	12
5. Regulation and Functions of NADPH oxidase 4 (Chen <i>et al.</i> , 2012).....	18
6. Putative mechanisms for the effects of probiotics treatment in diabetes. Green and red texts indicate hormones, systems and actions that are upregulated and downregulated, respectively. GLP: glucagon-like peptide; GABA: gama-amino butyric acid; LPS, lipopolysaccharide; SCFA: short chain fatty acid. (Patterson <i>et al.</i> , 2015).....	19
7. Proposed mechanisms by which dysbiosis mediates diabetic complications. ...	24
8. Experimental design of the butyrate treatment experiment.....	26
9. Experimental design of the colorectal cancer induction experiment.....	27
10. Experimental design of the microbiota inoculation experiment.....	29
11. Experimental design of the probiotics treatment experiment.....	30
12. Workflow for mothur microbial analysis (Saskia Hiltmann, B�erence Batut, Dave Clements, 2019 16S Microbial Analysis with mothur (extended) (Galaxy Training Materials). Online; accessed Mon, Apr 20, 2020).....	34
13. Body weight, blood glucose, HbA1c % and colon lengths of <i>MKR</i> mice compared to their control littermates. Results are expressed as mean \pm SD. * significantly different from <i>FVB-NJ</i> control mice at $p < 0.05$	43
14. Glucose tolerance test curve for <i>MKR</i> and control mice. Results are expressed as mean \pm SEM. * significantly different from <i>FVB-NJ</i> control mice at $p < 0.05$	44
15. Gross characteristics for colorectal cancer (CRC) and number of polyps in <i>FVB-NJ</i> and <i>MKR</i> CRC mice groups. Results are expressed as mean \pm SD. * significantly different from <i>FVB-NJ</i> control mice at $p < 0.05$	45
16. Polyp numbers of mice inoculated with fecal microbial transplant. Results are expressed as mean + SEM. * significantly different from <i>FVB-NJ</i> control mice at $p < 0.05$. # Significantly different from <i>FVB</i> FMT mice group at $p < 0.05$	46
17. Polyp numbers of <i>FVB</i> CRC mice treated with vehicle (PBS) or probiotics for 12 weeks. Results are expressed as mean \pm SD. * significantly different from <i>FVB</i> CRC mice at $p < 0.05$	47
18. Different microbial communities and butyrate-forming bacteria of <i>MKR</i> and control mice (n=3). Data are expressed as mean \pm standard deviation (SD). * statistically significant at $p < 0.05$ vs control.	48
19. Frequency histogram for the number of reads per sample in the 16S rRNA sequencing data.	49
20. Quality score per base in the 16S rRNA sequencing data.....	50
21. Richness of microbial features (operational taxonomic units) per sample in control, diabetic, colorectal cancer mice.	51

22. Richness of microbial features (operational taxonomic units) per sample in antibiotic-treated mice.	52
23. Rarefaction curve of samples of the antibiotic-treated mice.	53
24. Richness of microbial features (operational taxonomic units) per sample in control, diabetic and probiotics-treated diabetic mice.	53
25. Different phyla per sample in control, diabetic, colorectal cancer mice.	56
26. Different phyla per sample in antibiotic-treated mice.	57
27. Different phyla per sample in control, diabetic and probiotics-treated diabetic mice.	58
28. The principal coordinate analysis (PCoA) plot for the control, diabetic and cancer mice at early and late time points.	60
29. The principal coordinate analysis (PCoA) plot for the antibiotic-treated mice at early and late time points.	61
30. The principal coordinate analysis (PCoA) plot for the antibiotic-treated mice at late time point.	62
31. The principal coordinate analysis (PCoA) plot for the probiotics-treated mice at early and late time point. Note: the point for one of the late diabetic samples (1-diabetic) is plotted over another one making them appear as a single point.	63
32. The principal coordinate analysis (PCoA) plot for the probiotics-treated mice at late time point.	63
33. Microbiota composition of control <i>FVB-NJ</i> mice.	65
34. Microbiota composition of diabetic <i>MKR</i> mice.	66
35. Microbiota composition of colorectal cancer mice.	67
36. Volcano blot of analysis of microbial composition of control, diabetic and colorectal cancer mice.	70
37. Volcano blot of analysis of microbial composition of antibiotic-treated mice. .	70
38. Volcano blot of analysis of microbial composition of control, diabetic and probiotics-treated mice.	71
39. Butyrate content and its downstream molecular effects in <i>MKR</i> and control mice (n=3). Data are expressed as mean ± standard deviation (SD). * statistically significant at p<0.05 vs control.	77
40. Diabetes causes alteration of inflammatory cytokines and increases expression of IL-1β (n=3). Data are expressed as mean ± standard deviation (SD). * statistically significant at p<0.05 vs control.	78
41. Reactive oxygen species (ROS) production and protein expression of NADPH oxidase (NOX4) in <i>MKR</i> and control mice groups (n=3). Data are expressed as mean ± standard deviation (SD). * statistically significant at p<0.05 vs control. # statistically significant at p<0.05 vs <i>MKR</i> diabetic mice. NOX: NADPH oxidase.	79
42. Protein expression of IL-1β in colorectal cancer (CRC), <i>MKR</i> and control mice groups (n=3). Data are expressed as mean ± standard deviation (SD). * statistically significant at p<0.05 vs control. CRC: colorectal cancer.	80
43. Protein expression of NADPH oxidase (NOX4) in colorectal cancer (CRC), <i>MKR</i> and control mice groups (n=3). Data are expressed as mean ± standard deviation (SD). * statistically significant at p<0.05 vs control. CRC: colorectal cancer, NOX: NADPH oxidase.	81

44. Protein expression of IL-1 β in mice groups inoculated with fecal microbial transplants (n=3). Data are expressed as mean \pm standard deviation (SD). CRC: colorectal cancer, FMT: fecal microbial transplant.....	82
45. Protein expression of NOX4 in mice groups inoculated with fecal microbial transplants (n=3). Data are expressed as mean \pm standard deviation (SD). CRC: colorectal cancer, FMT: fecal microbial transplant.....	82
46. protein expression of NADPH oxidase (NOX4) in primary culture of colon tissue. Data are expressed as mean \pm standard deviation (SD). * statistically significant at $p<0.05$ vs control. # statistically significant at $p<0.05$ vs HG. HG: high glucose, NG: normal glucose, NOX: NADPH oxidase, TSA: Trichostatin A.	84
47. Body weight, random blood glucose, HbA _{1c} % and colon lengths of <i>MKR</i> and control mice (n \geq 3). A subset of <i>MKR</i> diabetic mice were treated with butyrate (20 mg/kg) interperitoneally for 8 weeks (from week 23 till week 31). Data are expressed as mean \pm standard deviation (SD). * statistically significant at $p<0.05$ vs control. # statistically significant at $p<0.05$ vs <i>MKR</i> diabetic mice.	85
48. Butyrate rectifies the overexpression of IL-1 β due to diabetes (n=3). Data are expressed as mean \pm standard deviation (SD). * statistically significant at $p<0.05$ vs control. # statistically significant at $p<0.05$ vs <i>MKR</i> diabetic mice.	85
49. Colon Lengths and ROS production in colon tissues. Results are expressed as mean + SEM. * significantly different from <i>FVB-NJ</i> control mice at $p<0.05$. # Significantly different from <i>MKR</i> mice at $p<0.05$. \$ statistically significant at $p<0.05$ vs <i>FVB</i> CRC.	86
50. Probiotics protects against the overexpression of IL-1 β caused by diabetes (n=3). Data are expressed as mean \pm standard deviation (SD). * statistically significant at $p<0.05$ vs control. # statistically significant at $p<0.05$ vs <i>MKR</i> diabetic mice.....	87
51. Probiotics protects against the overexpression of IL-1 β caused by colorectal cancer (n=3). Data are expressed as mean \pm standard deviation (SD). * statistically significant at $p<0.05$ vs control. # statistically significant at $p<0.05$ vs <i>FVB</i> CRC mice.	87
52. Probiotics protects against the overexpression of NOX4 caused by diabetes (n=3). Data are expressed as mean \pm standard deviation (SD). * statistically significant at $p<0.05$ vs control. # statistically significant at $p<0.05$ vs <i>MKR</i> diabetic mice.....	88
53. Probiotics protects against the overexpression of NOX4 caused by colorectal cancer (n=3). Data are expressed as mean \pm standard deviation (SD). * statistically significant at $p<0.05$ vs control. # statistically significant at $p<0.05$ vs <i>MKR</i> diabetic mice.	88

TABLES

Table	Page
1. Clinical trials for probiotics use in colorectal cancer (Hendler and Zhang, 2018).	20
2. List of primers.	37
3. Analysis of molecular variances (AMOVA) results for significance testing between control, diabetic and colorectal cancer mice. Significant p-values are in bold.....	68
4. Significantly characteristic bacteria in each mice group.....	71
5. Comparison between the antibiotic protocol used in this study and other protocols from literature.	91

LIST OF ABBREVIATIONS

AMOVA	Analysis of Molecular Variances
ANCOM	Analysis of Composition of Microbiome
ANOVA	Analysis of Variances
CRC	Colorectal Cancer
DM	Diabetes Mellitus
DMEM	Dulbecco's Modified Eagle's Media
DSS	Dextran Sulfate Sodium
FMT	Fecal Microbial Transplant
G-CSF	Granulocyte- Colony Stimulating Factor
GI	Gastrointestinal
HDAC	Histone Deacetylase
HFD	High Fat Diet
HPLC	High Performance Liquid Chromatography
IACUC	Institutional Animal Care and Use Committee
IBD	Inflammatory Bowel Disorder
IDF	International Diabetes Federation
IL	Interleukin
IP	Intraperitoneal
LEfSE	Linear Discriminant Analysis Effect Size
LPS	Lipopolysaccharides
MENA	Middle East North Africa
MS	Mass Spectrometry
NIH	National Institutes of Health
NOX	NADPH Oxidase
OTU	Operational Taxonomic Unit
PBS	Phosphate-buffered Saline
PCoA	Principal Coordinate Analysis
PERMANOVA	Permutational Multivariate Analysis of Variances

ROS	Reactive Oxygen Species
rt-PCR	Real-time Polymerase Chain Reaction
SCFA	Short Chain Fatty Acid
T1DM	Type 1 Diabetes Mellitus
T2DM	Type 2 Diabetes Mellitus
TNF	Tumor Necrosis Factor

CHAPTER 1

INTRODUCTION

1.1. Diabetes Mellitus Epidemiology

Diabetes Mellitus (DM) represents a huge health and economic burden in the region of Middle East North Africa (MENA). It is estimated that there are 54.8 million adults between the ages of 20 and 79 years old that suffer from diabetes in the MENA region ¹. This number represents 12.8% of the population of this age group in this area. It is more dreadful to know that 24.5 million adults of these 54.8 million are undiagnosed and they are suffering silently and may not be diagnosed till they suffer from diabetes-related complications ¹. Of all the regions surveyed by the International Diabetes Federation (IDF), the MENA region has the highest prevalence of diabetes according to 2019 statistics ¹ (**Figure 1**).

In 2019, there were 418,900 deaths attributed to diabetes and diabetes-related complication in the MENA region which represents 16.2% of all-cause mortality ¹. It is a non-trivial number which highlights the major health burden represented by this life-threatening condition. Intriguingly, more than half of the mortalities (58%) are people under the age of 60 years. Diabetes-related mortality is higher in women than in men in that region as reported by IDF ¹.

Most of the countries in the MENA region are middle-income countries with a rather fluctuating economy. Unfortunately, diabetes is further pressuring that economy by imposing health expenditure that approached 24.9 billion USD in 2019 and is projected to increase to 32.5 billion by the year 2030 ¹. In Lebanon, health expenditure

related to diabetes represents 20.4% of the total health expenditure, which is the highest proportion in the region after Sudan ¹.

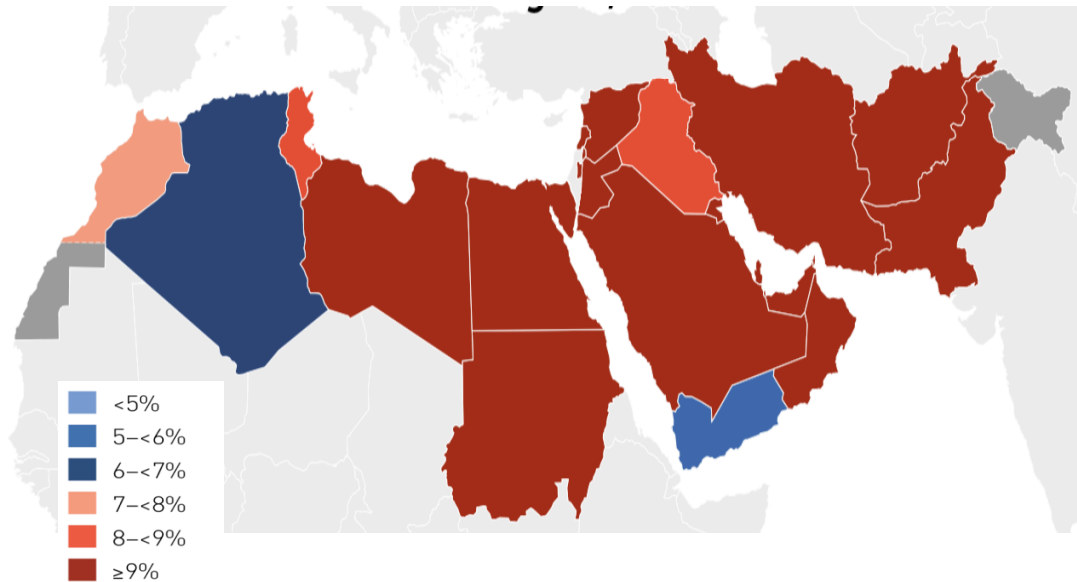


Figure 1: Epidemiology of Diabetes Mellitus in the Middle East-North Africa region (IDF, 2019).

Defects in either the insulin secretion by the pancreatic β -cells or in the insulin uptake by cells predispose DM. DM has two major types. Type 1 DM (T1DM) develops as a consequence for the auto-immune destruction of β -cells resulting in an adequate secretion of insulin while type 2 DM (T2DM) results from insulin resistance and inadequate insulin action ². Obesity is usually a co-morbidity seen with T2DM exacerbating the insulin resistance and facilitating the development of diabetic complications ².

1.2. Diabetes and Colorectal Cancer

The frequent diagnosis of diabetes mellitus and cancer is noteworthy which provoked the investigation of an association between both conditions. This interest was

first pursued by physicians as early as 1932³. Recently, epidemiologists tried to entangle this relation and it appears to be a causal association⁴. It is reported that there is 1.2-1.5 relative risk for colorectal cancer (CRC) when the patient suffers also from diabetes mellitus⁵. Astonishingly, medications for diabetes mellitus are reported to be associated with higher or lower risk of cancer while antineoplastic agents such as immune checkpoint inhibitors are associated with higher risk for diabetes mellitus⁶. Concerning mortality, diabetes is associated with higher mortality in patients with colorectal cancers compared to people with normal blood glucose levels⁷.

Many studies have reported an increased risk for CRC due to the presence of T2DM⁸. The association between colorectal cancer and T2DM is persistent regardless of the sex or the cancer sub-site⁹. An association between diabetes mellitus and colorectal cancer mortality was also previously recorded¹⁰. Some mechanisms have been proposed to link diabetes and CRC (reviewed in¹¹). However, more studies are warranted to further explore these links.

There are an estimated 500,000 deaths each year from CRC which places CRC as one of the most common worldwide cancers¹². CRC incidence is influenced by many factors including body mass index, obesity, low physical activity and diet¹³. The difference between dietary patterns reflects a difference in CRC epidemiology. Diet rich in animal protein, red and processed meat, refined grains, sweets, fat and alcohol (Western diet) was associated with higher risk for CRC while diet rich in vegetables, fruits, fibers, fish and olive oil (Mediterranean diet) showed protective effects^{14,15}. This dietary link is a pointer towards the role of microbiota in CRC.

Colorectal cancer is the cancer of the colon epithelium. The triggers for CRC are not completely known as 70% of CRC incidences are sporadic which may have been triggered by certain dietary or environmental factors ¹⁶. Age is also a risk factor for CRC as the diagnosis of CRC mainly occurs in patients over 50 years old ¹⁶. The environmental influence on CRC occurrence is notable as only 10% of CRC cases are due to hereditary factors ¹⁷.

There is a consensus theory on how CRC starts. Mutations in certain tumor suppressor genes namely *APC*, *CTNNB1* and *p53* or the oncogene, *KRAS* are believed to be the initiators of CRC phenotype ^{18,19}. The mutated colonic epithelial cells may have a selective advantage. It is believed that the triad consisting of the diet, **microbiota** and inflammation is the key surviving promoter for the mutated epithelial cells ²⁰⁻²⁵.

Treatments of CRC depends on the stage. Surgery is the first option in the early-stage as it will prevent the dissemination of the tumor ²⁶. In some cases of stage II and III patients, surgery with follow-up chemotherapy is the choice ²⁶. Radiation is an option in cases of rectal cancer with nodal disease ²⁶. The chemotherapy treatment protocol includes 5-fluorouracil and oxaliplatin. If CRC is metastasized, the treatments arsenal will also include irinotecan or oxaliplatin combined with a fluoropyrimidine and leucovorin ²⁷. Other agents that have proven noticeable efficacy are anti-Epidermal Growth Factor Receptor (anti-EGFR), panitumumab and anti-Vascular Endothelial Growth Factor (anti-VEGF) agents (bevacizumab, regorafenib) ²⁸.

1.3. Diabetes Mellitus, Colorectal Cancer and Dysbiosis

The association between T2DM and CRC enticed researchers to search for a link between both conditions. The gut and its microbial residences are suspected to be very important mediators for this relation. Gut microbiota have recently gained much interest as regulators of many metabolic and immunological functions of the host together with impacting the pathogenesis of many diseases as inflammatory bowel disorder (IBD), obesity, diabetes mellitus and cancer. The human body is a host of more than 100 trillion bacteria, a number that exceeds the total number of the host cells by ten times. The majority of microbiota belongs to phyla Firmicutes and Bacteroidetes with some bacterial proportions from Proteobacteria and Actinobacteria and a few members from Verrucomicrobia and Fusobacteria²⁹. Diet shapes the gut microbiota. Diets characterized by high intake of animal sources will enrich bacteria from Bacteroides and Ruminococcus while Prevotella bacteria will be enriched if the diet is composed mainly of plant sources³⁰. Many microbiota species can produce the beneficial butyrate such as Clostridium group IV bacteria (for example *Faecalibacterium prausnitzii*) and group XIVa, *Roseburia* spp., *Butyricoccus*, *Lactobacillus* and *Bifidobacterium*³¹⁻³³.

Gut microbiota influences many physiological functions including immune stimulation, production of essential nutrients, controlling pathogenic microorganisms, regulation of epithelial cell proliferation and differentiation³⁴⁻³⁶. These functions place gut microbiota in the center of physiology, metabolism and nutrition³⁴⁻³⁶.

The composition of gut microbiota differs between individuals due to many factors³⁷. These factors include diet, physical and psychological stress, age, different diseases, surgery, medications, radiation and chemicals which affect both the number and diversity of microbiota³⁸. Among these factors, diet appears to be the most

influential factor³⁹. The healthy status of the gastrointestinal tract of the host is governed by the interplay between microbiota and diet and their involvement in the inflammatory or metabolic pathways³⁶.

T2DM is strongly associated with disturbance of gut healthy microbiota^{40,41}, a condition known as diabetic dysbiosis. Several research groups tried to establish a microbial signature for type 1 and type 2 DM⁴²⁻⁴⁹. Despite the complex community of microorganisms that inhabit the digestive tract, and regardless of the conflicting findings, these studies were able to identify different flora signatures for T1DM, T2DM and obesity^{40,50}. A recent clinical study has found that the microbiota of obese patients with T2DM composed mainly of bacteria from phylum Firmicutes as well as Clostridia and Negativicutes, while they had lower abundance of bacteria from Verrucomicrobia, Bacteroidetes, Proteobacteria, and Elusimicrobia⁵¹. Evidence from literature suggests that gut microbiota plays a central role in the pathogenesis of T2DM⁵²⁻⁵⁵ (**Figure 2**), yet these studies relied on statistical correlations and educated hypotheses with no mechanistic foundations. Therefore, studies are warranted to delineate the molecular mechanisms by which gut microbiota mediates the pathogenesis of T2DM and its complications.

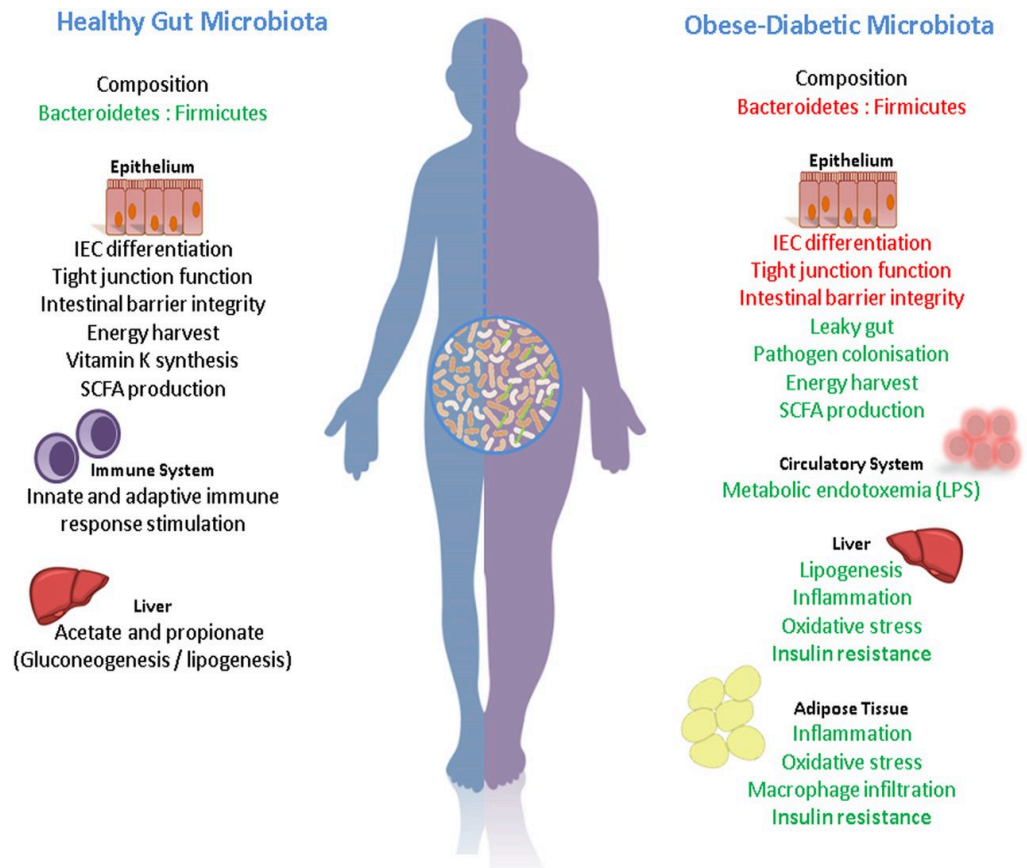


Figure 2: Compositional and functional alterations in the healthy gut microbiota versus the obese-diabetic microbiota (Patterson *et al.*, 2015).

Obesity is a major risk factor for T2DM and more than 80% of patients with T2DM are obese. The co-occurrence of both conditions made it difficult to separate changes in microbiota due to diabetes from those due to T2DM. Therefore, the majority of studies focused on the obesity microbiota and observational studies that can associate glucose intolerance (due to T2DM) with gut microbiota are scarce ⁵⁵.

T2DM is accompanied by a chronic inflammatory state ⁵⁶ and patients may exhibit endotoxemia ^{57,58}. Moreover, it is suggested that lipopolysaccharides (LPS) are one of the causes for this inflammatory state ⁵⁵. Mice, that are fed on high fat diet (HFD) to induce diabetes, show an increase in gut permeability and toxemia

concomitant with a unique gut microbial signature ⁵⁹. The term “metabolic infection” was coined to describe the contribution of gut microbiota in the endotoxemia-related inflammation associated with T2DM ^{60,61}. As early as in the pre-diabetic stage, the host microbiome was shown to be altered which can be manifested by the circulatory detection of Proteobacterial DNA ⁶¹.

The association between gut microbiota and CRC was investigated as early as 1950s. McCoy and Mason in 1951 published a case report mentioning an association between enterococcal endocarditis and carcinoma of the cecum ⁶². Since then, many efforts were undertaken to elucidate the underlying mechanism of this association. Gut microbiota is strongly implicated in keeping the mucosal barrier integrity, nutrient digestion, absorption and angiogenesis ⁶³. When the commensals in the gut are shifted to dysbiosis and selection of pathobionts (organisms with pathogenic potential), this dysbiosis will lead to a chronic inflammatory state that can precipitate CRC. Dysbiosis associated with CRC include “Drivers” which initiate CRC and “Passengers” which promotes CRC growth ⁶⁴. Two particular gut bacterial strains have been linked to CRC: *Bacteroides fragilis* and *Streptococcus bovis* ⁶⁵. Both *Bacteroides* and Bifidobacteria are associated with a higher risk for CRC while *Lactobacillus* and *Eubacterium aerofaciens* are believed to be protective ⁶⁶. CRC is associated by lower abundance of *Clostridium*, *Roseburia*, *Eubacteria* spp., and other butyrate-producing bacteria ^{67,68}. Although studies about the association between microbiota and CRC reported promising and interesting results, research progression in this area has been very slow. This slow progression arose from the difficulty in cultivating and culturing of intestinal bacteria ³⁹. Fortunately, the advance in whole DNA sequencing technologies made it possible to classify and quantify gut microbiota and identify its differential growth in

healthy and diseased subjects ³⁹. Many studies utilized these advanced genomic techniques to identify main bacterial species in healthy individuals and patients with IBD and CRC ⁶⁹. Using whole genome sequencing, Zeller *et al* identified 22 microbial species that are strongly associated with CRC ⁷⁰. Our main focus in this project will be on gut microbiota and its role in mediating diabetes-associated colorectal cancer (Figure 3).

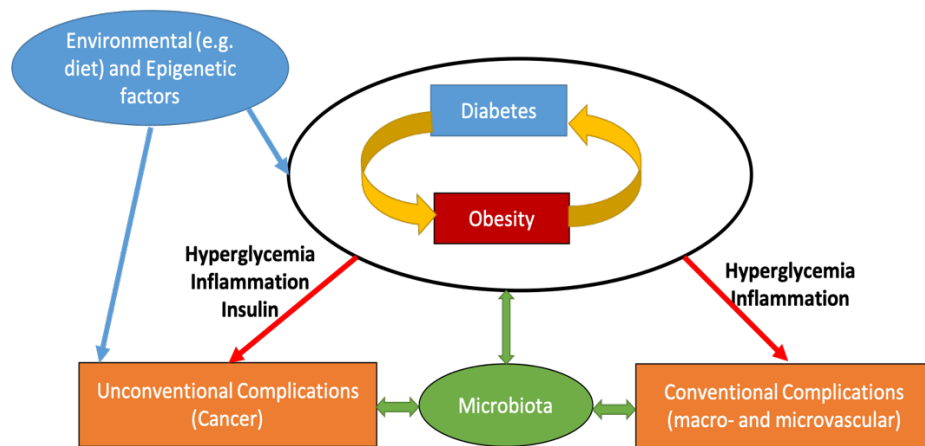


Figure 3: Interplay between diabetes, obesity and microbiota in the development of diabetic complications. Adapted from (Gonzalez *et al.*, 2017).

Microbiota is regulated by inflammasome secreted by the host which recognizes the host microbiota and ensures that it is in balance with the immune responses. Abnormal microbiota arises when there is a defect in any of the components of this inflammasome which will result in exaggerated gut inflammatory responses ⁷¹ and may even help in the tumorigenic transformation of the colon epithelium ⁷². Interestingly, these microbiota-induced inflammatory responses are believed to account for the transmissible nature of CRC in co-housed individuals ⁷³. Evidence from

literature suggests that insulin resistance can induce changes in the gut microbiota and the ensuing abnormal inflammatory responses ⁷⁴.

The integrative Human Microbiome Project (iHMP) studied the dysbiosis induced by T2DM as one of the models for the microbiome-associated human conditions ⁷⁵. Both T2DM and CRC share a microbial signature characterized by a reduction in the abundance of the butyrate-forming bacteria ^{22,76}. However, this signature was not studied in the context of the association between the two conditions.

1.4. Bacterial Metabolites

Besides the effect of microbiota itself, microbiota secrete very important metabolites that affect the host's health. The Gut microbiota ferments undigested dietary fibers producing short chain fatty acids (SCFAs) in the human intestines ⁷⁷. Microbiota- produced SCFAs include acetate, propionate and butyrate that are produced in the molar ratios of 60:25:15 ⁷⁸. SCFAs are important in differentiation, growth arrest and apoptosis as evidenced from experiments using colon cancer cell lines ⁷⁹. This was further proven epidemiologically as diet containing high fiber content was found to be associated with lower incidence and growth of colon cancers ⁸⁰. The anti-tumor effect of SCFAs in colon cancer cells was attributed to the induction of apoptotic cell death ⁸¹.

One of the metabolites produced by gut microbiota is butyrate that is produced by butyrate-producing bacteria upon digestion of dietary fibers and complex polysaccharides by anaerobic fermentation. After its production, butyrate is absorbed and metabolized by the epithelial cells of the colon to produce energy ⁸² while the excess butyrate is going to be transported by the hepatic portal vein to reach the liver ⁸³.

Some of the beneficial functions of butyrate involves regulation of hepatic lipogenesis and gluconeogenesis ⁸⁴. This action can have beneficial effects on colon cancer, non-alcoholic fatty liver disease and inflammation ⁸⁵. Butyrate acts as anti-inflammatory, anti-tumorigenesis and protects against pathogens. Butyrate is the preferred energy source for the colonic epithelium. The presence of butyrate guarantees healthy and proper epithelial functions such as maintaining the intestinal barrier function ⁸⁶ and suppressing tumorigenic transformation ⁸⁷⁻⁸⁹, orchestrates epigenetic regulation, inhibits inflammation and protects against DNA damage ⁹⁰. Moreover, it was proven that butyrate can inhibit proliferation and can induce apoptosis and autophagy in colorectal cancer cells ⁹¹. These effects are not limited to colorectal cancer and there are many clinical trials that have investigated the role of butyrate in other types of cancer ^{47,92}. Although it is almost a fact that butyrate beneficial effects on cancer are mediated through autophagy and apoptosis, the exact molecular mechanisms by which butyrate induces these processes are still under-researched.

In that spirit, butyrate is a widely known histone deacetylase enzyme (HDAC) inhibitor ^{44,45}. HDAC inhibition by butyrate regulate cellular proliferation, differentiation and energy metabolism and has been described to play a direct role in the pathogenesis of DM ^{46,47} by increasing the differentiation and the gene expression of insulin in β -cells ⁴⁸. Moreover, butyrate was associated with reduction of plasma glucose, insulin resistance and body weight in diabetic mice fed with high-fat diet ^{47,49}. Moreover, butyrate deficiency was portrayed to be altering glucose metabolism and to aggravate diabetic pathogenesis ⁹³ by inducing inflammation and oxidative stress ^{94,95}. **Figure 4** shows the proposed mechanisms by which butyrate inhibits HDAC contributing to the pathogenesis of diabetes mellitus ⁹³.

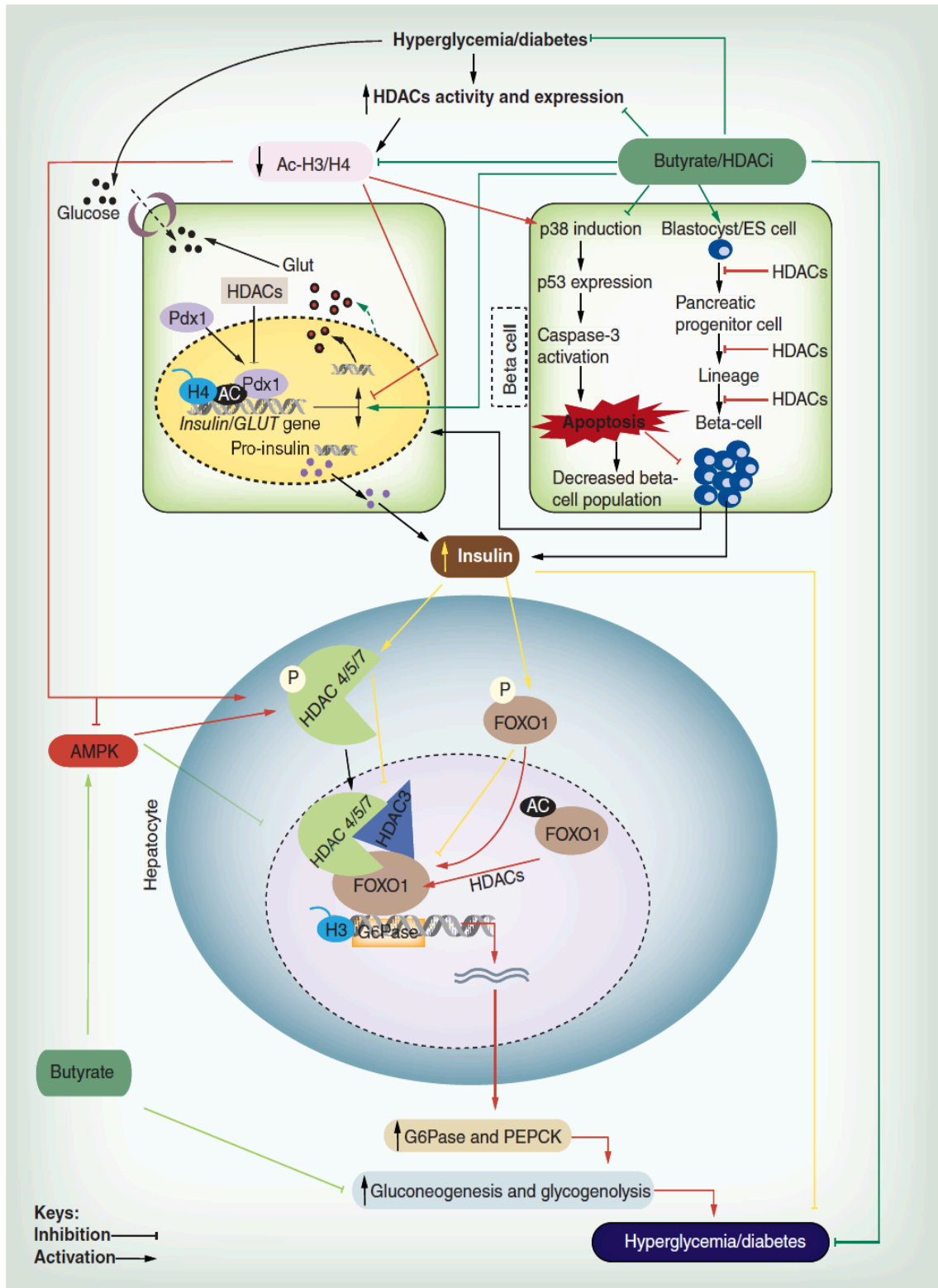


Figure 4: Proposed mechanisms of butyrate in the pathogenesis of diabetes (Khan *et al.*, 2015).

1.5. Histone Deacetylase (HDAC) in Diabetes

From the HDAC family of enzymes that epigenetically regulates cellular processes, HDAC3 appears to be the most significant in mediating diabetic pathogenesis. HDAC3 selective inhibition can limit pancreatic islet infiltration, abolish the death of β -cells and protect against development of T1DM in non-obese diabetic (NOD) mice ⁹⁶. In their review on the effect of HDAC3 inhibition, Meier and Wagner concluded that selective inhibition of HDAC3 could be a promising strategy in the treatment of metabolic diseases ⁹⁷. Furthermore, HDAC3 was associated with the onset and development of diabetic complications. A clinical association study assessed the activity of HDAC3 in peripheral blood mononuclear cells of patients with T2DM and found that its activity is higher than that of the control. Yet the underlying cause of the observed effect was not well highlighted despite the subtle hint of an alteration in the levels of the systemic inflammatory cytokines ⁹⁸. When it comes to epigenetic alteration, HDAC3 inhibition prevented diabetic cardiomyopathy onset by regulating DUSP5-ERK1/2 pathway in OVE26 mice ⁹⁹. Likewise, inhibition of HDAC3 protected diabetic mice from diabetes-induced liver damage ¹⁰⁰. HDAC3 inhibition can also improve glycaemia and insulin secretion in obese diabetic rats ¹⁰¹.

1.6. Dysbiosis and Immunity

Resident microbiota are critical for priming the immune system in the gut and protecting against pathogen infection. To avoid unnecessary or excessive immune response to the resident microbiota, the immune system has evolved mechanisms to prevent activation of inflammatory responses by microbiota. For instance, the gut immune system does not respond to the Toll-like receptor (TLR) ligands such as LPS

that are secreted by the microbiota ^{102,103}. Other mechanisms like mucus production and secretion of antimicrobial peptides secreted by the intestines limit the contact between microbiota and the immune system and hence imparting intestinal homeostasis ¹⁰⁴. Dysregulation of normal gut microbiota can lead to colonic inflammation which can be abolished if microbiota has been depleted using antibiotics ^{105–108}. Some species of bacteria are associated with intestinal inflammation and colonic pathology such as *Bacteroides* species and members of the *Enterobacteriaceae* family including *Klebsiella pneumoniae* and *Proteus mirabilis* ^{109,110}. The stimulation of immune system and the role of cytokines in promoting colonic inflammation have been the subject of intensive research.

The inflammasome is a major signaling pathway for the innate immunity. It consists of a multi-protein cascade that leads to the activation of caspase-1 which in turn will cleave pro-interleukin-1 β to active **IL-1 β** ¹¹¹.

The intracellular Nod-like receptor (NLR) is a major component for the inflammasome ¹¹². NLRP1, NLRP3 and NLRC4 are all functioning inflammasomes that include NLR ¹¹². Dysbiosis disturbs the inflammasome proper response and can lead to overproduction of IL-1 β ¹¹³. IL-1 β has a major role in colitis and blocking the IL-1 β signaling pathway has been shown to protect against intestinal inflammation in animal models ^{114,115}. Several bacteria can induce IL-1 β via the NLRP3 inflammasome ¹¹³. However, the ability of microbiota to induce IL-1 β *in vivo* has not been well studied.

In the diabetic milieu, dysbiosis affects the intestinal immune system directly and impacts the lymphocyte-homing receptors which can lead to the development of autoimmune diabetes ^{93–97}, a finding that can explain the alteration in the inflammatory

markers observed in diabetes. **IL-1 β** is a very important key player in the loss of β -cell mass in T2DM ¹¹⁶. Evidence from *in vitro* and *in vivo* studies all support this causative role ¹¹⁶. IL-1 β initiates an autoinflammatory process against β -cells resulting in the eventual destruction of these cells contributing to the pathogenesis of diabetes and its complications ¹¹⁶. Blocking IL-1 β signaling by inhibition of its receptor IL-1Ra or the neutralization of IL-1 β by antibodies have been proven beneficial in T2DM as testified from clinical trials ¹¹⁶. This blockade may correct β -cell dysfunction, protect against its destruction and may even allow its regeneration ¹¹⁶.

Likewise, immunity plays a key role in the pathogenesis of CRC. The microenvironment surrounding the cancer cells can promote tumor growth through aberrant inflammatory signals ¹¹⁷. Cancer-promoting inflammation is mediated by many mediators and cytokines, one of them is IL-1 β ¹¹⁸. Not only immune cells can secrete IL-1 β but also stromal and tumor cells ¹¹⁸. High circulatory levels of IL-1 β have been detected in serums of patients with CRC and has been associated with poor prognosis ^{119,120}. Moreover, the cross talk between immune cells in the tumor microenvironment and cancer cells have been shown to induce the secretion of IL-1 β ^{121,122}. IL-1 β is also believed to promote cancer growth and invasion ^{123,124}.

Interestingly, it has been discovered that the expression of IL-1 β is under control of HDAC3. When Lagosz *et al.* inhibited all HDAC enzymes, they reported a significant reduction of inflammatory cytokines ¹²⁵. They tried to pinpoint the specific type of HDAC responsible for this inhibition, they found that HDAC3 inhibition resulted in the reduction of pro-inflammatory cytokines including IL-1 β ¹²⁵.

These evidences for the fundamental role of IL-1 β in T2DM, colonic

inflammation and CRC imply that IL-1 β represents one of the missing links by which diabetes is predisposing CRC.

1.7. Reactive Oxygen Species (ROS) in Diabetes and Cancer

Brownlee in 2005 has investigated the possible underlying mechanisms that predispose diabetic complications ¹²⁶. He has reached the conclusion that oxidative stress and ROS production are the unifying mechanisms common in the development of all diabetic complications ¹²⁶. ROS relay intracellular signals contributing to the pathogenesis of diabetes and its complications. Oxidative stress is a major player in gastrointestinal inflammation and CRC carcinogenesis ¹²⁷. Our group and others have studied the involvement of ROS production in diabetic complications and in diabetes-associated CRC in particular ¹²⁸⁻¹³¹. Overproduction of ROS are responsible for cellular senescence, apoptosis and cellular death. A physiological role has been assigned to low levels of ROS, which are essential to regulate cell growth, differentiation, apoptosis and gene expression ¹³². Oxidative stress is also regulated by nutrition and the resident microbiota and any tampering with this balance can lead to inflammation in the bowels ^{133,134}. Since the inhibition of total ROS production has been proven not to be the perfect strategy, we are going to focus on a specific source for ROS production in diabetes and CRC which is NADPH oxidase 4 (**NOX4**).

The NADPH oxidase family include 7 members (NOX1–5 and dual oxidase “DUOX”1–2) ¹³⁵. Many of these members have been associated with diabetic complications ^{128-131,136} as well as cancer development and progression ¹³⁷. NOX1 is believed to be fundamental for the oncogenic Ras transformation ¹³⁸ while NOX5 has

been involved in cell viability ¹³⁹. However, **NOX4** is the most important member of the NOX family in the cancer milieu. NOX4 is overexpressed in various types of cancer such as prostate cancer ¹⁴⁰, glioblastoma ¹⁴¹, liver cancer ¹⁴² and melanoma ¹⁴³. These studies have also described the role of NOX4 in cancer transformation, proliferation, apoptosis, metastasis and treatment resistance. NOX4 predicts poor prognosis and promotes cancer progression in CRC ¹⁴⁴.

NOX4 is different from other members of the NOX family in many aspects. It is highly expressed in the cardiovascular tissue and it has unique enzymatic properties. Regulation of ROS production by NOX4 is only possible by controlling its expression as it is constitutively active ¹⁴⁵. However, there is a recent evidence of a possible post-translational control ¹⁴⁶. Other characteristics for NOX4 that distinguishes it from other NOX family members are emission of different pattern of ROS, subcellular localization, tissue distribution and effect on signaling pathways ^{147,148}. **Figure 5** summarizes the regulation and functions of NOX4 ¹⁴⁸.

Several studies showed that the expression of NOXs is under the regulation of HDAC3 ¹⁴⁹. However, the crosstalk between NOXs and HDAC3 is not described in a diabetic context. This allured us to investigate if NOXs expression is correlated with HDAC3 inhibition in diabetes-induced gastrointestinal (GI) complications and CRC.

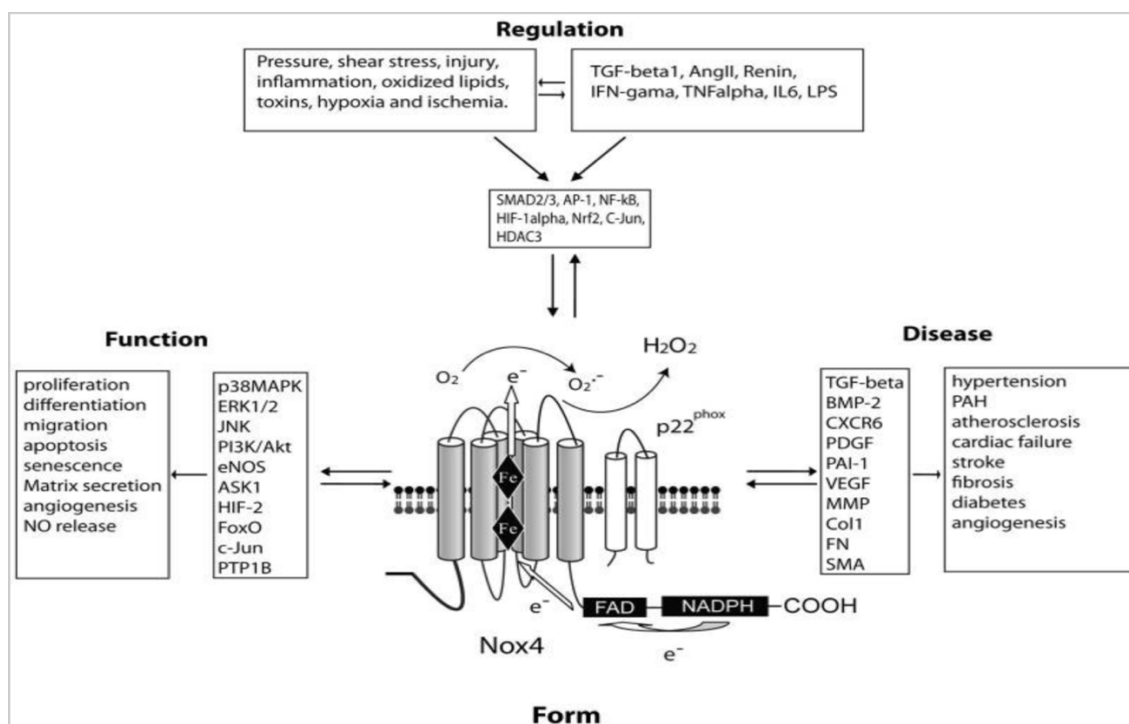


Figure 5: Regulation and Functions of NADPH oxidase 4 (Chen *et al.*, 2012).

1.8. Probiotics in Diabetes and CRC

There is a growing body of evidence that manipulating the gut microbiota is a promising therapeutic strategy for metabolic diseases¹⁵⁰. Probiotic administration is the most effective and safest strategy to alter the gut microbiota eventually leading to enhanced metabolic status and overall health¹⁵¹. The first studies investigating the effects of probiotics on T2DM have applied non-targeted approaches^{152,153}. They lacked any prior molecular hypothesis for the experimentation. Recent studies have reported that probiotics can actually affect the inflammatory responses and reduce endotoxemia^{154,155}. There is no doubt about the beneficial effect of reducing inflammation in T2DM and its complications. However, there was no solid evidence on the specific pathway that probiotics are targeting. Delzenne and Cani have formulated

many theories about the metabolic targets for probiotics and targeting the diabetic microbiome ¹⁵⁶. **Figure 6** shows the putative mechanisms for the effects of probiotics treatments on the host metabolic health in diabetes.

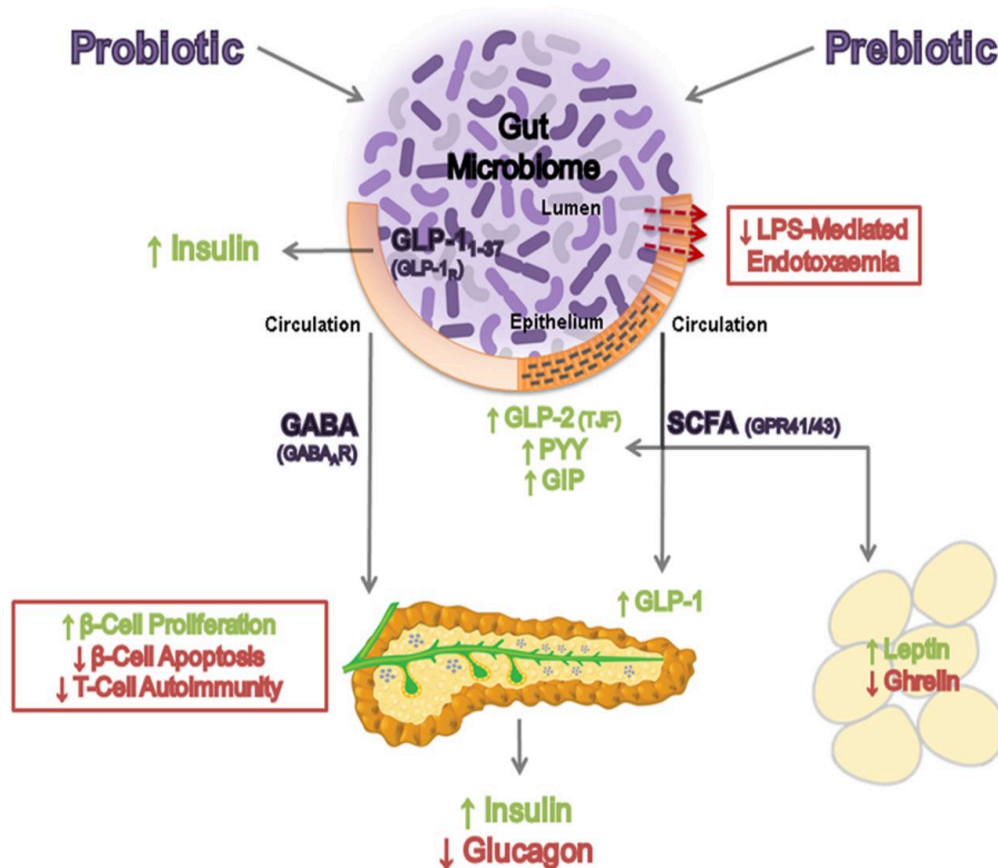


Figure 6: Putative mechanisms for the effects of probiotics treatment in diabetes. Green and red texts indicate hormones, systems and actions that are upregulated and downregulated, respectively. GLP: glucagon-like peptide; GABA: gamma-amino butyric acid; LPS, lipopolysaccharide; SCFA: short chain fatty acid. (Patterson *et al.*, 2015).

Likewise, CRC is believed to be ameliorated by the manipulation of gut microbiota through the use of probiotics ¹⁵⁷. Many clinical trials have been conducted and are still conducted to investigate the effect of probiotics on the outcome of CRC.

Table 1 summarizes the outcomes of clinical trials that used probiotics intervention for patients with CRC ¹⁵⁸.

Table 1: Clinical trials for probiotics use in colorectal cancer (Hendler and Zhang, 2018).

Study Name	Study Type	Population	Intervention	Summary of Key Results
Studies evaluating probiotics and cancer prevention:				
Rafter 2007 159	RCT ¹	Colon cancer (<i>n</i> = 37) & polypectomized (<i>n</i> = 43) patients	SYN1 ² + LGG ³ + BB12 ⁴ vs. placebo	Several CRC ⁵ biomarkers altered favorably (e.g., decreased genotoxin exposure, IL-2 ⁶ , and IFN γ ⁷)
Ishikawa 2005 160	RCT	Tumor-free patients with history of ≥ 2 colorectal tumors removed (<i>n</i> = 398)	Wheat bran vs. <i>Lactobacillus casei</i> vs. neither	No significant difference in colorectal tumor occurrence rate with wheat bran or <i>L. casei</i> . However, atypia of tumors was lower in the <i>L. casei</i> group.
Pala 2011 161	Prospective cohort study	EPIC-Italy cohort (<i>n</i> = 45,241)	Yogurt intake by tertile ⁸	CRC occurrence was significantly lower in highest vs. lowest tertile of yogurt intake. HR ⁹ = 0.62 (95% CI ¹⁰ , 0.46–0.83).
Studies evaluating probiotics and alleviating adverse effects of cancer therapy:				
Mego 2015 162	RCT	CRC patients starting treatment with	Colon Dophilus TM	Reduced incidence in probiotic group of

Study Name	Study Type	Population	Intervention	Summary of Key Results
		irinotecan-based therapy ($n = 46$) ¹¹	probiotic formula vs. placebo	severe diarrhea (0% vs. 17.4%, $p = 0.11$) and diarrhea overall (39.1% vs. 60.9%, $p = 0.11$), but not statistically significant.
Osterlund 2007 163	RCT	Post-resection CRC patients requiring adjuvant chemotherapy ($n = 150$)	Randomized to 5-FU via Mayo regimen vs. de Gramont regimen, then randomized to LGG vs. no probiotic	Less grade 3–4 diarrhea in patients receiving LGG (22% vs. 37%, $p = 0.027$)
Fuccio 2009 164	Meta-analysis	Three RCTs evaluating probiotic supplementation to prevent radiation induced diarrhea ($n = 632$). One RCT evaluating therapeutic role.	Probiotic supplementation vs. placebo/control	No significant difference in rates of radiation-induced diarrhea between probiotic and control arms in preventative trials (OR ¹² 0.47, 95% CI 0.13–1.67) or in the single therapeutic trial
Kotzampassi 2015 165	RCT	Patients undergoing surgery for CRC ($n = 168$) ¹³	Probiotic formulation ¹⁴ vs. placebo	Significant decrease in all major post-operative complications in probiotics arm (28.6% vs. 48.8%, $p = 0.010$, OR 0.42)
Krebs 2016	RCT	Patients undergoing	Preoperative prebiotics ¹⁵ vs.	No statistical difference in

Study Name	Study Type	Population	Intervention	Summary of Key Results
¹⁶⁶		surgery for CRC (<i>n</i> = 73)	preoperative synbiotics ¹⁶ vs. mechanical bowel cleansing	systemic inflammatory response, postoperative course, or complication rate

¹ Randomized control trial. ² Synbiotic preparation-oligofructose-enriched inulin. ³ *Lactobacillus rhamnosus* GG. ⁴ *Bifidobacterium lactis* Bb12. ⁵ Colorectal cancer. ⁶ Interleukin-2. ⁷ Interferon gamma. ⁸ As assessed by a dietary questionnaire. ⁹ Hazard ratio. ¹⁰ Confidence interval. ¹¹ Study prematurely terminated due to slow accrual. ¹²Odds ratio. ¹³ Study prematurely stopped due to efficacy in the primary outcome. ¹⁴ Consisting of *Lactobacillus acidophilus*, *L. plantarum*, *Bifidobacterium lactis*, and *Saccharomyces boulardii*. ¹⁵ Consisting of betaglucan, inulin, pectin, and resistant starch. ¹⁶ Consisting of the prebiotic formulation plus *Pediococcus pentosaceus* 5–33:3, *Leuconostoc mesenteroides* 32–77:1, *Lactobacillus casei* subspecies *paracasei* 19, and *Lactobacillus plantarum* 2362

Moreover, in diabetes-associated colorectal cancer, probiotics were shown to be protective ¹⁶⁷. It is believed that their action is mediated through maintaining ROS homeostasis and reduction of proinflammatory cytokines ¹⁶⁷. The use of probiotics with an antidiabetic drug such as metformin is proposed to impart protection against the oncogenic transformation of the colon ¹⁶⁸.

Given the important role of dysbiosis in the pathogenesis and the reported epidemiological association between diabetes and CRC, we are interested in entangling the role of diabetic microbiota in development of CRC. We hypothesize that gut microbiota is a key factor in the pathogenesis of diabetes-associated CRC. In our study, we aimed to identify a unique microbial signature of diabetes-associated CRC. We also tried to study the underlying molecular, metabolic and immunological pathways that mediate the interaction between the host and microbiota in diabetes-associated CRC.

CHAPTER 2

AIMS

Increasing body of evidence suggests an association between diabetes and CRC. However, the exact mechanisms of how diabetes can lead to gastrointestinal complications and CRC are unknown. Diabetes changes the body metabolism and an important site of this action is the gut. Since the gut harbors a huge diverse population of microbiota, these residents will be affected with a shift favoring the growth of pathological and harmful bacteria over beneficial communities. It is also unknown whether this shift is the cause or the result of diabetes and CRC. This project is an effort to identify this change and how it affects the host mediating diabetic complications with focus on CRC. Our long-term objective is to elucidate how diabetes-associated dysbiosis contributes to the pathogenesis of diabetes-associated GI complications and CRC.

To explore our hypothesis, we focused on the following aims:

- **Aim 1-** Establish if dysbiosis plays a key role in diabetes-associated CRC.
- **Aim 2-** Investigate if restoring the homeostatic balance of gut microbiota can protect against diabetes-associated CRC.
- **Aim 3-** Identify the microbial signature associated with diabetes and CRC.
- **Aim 4-** Associate the identified microbial communities to the underlying pathogenesis of both conditions.
- **Aim 5-** Identify the signaling mechanism altered by dysbiosis and leading to the progression of CRC in diabetes.

Figure 7 illustrates a proposed mechanism by which diabetes-associated microbiota mediates its gastrointestinal complications and colorectal cancer.

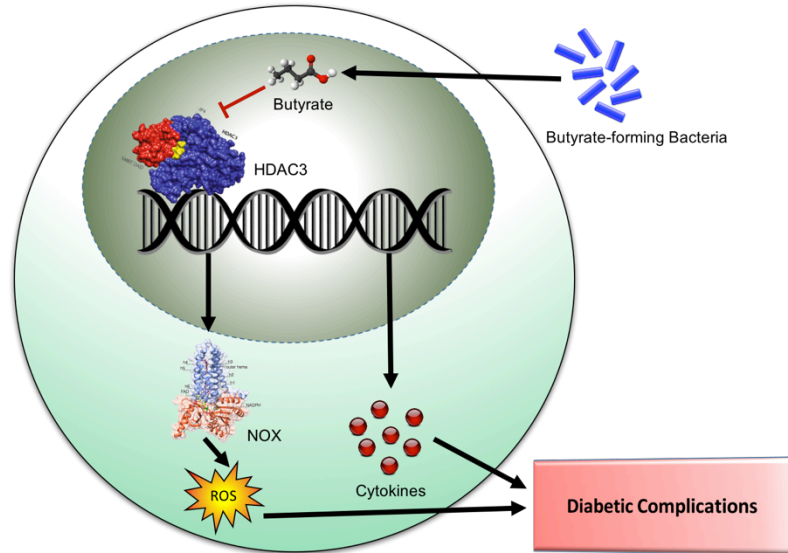


Figure 7: Proposed mechanisms by which dysbiosis mediates diabetic complications.

This microbial signature obtained for diabetes and CRC can serve as a novel non-invasive biomarker. By the end of the project, we are going to have insights about the molecular mechanisms by which diabetic dysbiosis affects the host mediating GI complications and CRC.

CHAPTER 3

MATERIALS AND METHODS

3.1. Animal Studies

All animal procedures were approved by the Institutional Animal Care and Use Committee (IACUC) of the American University of Beirut, Lebanon following the National Institutes of Health (NIH) animal care guidelines. Our present study included *MKR* male mice that were purchased from The Jackson Laboratory (Bar Harbor, Maine). *MKR* male mice have a mutation in their muscle insulin receptor that makes them susceptible for insulin resistance and the development of T2DM at adulthood¹⁶⁹. They were developed on *FVB-NJ* background, so these wildtype mice were used as controls. These mice have been shown to develop diabetic GI complications resembling those seen in humans.

Our central hypothesis is that dysbiosis, observed in diabetes mellitus, play a key role in the pathogenesis of cancer progression in CRC through modulating the host inflammatory and ROS production. To test this hypothesis, we are going to perform the following experiments:

3.1.1. Assessment of the effect of butyrate on MKR mice

This experiment included 3 groups of non-obese male mice, the first group contained *FVB-NJ* mice and served as the control, the second group contained non-

obese diabetic *MKR* mice treated with vehicle (phosphate-buffered saline “PBS”) while the third group comprised non-obese diabetic *MKR* mice treated with sodium butyrate (Sigma-Aldrich, USA) dissolved in PBS with a daily intraperitoneal (IP) dose of 20 mg/kg for 8 weeks (from week 23 till week 31 of age) (**Figure 8**). The dose of butyrate should be sufficient to provide 10 μ M of butyrate concentration in the plasma which is reported to be the concentration of a healthy gut milieu ¹⁷⁰. Mice were housed in the animal care facility, American University of Beirut and were fed with autoclaved food *ad libitum* and maintained in fixed temperature and humidity in 12-hour light/dark cycles. At 31 weeks of age, fecal samples were collected from each mouse under sterile condition and stored at -80°C fridge for further extraction of bacterial genomic DNA for microbial identification.

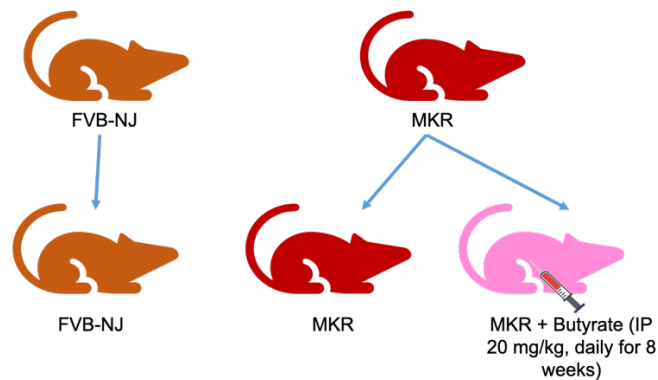


Figure 8: Experimental design of the butyrate treatment experiment.

3.1.2. Establishing if dysbiosis play a key role in diabetes-associated CRC

In this set of experiment, four groups of male mice (n=4) were used: 1) Control mice or *FVB-NJ* mice, 2) non-obese type 2 diabetic *MKR* mice, 3) *FVB-NJ* mice treated

with azoxymethane and dextran sulfate sodium (DSS), known to induce CRC, and 4) non-obese type 2 diabetic *MKR* mice treated with azoxymethane and DSS.

The azoxymethane-DSS protocol¹⁷¹ involves an initial intraperitoneal injection with the genotoxic azoxymethane (10 mg/kg) then after one week, mice were supplied with 2.5% DSS solution instead of drinking water for one week. Mice were allowed to rest for two weeks then the DSS cycle was repeated for two additional times (**Figure 9**).

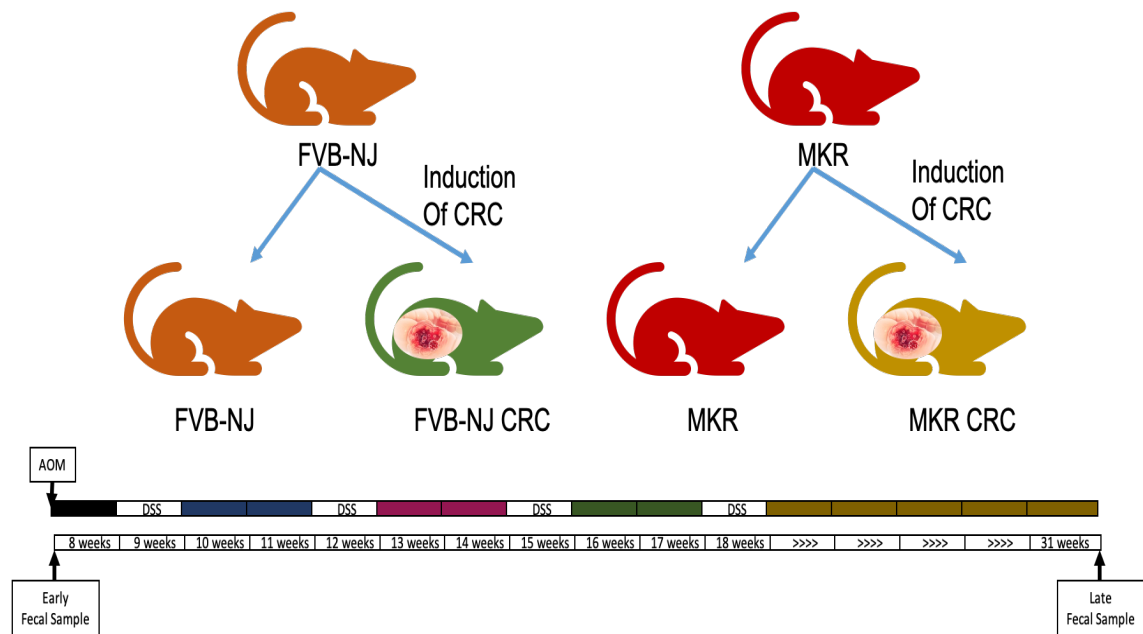


Figure 9: Experimental design of the colorectal cancer induction experiment.

Fecal samples were collected before the initiation of the experiment (at 7 weeks of age) and another fecal sample was collected before sacrifice at 31 weeks of age. Fecal samples were stored at -80°C for analysis. Body weight and blood glucose were monitored throughout the study.

3.1.3. Microbiota depletion and fecal microbial transplant

In a parallel set of experiments, *FVB-NJ* male mice were treated with antibiotic cocktail to deplete their colonic microbiota. The antibiotic cocktail consisted of amoxicillin (0.5 mg/mL), vancomycin (2.5 mg/mL), metronidazole (0.5 mg/mL), amphotericin B (0.025 mg/mL), streptomycin (0.025 mg/mL), penicillin (25 U/mL) and ciprofloxacin (0.0625 mg/mL). The antibiotic cocktail was supplied in the mice drinking water at their weaning age (3-month of age) and for 5 consecutive weeks. Fecal samples were collected immediately after the end of the antibiotic treatment to ensure microbiota depletion by 16S rRNA sequencing. The antibiotic cocktail was optimized through experimentation on small number of animals till the optimum concentrations were achieved. From the 50 mice that were first included in the antibiotic microbiota-depletion experiment, 30 mice died from complications related to the antibiotic treatment before the optimum dose of antibiotics was achieved.

The microbiota-depleted *FVB-NJ* mice were divided into 5 groups (n=4) (**Figure 10**). The first group served as the control. The other four groups were conventionalized in the cages of the 4 groups mentioned in the previous animal experiment. After two weeks of conventionalization, these mice were inoculated with fecal microbial transplant (FMT) obtained from mice from the previous experiment. FMT were prepared by homogenization of fecal pellets in PBS supplied with 0.05% of L-cysteine and allowed to pass through 40 µm cell strainer. Fecal samples were collected at early and late time points to ensure the stability of transplanted microbiota.

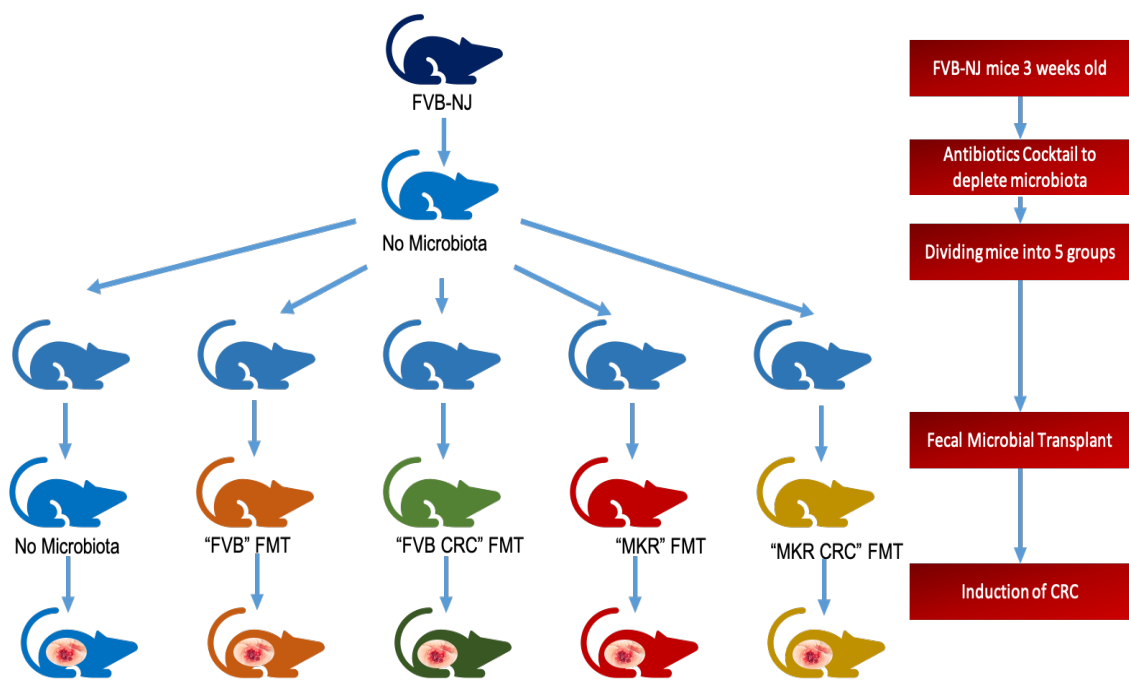


Figure 10: Experimental design of the microbiota inoculation experiment.

Colorectal cancer was induced in all groups using the azoxymethane-DSS protocol as previously described and fecal samples were collected at different time points for 16S rRNA sequencing. At the end of the experiment, mice were sacrificed for histological and biochemical analysis of different tissues and assessment of CRC severity.

3.1.4. Probiotics treatment

In order to assess if restoring the homeostatic balance of the gut microbiota can delay the onset of diabetes-associated GI complication, our different group of mice were treated with probiotics (ProbioLife; Valio Ltd., Finland). ProbioLife contains a mixture of complex probiotics including *Lactobacillus acidophilus*, *Bifidobacterium lactis*,

Lactobacillus plantarum, *Bifidobacterium breve*, *Saccharomyces boulardi*,
Lactobacillus rhamnosus, *Lactobacillus reuteri*, and zinc as a prebiotic.

In this set of experiments, 5 groups of male mice were used: Control *FVB-NJ* mice, 2) *non obese type 2 diabetic MKR mice* treated with PBS (vehicle); 3) *MKR* mice receiving probiotics (ProbioLife) dissolved in PBS at a dose of 5 mg/kg body weight by oral gavage for 12 weeks (from week 19 of age till week 31 of age); 4) *FVB-NJ* mice with CRC treated with PBS (vehicle); and 5) *FVB-NJ* mice with CRC and treated with probiotics (ProbioLife) dissolved in PBS at a dose of 5 mg/kg body weight by oral gavage for 12 weeks (from week 19 of age till week 31 of age) (**Figure 11**).

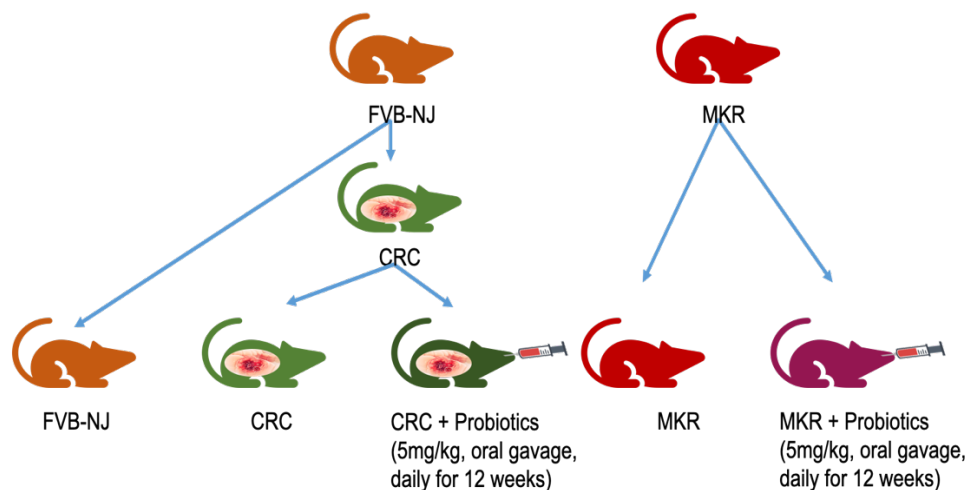


Figure 11: Experimental design of the probiotics treatment experiment.

Fecal samples were collected at early and late time points to investigate the difference in microbiota. After the end of the treatment period, all mice were sacrificed and colon tissue extracted, and analysis performed to assess the development of CRC and polyps and the severity of CRC as well as for metabolic and biochemical analysis.

3.2. 16S rRNA sequencing

The isolated genomic DNA (gDNA) from the mice feces was used for 16S rRNA sequencing of microbiota. Sequencing procedures were performed at Avera Institute for Human Genetics (USA) using the following universal primers for the conserved V4 region (GTGCCAGCMGCCGCGGTAA (V4f) and GGACTACHVGGGTWTCTAAT (V4r)) to amplify the V4 region and give an amplicon length of 250 bp. The wetlab procedures were adapted from MiSeq Wetlab SOP available from Schloss lab at https://github.com/SchlossLab/MiSeq_WetLab_SOP (accessed on October 7, 2019). The ZymoBIOMICS™ Microbial Community Standard II kit (USA) was used to provide the MOCK community to assess the performance of microbiomics workflow. We performed sequencing of 105 samples representing $n \geq 3$ of each group at different time points and from different experiments. The initial QC on the sub-set of the sequenced samples showed that all but 4 samples passed. Raw sequencing files are available at <https://basespace.illumina.com/s/4CNcuYouds0q>. The average yield was 142,000 reads per sample which implies an excellent coverage and allowed us to discover low abundant microbial communities.

The obtained Fasta files were used for analysis as follows. For each experiment, we generated a “.files” file that compiles the 2 sequencing files of each sample and gave it the name of the samples and we created “.design” and “.metadata” files that describes the respective group and time point of each sample. Analysis of the 16S rRNA sequencing data was performed in the labs of the American University of Beirut using the High-Performance Computing (HPC) facility available on campus. The analysis was performed on Arza cluster computer using 32 cores and 20 Gb RAM. A

complete description of the hierarchy of Arza HPC is available at <https://servicedesk.aub.edu.lb/TDClient/Requests/ServiceDet?ID=29747> (accessed on October 7, 2019). We used the mothur tool ^{172,173} to analyze our samples according to the published SOP available at https://www.mothur.org/wiki/MiSeq_SOP (accessed on October 7, 2019) . We customized the job batch file according to our files, design and required analysis and we submitted our jobs to Arza. We used the latest SILVA v132 data for alignment. SILVA contains 88247 bacteria, 4626 archaea, and 20246 eukarya sequences. It can be downloaded from <https://www.arb-silva.de/download/> (accessed on October 7, 2019). Classification of operational taxonomic units (OTUs) was done using the RDP training set release 11 (available at <https://rdp.cme.msu.edu/>, accessed on October 7, 2019). The script used for the analysis is attached in appendix 2.

Briefly, primers were first removed from sequencing reads via cutadapt v1.4. The error tolerance was set at 0.1 for both primers which enabled us to remove sequences containing more than one base error per 10 bases of primers. The reads were then aligned against sequences obtained from SILVA database after curating the database to start at 11894 and end at 25319 to save computational power. This was followed by removing sequences that failed to align, or had ambiguous bases, or contained more than 275 bp, or had homopolymers larger than 8 bases to reduce any error resulting from PCR amplification. To further save computational power, contigs were generated and duplicates were removed to leave only unique sequences. The UCHIME algorithm was used as an integrated part of the mothur package to identify and remove chimeras. Likewise, Sequences originated from nonbacterial species such as mitochondria, chloroplasts and Archea or from unknown origin were removed. We

then removed the MOCK groups after the determination of the error rates and clustered the remaining sequences into OTUs with 97% similarity.

Subsampling against the number of reads in the least abundant sample was used for standardization. Good's coverage estimator and rarefaction curves showed that our data has adequate sequencing coverage. Alpha-diversity within samples was measured using Chao-1, Shannon Diversity Index and Simpson's Index. The alpha-diversity matrices were tested for differences within samples using Mann-Whitney tests. For beta-diversity analysis, Yue and Clayton theta similarity coefficient was used to generate the distance matrices. Mothur used the distance matrices to create principal coordinate analysis (PCoA) to determine the major differences between groups. Testing the dissimilarities between groups was statistically performed using Analysis of molecular variance (AMOVA) test. LEfSe test was used to determine OTUs that are responsible for the differences in each group . **Figure 12** illustrates the general workflow for mothur microbial analysis. Qiime2 was additionally used to validate all the results obtained from mothur (script attached in appendix 2). Graphs were generated using the BIOM file generated via mothur or Qiime2 and using tools available in R (using vegan, ggplot2 and phyloseq packages), Galaxy Krona and Phinch.



Figure 12: Workflow for mothur microbial analysis (Saskia Hiltemann, Bérénice Batut, Dave Clements, 2019 16S Microbial Analysis with mothur (extended) (Galaxy Training Materials). Online; accessed Mon, Apr 20, 2020).

3.3. Oral Glucose Tolerance Test

After fasting for 8 hours, *MKR* mice were challenged intraperitoneally with D-glucose (Sigma Chemical Co., St. Louis, MO, USA) at a dose of 2 g/kg body weight which was administered via oral gavage. Blood samples were taken from the tail tip at 0 (before glucose injection), 30, 60, 90 and 120 min after the glucose challenge for blood glucose determination.

3.4. Sacrifice and Organ Harvesting

After 31 weeks of age, all mice were sacrificed by spinal dislocation after anaesthetizing them with isoflurane. Subsequently, distal colon segments were harvested for protein extraction and determination of HDAC3 and histone acetylase (HAT) activity in colon tissues. Colon lengths were recorded (from just underneath the cecum till the anus) to assess the effect of diabetes and treatments on the colon anatomy. Blood was collected via cardiac puncture under anesthesia in heparin vacutainers for determination of inflammatory cytokines. In total, 1 ml of blood was withdrawn from the heart. Blood was centrifuged at 3000 rpm for 15 minutes at 4°C and plasma was collected and stored at -80°C for further analysis. Cecal and fecal contents were collected for determination of their butyrate content.

3.5. Determination of Random Blood Glucose and Circulatory Cytokines

Random blood glucose was measured weekly between 10 AM and noontime using a glucometer (Accu-Chek Performa, Roche, USA) in blood obtained from the tail vein (5 µl) utilizing the glucose oxidase-peroxidase method. Random blood glucose was measured weekly from 7 weeks of age till 31 weeks of age. Plasma inflammatory

markers were determined in the blood obtained on sacrifice day using Inflammatory Cytokines Multi-Analyte ELISArray Kits (Cat. No. MEM-004A, Qiagen, Germany). This multi-array kit detects mouse inflammatory cytokines using a conventional ELISA protocol. This kit was used to determine circulatory interleukin IL-10, IL-17 α , tumor necrosis factor (TNF)- α and granulocyte- colony stimulating factor (G-CSF) according to manufacturer's instructions.

3.6. Determination of glycated hemoglobin (HbA_{1c})

An aliquot of the whole blood (50 μ l) was used for the determination of HbA_{1c} to determine the presence of chronic diabetic state. HbA_{1c} levels were determined with a Mouse HbA_{1c} Kit (Catalogue #80310, Crystal Chem, USA), according to the manufacturer's instructions and normalized against total hemoglobin to get HbA_{1c} %.

3.7. Isolation of fecal DNA and Microbial Gene Analysis

Feces were collected at early and late time points from all mice under aseptic conditions and stored at -80°C for further analysis. Bacterial DNA was extracted from feces using DNeasy PowerSoil Kit (Cat. No. 12888-100, Qiagen, Germany) according to manufacturer's instructions. Real-time polymerase chain reaction (rt-PCR) was used to determine the different microbial communities. Herein, we studied the butyrate-forming bacterial communities that were previously described by Vital *et al.* as the major contributors for butyrate formation¹⁷⁴. Bacterial communities were identified using specific primers for these communities and for the butyrate kinase gene (**Table 2**). Results are normalized against 16S rRNA gene levels in each sample and are compared to controls.

Table 2: List of primers.

Primer	Sequence	Reference
<i>Akkermansia muciniphila</i> Forward	CAGCACGTGAAGGTGGGGAC	175
<i>Akkermansia muciniphila</i> Reverse	CCTTGCGGTTGGCTTCAGAT	
Alistipes spp Forward	TTAGAGATGGGCATGCGTTGT	176
Alistipes spp Reverse	TGAATCCTCCGTATT	
Anaerstipes spp Forward	GCGTAGGTGGCATGGTAAGT	177
Anaerstipes spp Reverse	CTGCACTCCAGCATGACAGT	
Bacteroidaceae Forward	GAAGGTCCCCACATTG	178
Bacteroidaceae Reverse	CGCKACTTGGCTGGTTCAG	
<i>Bacteroides fragilis</i> Forward	ATACGGAGGATCCGAGCGTTA	179
<i>Bacteroides fragilis</i> Reverse	CTGTTTGATACCCACT	
Butyrate kinase Forward	GCAGGCCTAACACATGCAAGTC	180
Butyrate kinase Reverse	CTGCTGCCTCCCGTAGGAGT	
Butyricococcus spp Forward	ACCTGAAGAATAAGCTCC	181
Butyricococcus spp Reverse	GATAACGCTTGCTCCCTACGT	
Butyrivibrio Reverse	GTTAGCGACGGCACTGA	
Butyrivibrio spp Forward	CTATCAGCAGGGAAGAAAG	
<i>Coprococcus comes</i> Forward	GTGACCGCGTGTAATGACG	182
<i>Coprococcus comes</i> Reverse	CAGAGTGCCCATCCGAATTG	
<i>Coprococcus eutactus</i> Forward	CTGGAGCTTGCTCCGGCCGATTT	
<i>Coprococcus eutactus</i> Reverse	GTCAGTAGCAGTCCAGTAAGT	
Enterobacteriaceae Forward	GACCTCGCGAGAGCA	183
Enterobacteriaceae Reverse	CCTACTTCTTTTGCAACCCA	
<i>Eubacterium hallii</i> Forward	GTGTCGGGGCCGTATAGG	182
<i>Eubacterium hallii</i> Reverse	GTTTCGCCTCACTCTGTGAC	
<i>Eubacterium rectale</i> Forward	CATIGCTICTCGGTGCCGTC	184
<i>Eubacterium rectale</i> Reverse	ATITGCTCGGCTTCACAGCT	
<i>Eubacterium ventriosum</i> Forward	GTCGGGGGACAATAGTCC	182
<i>Eubacterium ventriosum</i> Reverse	ATTTGCTTACCCTCACGGGG	
<i>Faecalibacterium prausnitzii</i> Forward	TGTAAACTCCTGTTGTTGAGGAAGATAA	185
<i>Faecalibacterium prausnitzii</i> Reverse	GCGCTCCCTTTACACCCA	
Lachnospiraceae Forward	CGGTACCTGACTAAGAAGC	178
Lachnospiraceae Reverse	AGTTYATTCTTGCGAACG	
<i>Odoribacter splanchnicus</i> Forward	ATGTAATGATGAGCACTCTAACGG	186
<i>Odoribacter splanchnicus</i> Reverse	GGCTTTTGAGATTGGCATCC	
Oscillospira spp Forward	ACGGTACCCCTGAATAAGCC	187

Oscillospira spp Reverse	TCCCCGCACACCTAGTATTG	
Roseburia intestinalis Forward	GCACAGGGTCGCATGACCT	182
Roseburia intestinalis Reverse	AACACATTACATGTTCTGTCATC	
Ruminococcaceae Forward	TTAACACAATAAGTWATCCACCTGG	178
Ruminococcaceae Reverse	ACCTTCCTCCGTTTTGTCAAC	
Universal 16S rRNA Forward	GTGSTGCAYGGYYGTCGTCA	178
Universal 16S rRNA Reverse	ACGTCRTCCMCNCCTTCCTC	

3.8. Real Time PCR

Real Time PCR was conducted using Bio-Rad CFX384 RT-PCR system using 10 ng of DNA, 300 nM of each primer, SYBR Green Master Mix (Applied Biosystems) and RNase-free water to reach final volume of 10 µl as previously described ¹⁸⁸.

Cycling conditions included an initial pre-heating step to 95°C for 2 minutes followed by 40 cycles of denaturation (95°C for 15 seconds), annealing (60°C for 30 seconds) and extension (72°C for 15 seconds) and a final extension step at 72°C for 2 minutes. Each sample was performed in triplicates.

3.9. Determination of Fecal and Cecal Butyrate Content

High Performance Liquid Chromatography (HPLC)/Mass Spectrometry (MS) technique was used to quantify butyrate content in feces and cecal contents of mice according to the method described by Parise *et al.* ¹⁸⁹. The LTQ-FT system (Thermo Scientific, Germany) was used with the application of a Phenomenex Synergi Polar-RP column (Phenomenex, USA). Results are expressed as mg butyrate per g of feces or cecal content.

3.10. Determination of Histone acetylase and histone deacetylase 3 activities

The enzymatic activities of HAT and HDAC3 in distal segments of colon tissues were determined using HAT and HDAC3 Activity Assay Kits (Cat. No. EPI001 & EPI004, Sigma-Aldrich, Germany) according to manufacturer's instructions.

3.11. Detection of reactive oxygen species production in colon tissues using HPLC

Determination of ROS production in distal segments of colon tissues was assessed using HPLC method as previously described¹⁸⁸. Briefly, sections of the colons were washed twice with Hanks' balanced salt solution (HBSS)-diethylenetriaminepentaacetic acid (DTPA), homogenized and incubated for 30 min with 50 μ M DHE (Sigma-Aldrich) in HBSS–100 μ M DTPA. This step was followed by the addition of acetonitrile and centrifugation at 12,000 \times g for 10 min at 4°C). The homogenate was dried under vacuum and analyzed by HPLC with fluorescence detectors. Quantification of DHE, EOH, and ethidium concentrations was performed by comparison of integrated peak areas between the obtained and standard curves of each product under chromatographic conditions identical to those described above. EOH and ethidium were monitored by fluorescence detection with excitation at 510 nm and emission at 595 nm, whereas DHE was monitored by ultraviolet absorption at 370 nm. The results are expressed as the amount of EOH produced (nmol) normalized for the amount of DHE consumed (*i.e.*, initial minus remaining DHE in the sample; μ mol).

3.12. Primary Culture

To assess the role of HDAC in regulating NOX4 protein expression, part of the distal segments of colon of control mice (*FVB-NJ*) was extracted and used for *ex vivo*

culture¹⁹⁰. Briefly, the extracted colons were cleaned with ice-cold PBS and feces were completely removed. Afterwards, the colon was cut into pieces with 1 cm length and weighed. For the organ culture, a cell strainer (100 µm) was placed on a 6-well plate to which all the colon pieces were transferred. Dulbecco's modified eagle's media (DMEM) was used and was supplied with 2% FBS and 1% Penicillin-Streptomycin (1x). the colon pieces were left to rest in the media for 24 hours, before incubating the pieces with either normal glucose NG (5 mM), high glucose (25 mM), high glucose with sodium butyrate (4 mM), high glucose with the HDAC specific inhibitor (Trichostatin A "TSA", 0.5 µM) or high glucose with combination of butyrate and TSA for 48 hours, before proceeding to protein extraction.

3.13. Western Blot

Total proteins from homogenates of the distal segments of the colon were obtained using 200 µl of radioimmune precipitation assay buffer containing 20 mmol/l Tris.HCl, pH 7.5, 150 mmol/l NaCl, 5 mmol/l EDTA, 1 mmol/l Na₃VO₄, 1 mmol/l PMSF, 20 µg/ml aprotinin, 20 µg/ml leupeptin, and 1% NP-40 then incubated overnight on a rotator at 4°C. Subsequently, samples were centrifuged at 13,700 rpm for 30 min at 4°C. Total protein content of each sample was quantified using the Lowry Protein Assay¹⁹¹. Samples (containing 30 µg of proteins) were loaded on 15% SDS-PAGE and transferred to nitrocellulose membrane. Blots were incubated with rabbit polyclonal anti-NOX4 (1:500, Santacruz, USA), rabbit polyclonal anti-IL-1β (1:500, Abcam, USA), mouse polyclonal HSC-70 (1:1000, Santacruz, USA), or mouse polyclonal β-actin (1:1000, Santacruz, USA). The primary antibodies were detected using horseradish peroxidase-conjugated IgG (1:20000). Bands were visualized by enhanced

chemiluminescence. Densitometric analysis was performed using National Institutes of Health ImageJ software.

3.14. Statistical Analysis

Statistical analysis was performed using Graphpad Prism Software (Graphpad, version 6.0, CA, USA) ¹⁹². Sample size was calculated to give 80% power and $p \leq 0.05$. All results are expressed as mean \pm SD (standard deviation). We used a two-tailed student's t test or Analysis of Variances (ANOVA) to determine significance and $p \leq 0.05$ was considered statistically significant. We used Levene's test to test for differences in group variances and chose the t test calculation method accordingly.

CHAPTER 4

RESULTS

In this current study, we investigated the role of microbiota in diabetes-associated colorectal cancer. To test this hypothesis, we performed multiple experiments to: (1) identify the microbial signature associated with diabetes; (2) investigate if diabetes-associated microbiota is influencing its gastrointestinal complications and colorectal cancer development; (3) pinpoint the underlying molecular mechanisms responsible for this effect; and (4) investigate the effect of rectifying this microbial signature by the use of probiotics on the development of the GI complications. Our results are presented in the following section.

4.1. *MKR* mice develop type 2 diabetes without obesity and suffer from gastrointestinal dysfunction

First, we assessed the diabetic status of *MKR* mice, and their GI health compared to that of the control mice. Body weight and random blood glucose were measured at sacrifice (31 weeks of age) for *MKR* mice and the *FVB-NJ* controls. Although the body weight of *MKR* mice was comparable to that of the controls (indicating no signs of developing obesity) (**Figure 13a**), blood glucose levels and HbA_{1c} % were significantly elevated in diabetic mice compared to those of the control group (**Figure 13b, c**). Concerning GI health, we measured colon lengths and found that *MKR* mice have shorter colons than their control littermates which reflects a reduced nutrient absorption and GI dysfunction (**Figure 13d**).

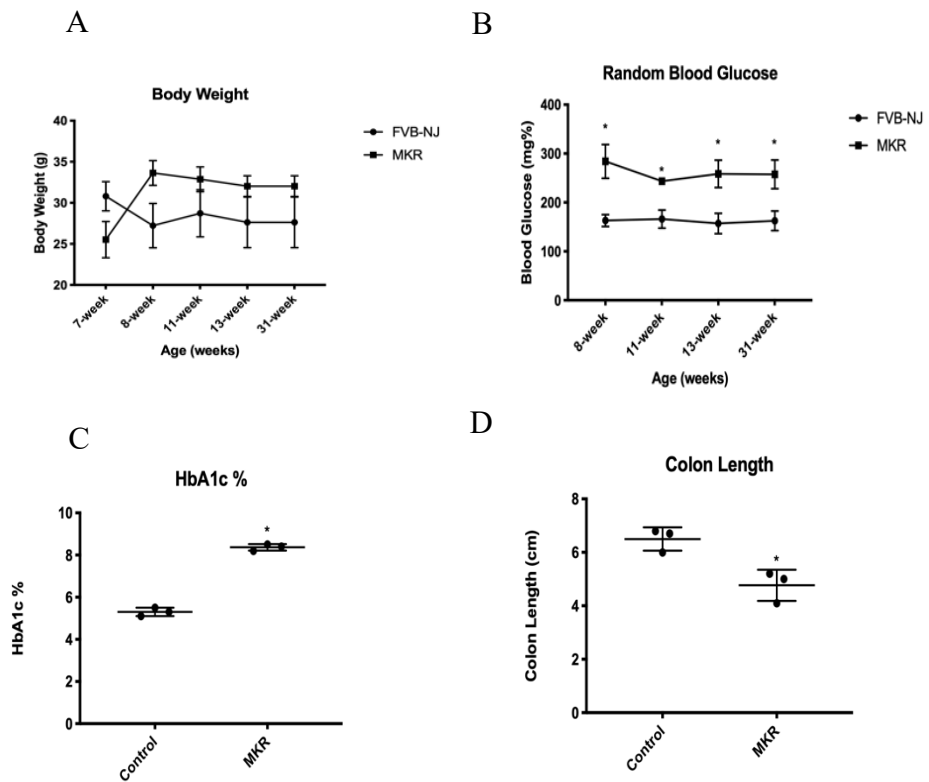


Figure 13: Body weight, blood glucose, HbA1c % and colon lengths of *MKR* mice compared to their control littermates. Results are expressed as mean \pm SD. * significantly different from *FVB-NJ* control mice at $p < 0.05$.

4.2. *MKR* mice have impaired glucose utilization

We performed IP glucose tolerance test to assess the insulin resistance of *MKR* mice. *MKR* mice showed impaired glucose utilization marked by high fasting blood glucose and significant elevation of blood glucose after glucose injection that slowly declines and did not reach normal levels after 90 minutes of injection (**Figure 14**).

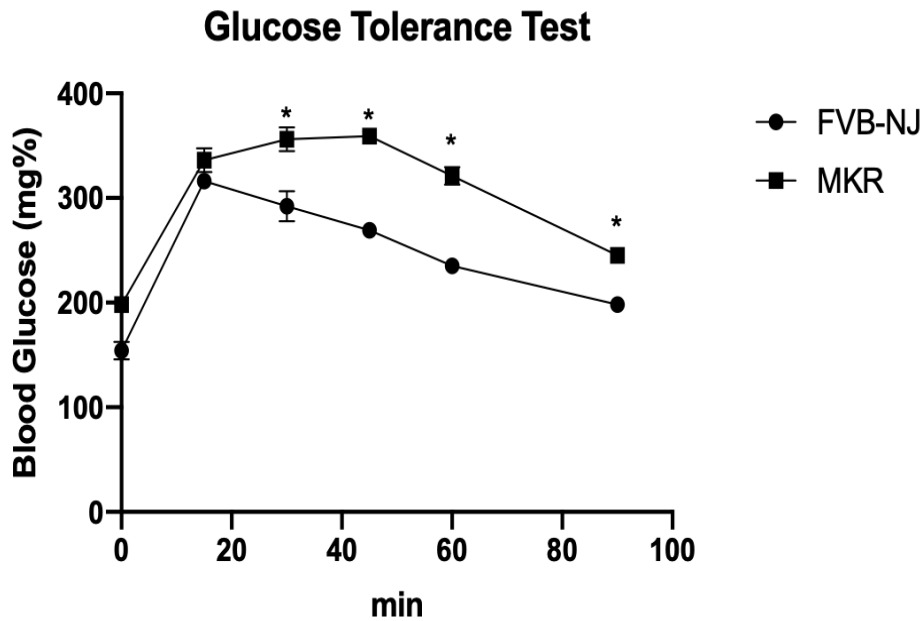


Figure 14: Glucose tolerance test curve for *MKR* and control mice. Results are expressed as mean \pm SEM. * significantly different from *FVB-NJ* control mice at $p < 0.05$.

4.3. Diabetes results in more aggressive colorectal cancer phenotype

Colorectal cancer was induced in a subset of *FVB-NJ* and *MKR* mice using the azoxymethane/DSS protocol. At 31 weeks of age, all mice were sacrificed, and colons were harvested. CRC mice showed some gross findings of CRC (rectal bleeding, inflamed bleeding colon, fecal impaction and polyps). As expected, diabetes resulted in a more aggressive form of CRC confirmed by higher number of polyps compared to that in the *FVB-NJ* CRC group (**Figure 15**).

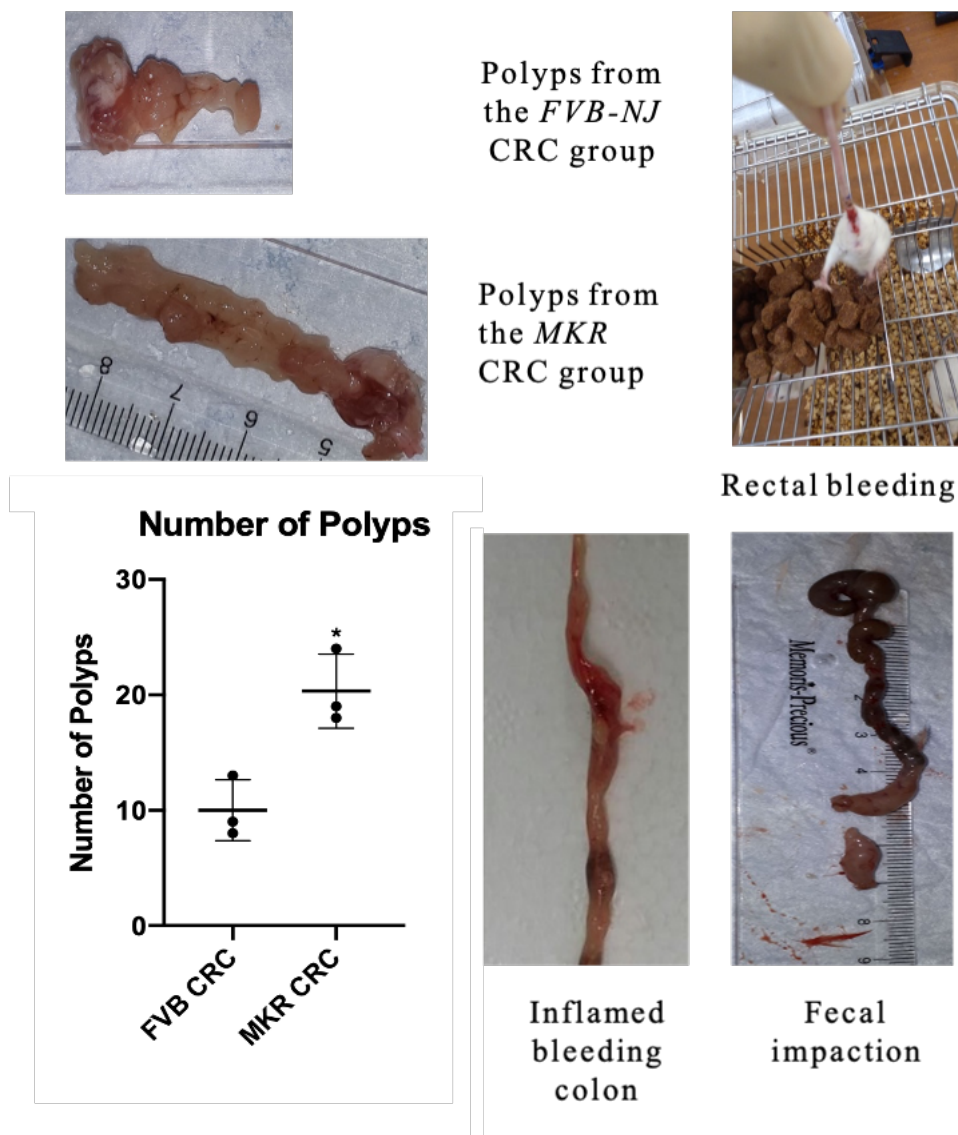


Figure 15: Gross characteristics for colorectal cancer (CRC) and number of polyps in *FVB-NJ* and *MKR* CRC mice groups. Results are expressed as mean \pm SD. * significantly different from *FVB-NJ* control mice at $p < 0.05$.

4.4. Fecal microbial transplant of diabetic and cancer microbiota results in more aggressive colorectal cancer phenotype.

We performed a set of experiments where we depleted the microbiota of control mice with antibiotic cocktail (detailed in the methods section) after weaning followed by inoculating them with FMT from control mice, mice with CRC, mice with

diabetes and mice with CRC and diabetes. Additionally, all mice received azoxymethane/ dextran sulfate sodium to induce CRC. Our data presented in **Figure 16** shows that mice inoculated with FMT from mice with diabetes or mice with both CRC and diabetes have a higher number of polyps compared to control mice or mice inoculated with control FMT.

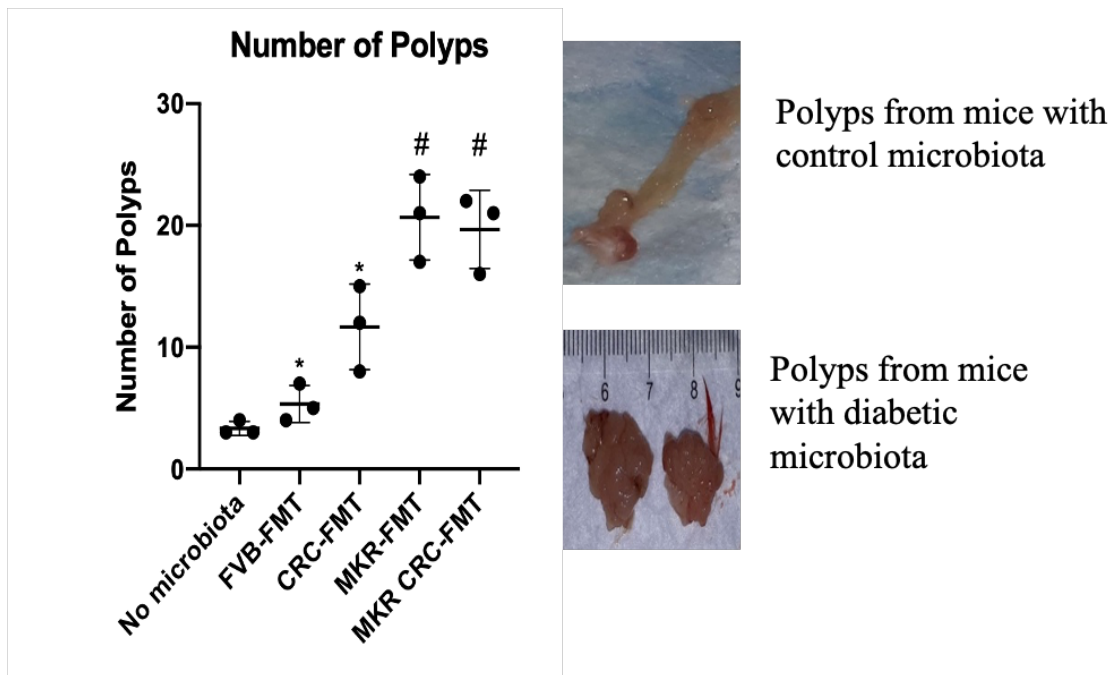


Figure 16: Polyp numbers of mice inoculated with fecal microbial transplant. Results are expressed as mean + SEM. * significantly different from *FVB-NJ* control mice at $p < 0.05$. # Significantly different from *FVB* FMT mice group at $p < 0.05$.

Likewise, mice that were treated with probiotics had a smaller number of polyps compared to the CRC group (**Figure 17**).

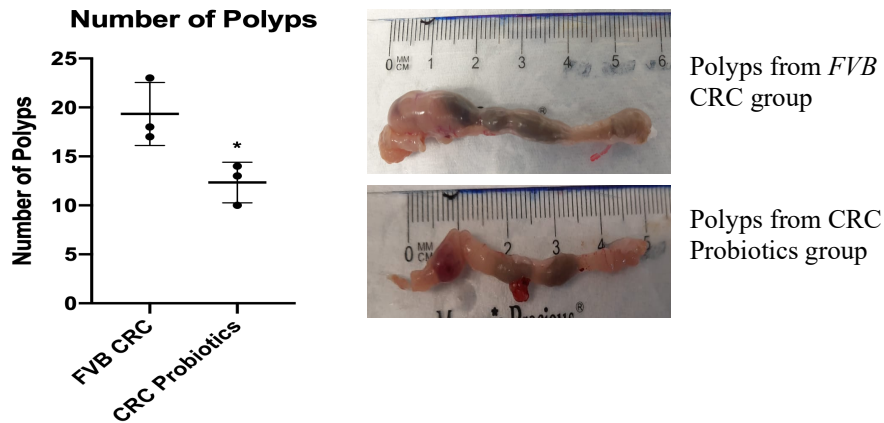


Figure 17: Polyp numbers of FVB CRC mice treated with vehicle (PBS) or probiotics for 12 weeks. Results are expressed as mean \pm SD. * significantly different from FVB CRC mice at $p < 0.05$.

4.5. Diabetic mice microbiota contains less *Bacteroid fragilis* and butyrate-forming bacteria

In order to assess the difference in gut microbiota that resulted from the disturbance in carbohydrate metabolism, RT-PCR, using specific primers for different bacterial communities and primers for the total butyrate kinase genes (**Table 2**), was performed. Our results show the presence of a significant difference between the microbiota of the MKR mice and that of the control mice that is highlighted by the reduction of *B. fragilis* and the most relevant butyrate-forming bacteria¹⁷⁴ (**Figure 18a**), *Butyricoccus spp*, *Butyrivibrio spp*, *Coprococcus comes*, *Eubacterium hallii*, *Eubacterium rectale*, *Eubacterium ventriosum*, and *Roseburia intestinalis* (**Figure 18b**). These findings were also reflected by the reduced abundance of the total butyrate kinase gene expression (**Figure 18c**). Furthermore, the MKR mice and their control littermates had similar abundance of *Akkermansia muciniphila*, Bacteroidaceae, Enterobacteriaceae, *Faecalibacterium prausnitzii*, Lachnospiraceae and Ruminococcaceae, that were previously shown to be associated with other metabolic

conditions ^{175,176,193–201}. Taken together these results suggest that diabetes-associated dysbiosis affects mainly the butyrate-forming bacterial communities.

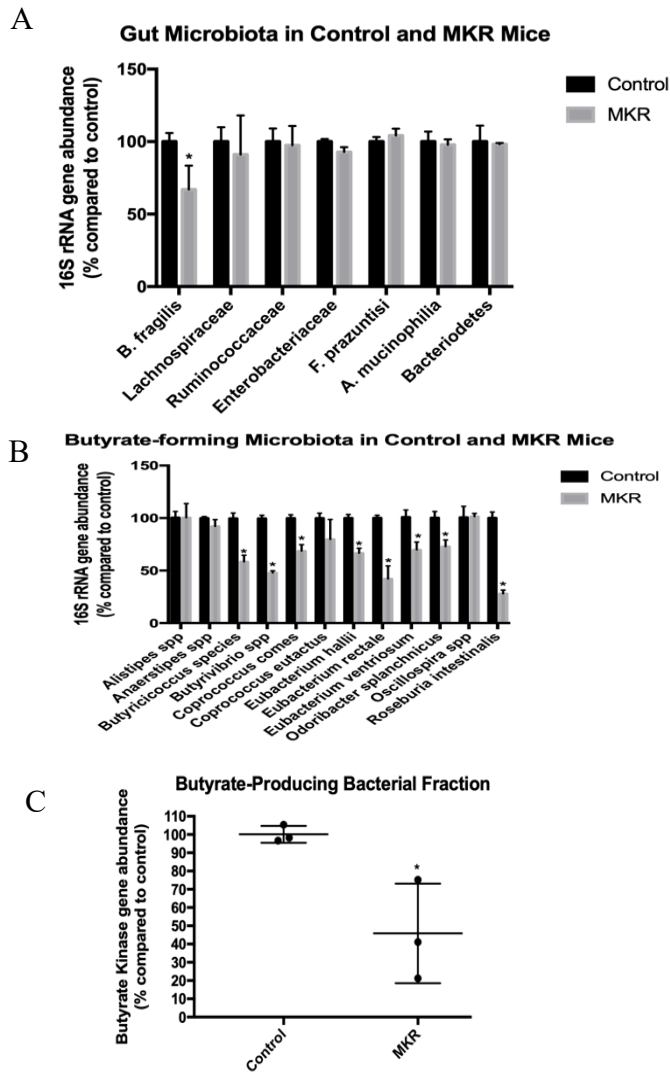


Figure 18: Different microbial communities and butyrate-forming bacteria of *MKR* and control mice (n=3). Data are expressed as mean \pm standard deviation (SD). * statistically significant at $p < 0.05$ vs control.

4.6. Quality control of 16S rRNA sequencing data

We sequenced microbiota 16S rRNA V4 region obtained from fecal samples of all mice included in our experiments. The obtained sequencing data was subjected to quality control where we identified the number of reads per each sample (**Figure 19**). The median number of reads per sample was found to be 80653.5 and the minimum number of reads was 1266 in the non-template control sample. We also inspected the quality control scores for different bases (**Figure 20**). These plots were generated using a random sampling of 10000 out of 8776316 sequences without replacement. The minimum sequence length identified during subsampling was 247 bases. According to the quality control data, we trimmed our reads at 0 and 120 positions to get rid of low-quality reads. All samples passed quality control except for 4 samples in the late time point in the experiment involving antibiotic-treated mice leaving many groups at that time point with only 2 mice per group.

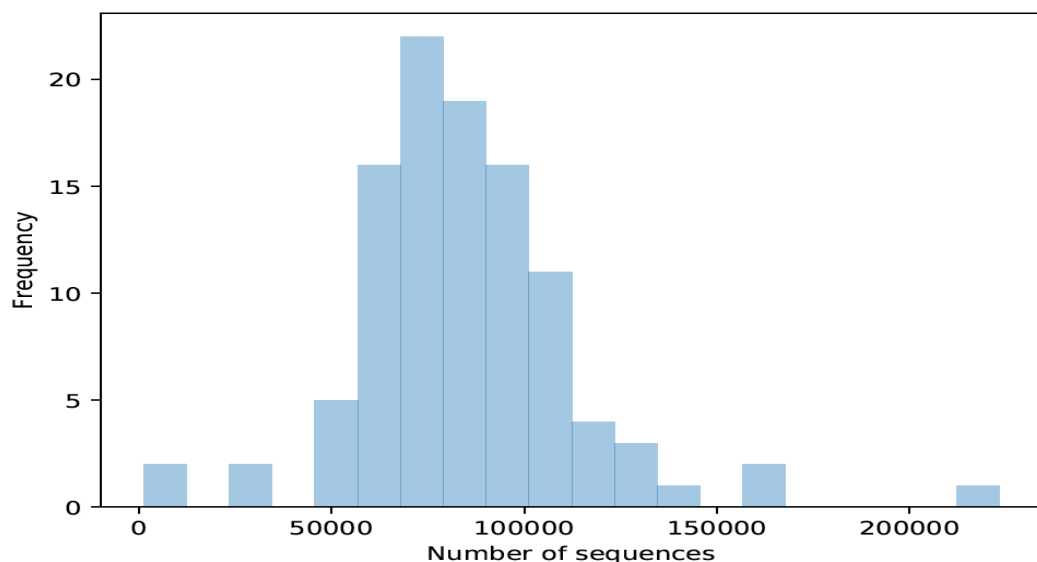


Figure 19: Frequency histogram for the number of reads per sample in the 16S rRNA sequencing data.

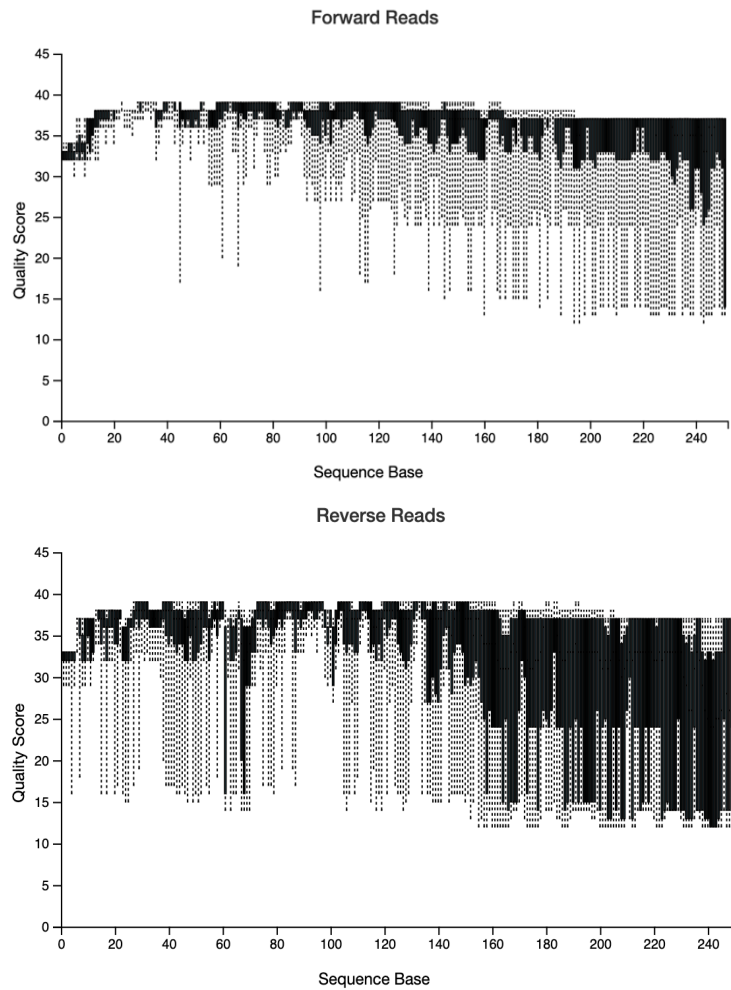


Figure 20: Quality score per base in the 16S rRNA sequencing data.

We performed rarefaction analysis for all samples to ensure that the samples were sequenced deep enough to detect all available OTUs. This was done computationally through random selection of 1000 reads per sample followed by OTUs detection then incrementing by 1000 reads and so on. Our results show that all the samples were sequenced deep enough to detect all features (**Supplementary Figures 1-2 and Figure 23**).

4.7. 16S rRNA microbiota sequencing results

4.7.1. Alpha diversity

In our effort to identify a microbial signature for diabetes and colorectal cancer, we sequenced 16S rRNA DNA obtained from fecal samples of control (*FVB-NJ*) mice, *MKR* diabetic mice, *FVB-NJ* mice with chemically induced CRC and *MKR* mice with CRC. Fecal samples were obtained from early (7 weeks of age) and late (31 weeks of age) time points. The first type of metric that we investigated was alpha diversity, with detection of richness. Richness refers to how many different *types* of organisms (also known as features or operational taxonomic units “OTUs”) are present in a sample. Our results show that our samples had different degrees of richness with the least number of features represented in the control group while the highest number was in the diabetic and diabetic with CRC groups (**Figure 21**). Noteworthy, ageing has increased the number of features in the control and CRC mice.

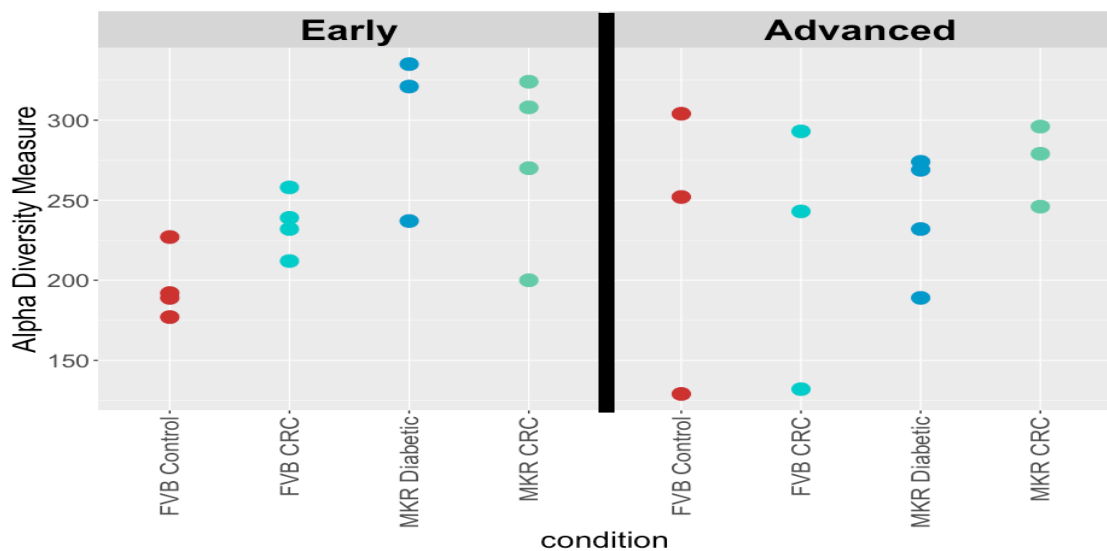


Figure 21: Richness of microbial features (operational taxonomic units) per sample in control, diabetic, colorectal cancer mice.

In the set of mice that were pre-treated with antibiotics, alpha diversity analysis showed a severe reduction of the number of features in the early time point. These mice were inoculated with FMT from different mice groups then CRC was chemically induced in all mice. The analysis of sequencing data from the late time points show an increase in richness in all samples (**Figure 22**). This was also confirmed by rarefaction analysis (**Figure 23**) which shows that the low number of features detected in the samples of the early time point was not due to low read counts but rather due to the nature of the sample composition itself (**Figure 23**).

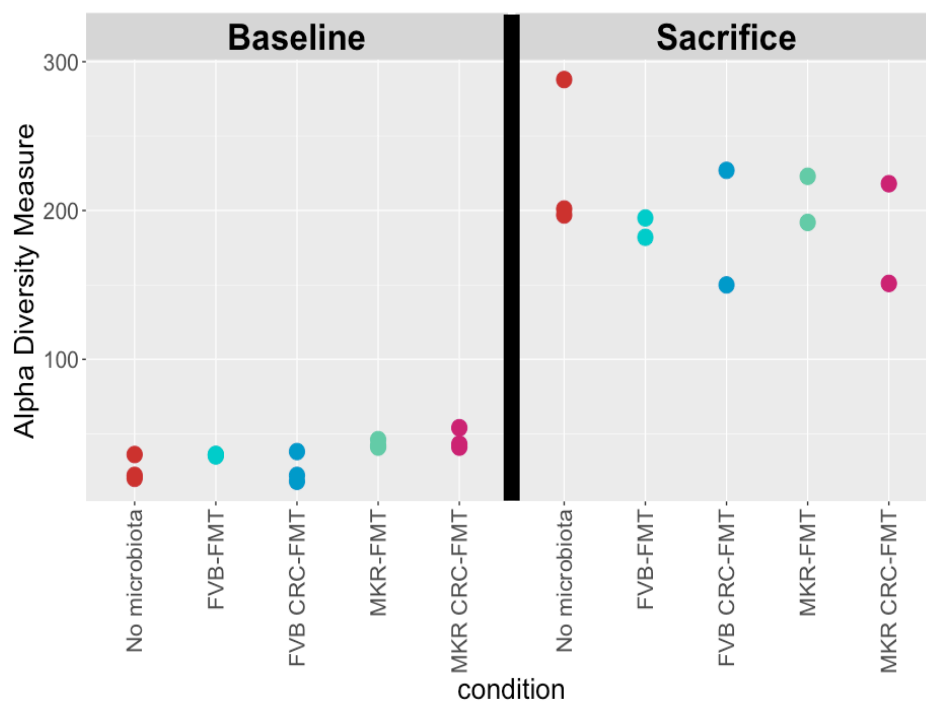


Figure 22: Richness of microbial features (operational taxonomic units) per sample in antibiotic-treated mice.

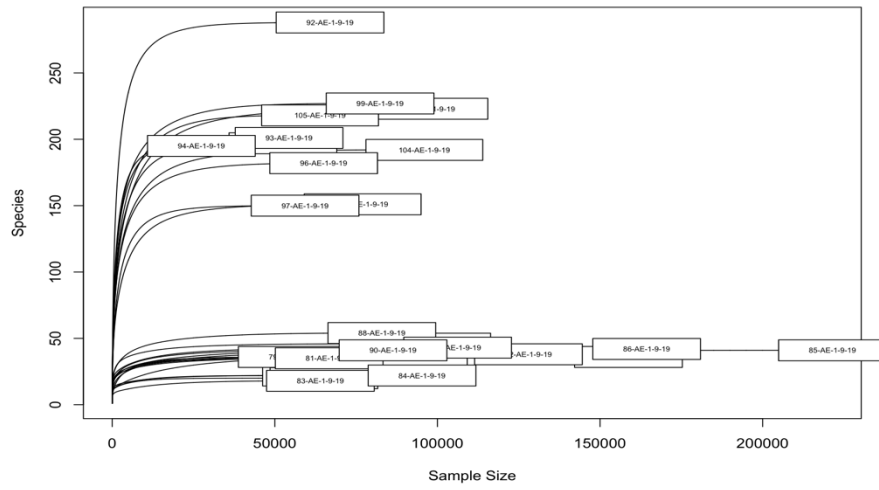


Figure 23: Rarefaction curve of samples of the antibiotic-treated mice.

When a subset of *MKR* mice was treated with probiotics, there was no difference in the richness or the number of OTUs (**Figure 24**). This finding shows that probiotics treatment doesn't affect the number of OTUs but rather its type.

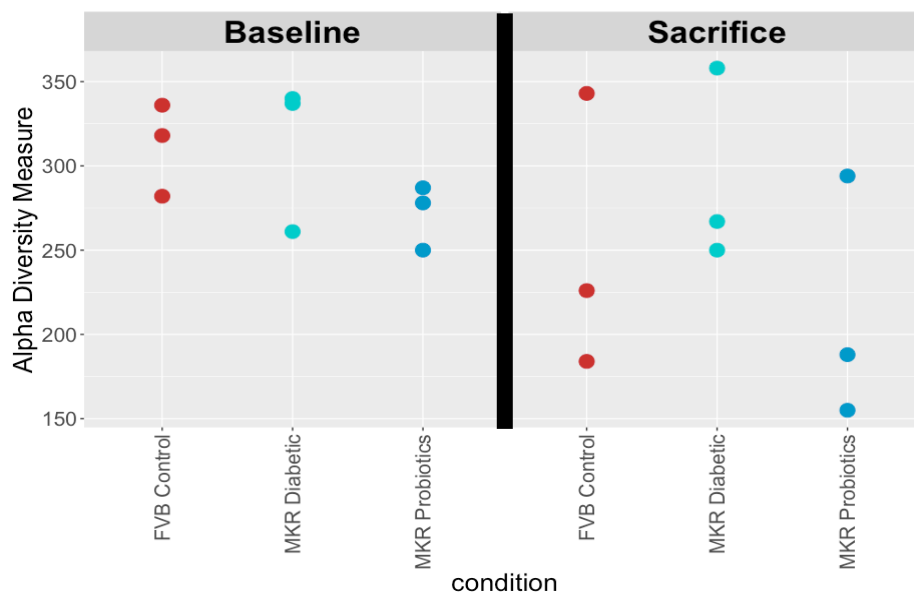


Figure 24: Richness of microbial features (operational taxonomic units) per sample in control, diabetic and probiotics-treated diabetic mice.

Additionally, we performed alpha diversity analysis using Shannon's index which accounts for both the evenness as well as the richness of samples²⁰². Notably, samples with high richness showed less evenness (contained different number of bacteria for different species) while samples that showed low richness had higher evenness (**Supplementary Figures 3-5**).

4.7.2. Taxonomy

In the next step of analysis, we assigned the discovered feature to its corresponding bacterium. We are presenting here the results on the phylum level for simplicity and because it aggregates the differences observed on higher levels of taxonomy.

Concerning the differences in microbial phyla in the diabetic and cancer mice compared to that of the control mice, we observed that the late time point was characterized by higher abundance of Verrucomicrobia compared to the early time point. Interestingly, we observed that diabetic mice have more bacteria belonging to phylum Firmicutes compared to their control littermates. The higher percentage of Firmicutes resulted in lower percentage of Bacteroidetes in *MKR* mice compared to their control littermates (**Figure 25**).

The most interesting differences observed in the microbial phyla were in the antibiotic treated mice (**Figure 26**). At the early time point, all mice harbored Verrucomicrobia whose abundance decreased significantly in the late time point except in the CRC mice. All samples at the early time point also hosted a significant amount of

Proteobacteria which disappeared at the late time point. Another significant difference was observed at the late time points in the mice inoculated with diabetic FMT or diabetic and CRC FMT where these mice had significant amount of Cyanobacteria.

In the probiotics-treated mice, the most significant difference on the phylum level was observed in Bacteroidetes and Cyanobacteria. Probiotics treatment increased the levels of Bacteroidetes and decreased that of Cyanobacteria compared to diabetic mice at the late time point (**Figure 27**).

We also assigned taxonomies to the discovered OTUs to the level of bacterial orders (level 4). **Supplementary Figures 6-8** show the bar plots for different families assigned to the OTUs for each sample in different experiments.

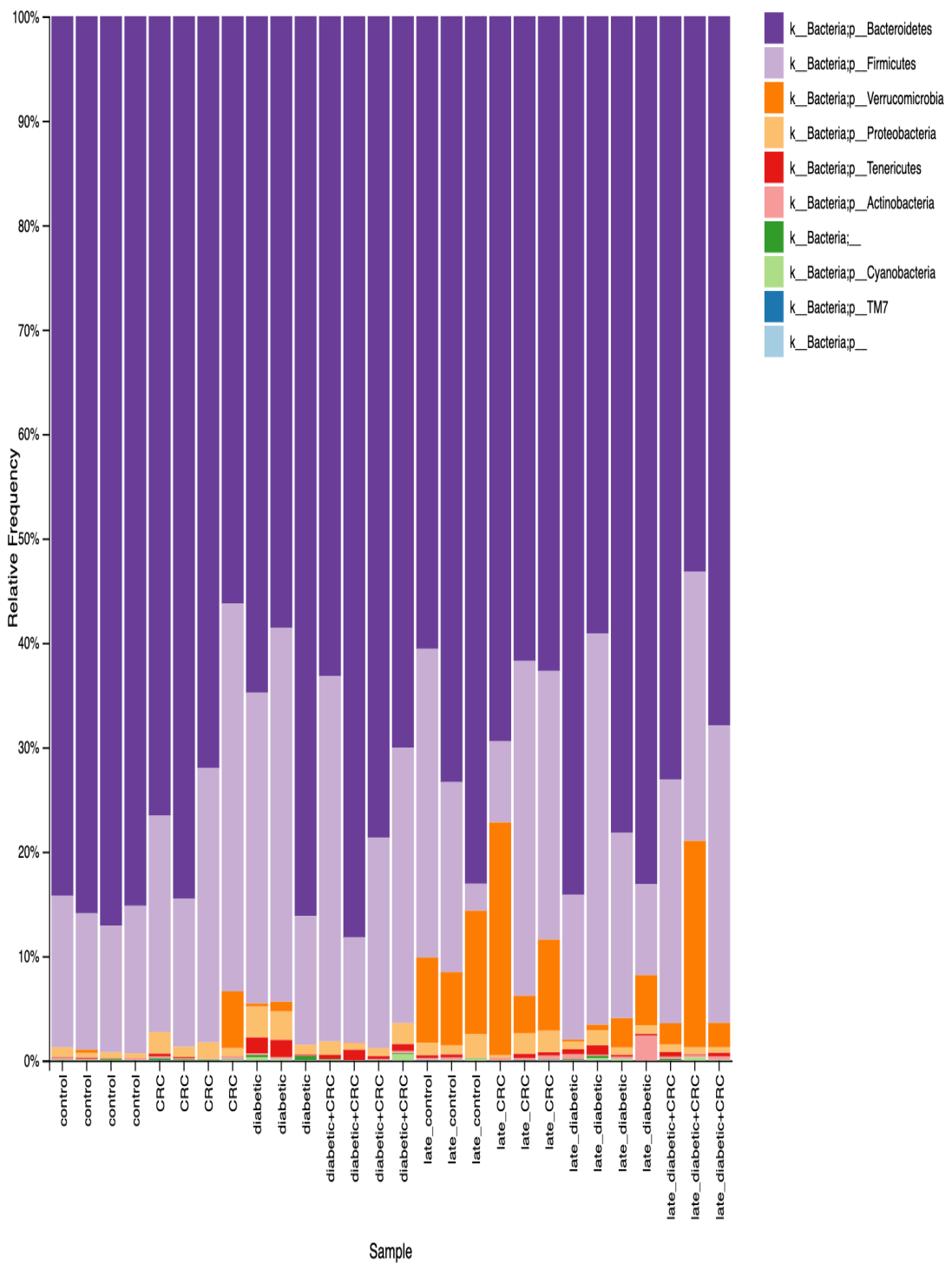


Figure 25: Different phyla per sample in control, diabetic, colorectal cancer mice.

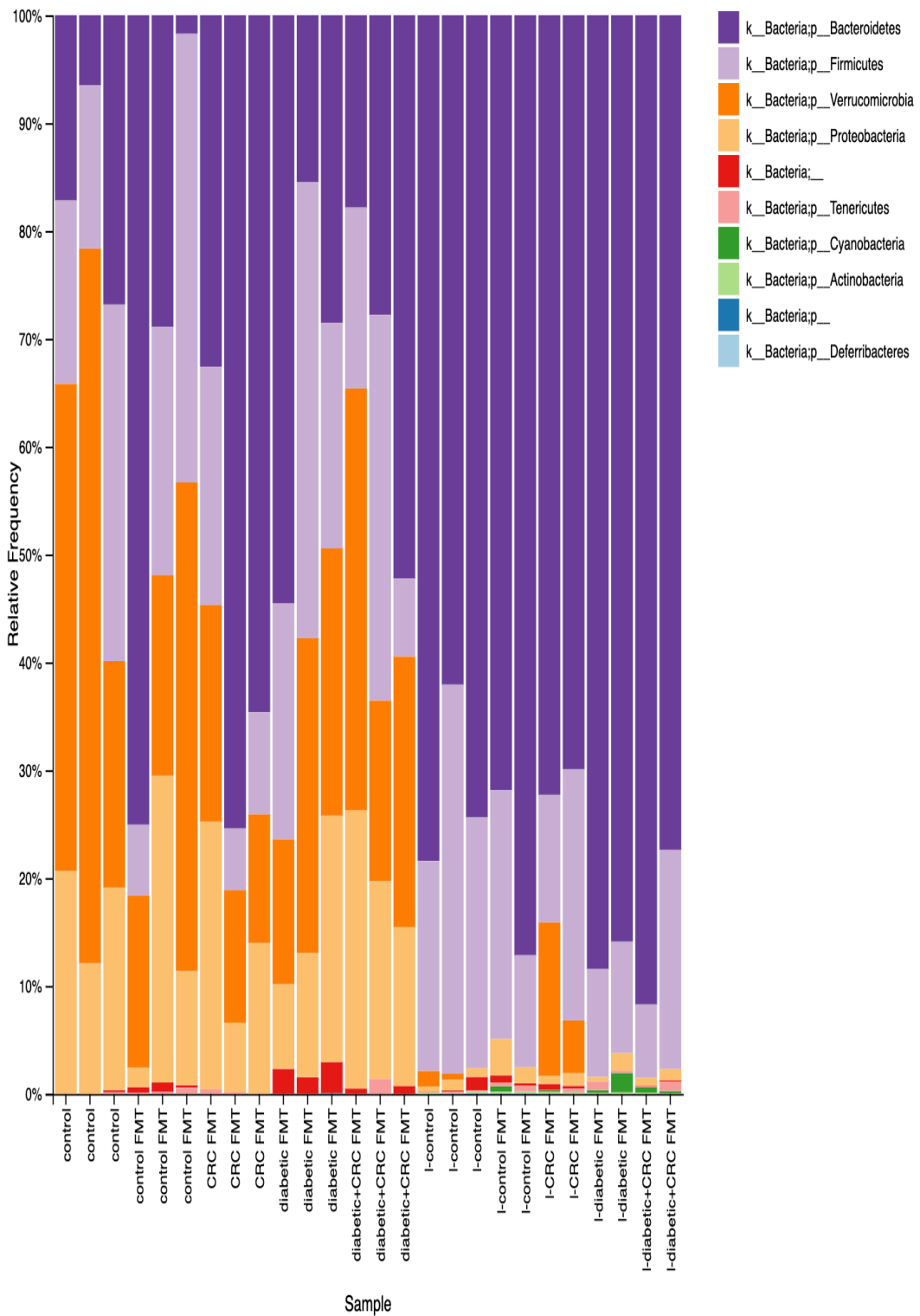


Figure 26: Different phyla per sample in antibiotic-treated mice.

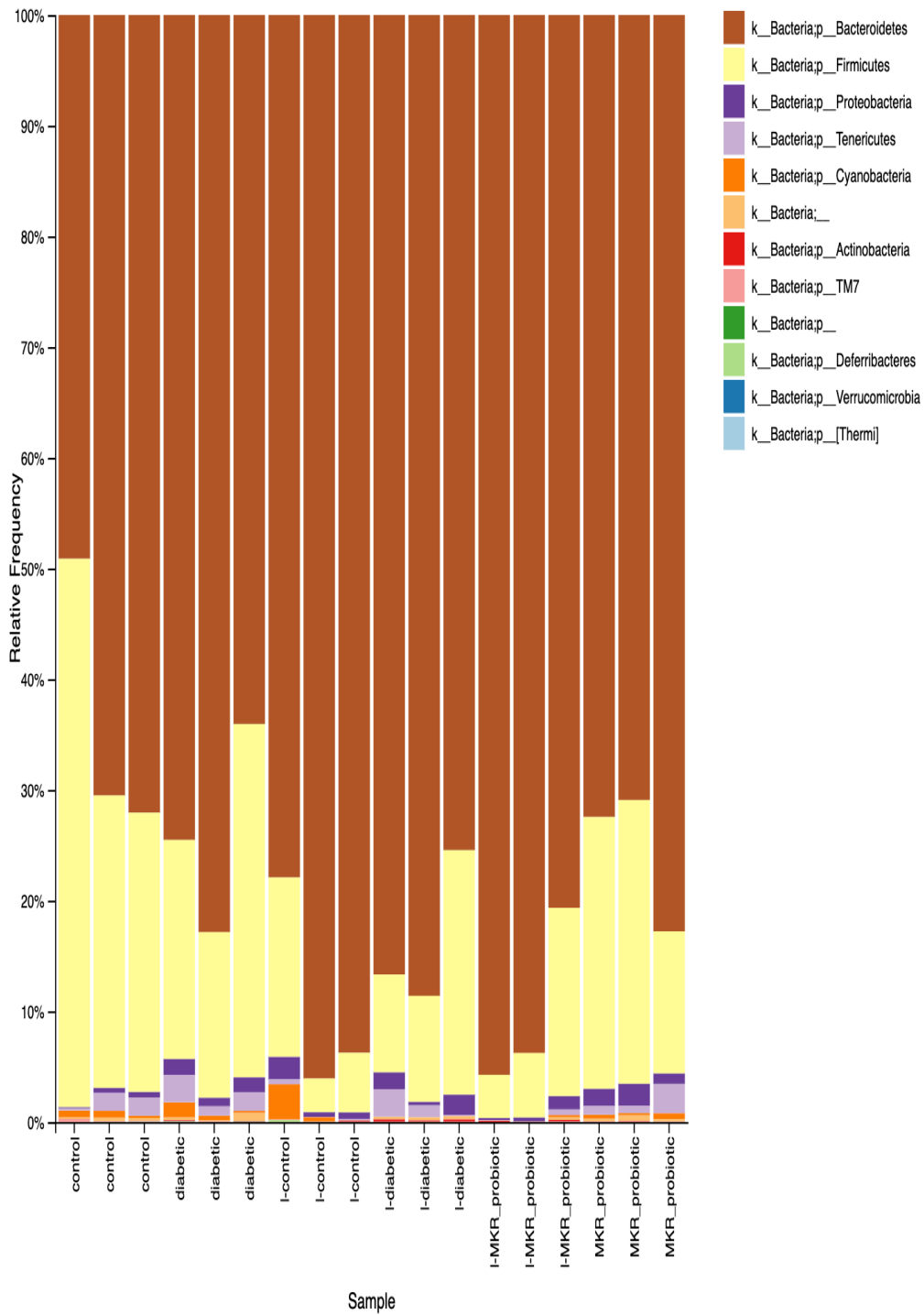


Figure 27: Different phyla per sample in control, diabetic and probiotics-treated diabetic mice.

4.7.3. Beta diversity

The complexity of microbiota makes it difficult to detect significant differences between mice groups by just observing the OTUs present in each sample. Beta diversity calculate the differences between samples while taking into account the number and type of different OTUs present in each sample. We calculated the beta diversity between our samples using the unweighted UniFrac method²⁰³ which is superior to the Bray-Curtis distance matrix as it takes the phylogenetic diversity into account.

The principal coordinate analysis (PCoA) plots cluster samples according to the calculated UniFrac matrix through unsupervised machine learning algorithm which removes any bias due to prior assignment of samples to different conditions. The PCoA plot for the control, diabetic and cancer mice at early and late time points show that the *FVB-NJ* mice are clustered together at the early time point (before induction of CRC) and the *MKR* mice are clustered together which reflects a significantly different microbial signature for diabetic mice (**Figure 28**). At the late time point, it is difficult to discern unique clusters for each condition. However, the *MKR* mice are segregated away from the control mice. Interestingly, the difference in microbial signatures between control and diabetic mice is more pronounced than that between control and CRC mice. Moreover, the segregation of the late control samples from the early control samples reflects a deleterious role for the microbiota hosted by aged mice.

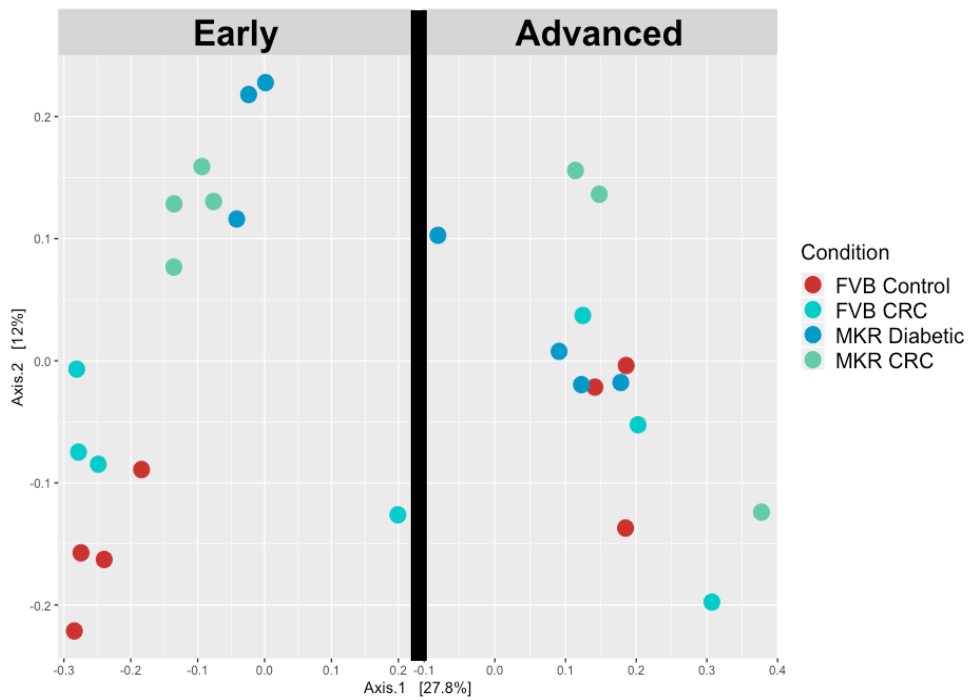


Figure 28: The principal coordinate analysis (PCoA) plot for the control, diabetic and cancer mice at early and late time points.

The PCoA plot for the antibiotic-treated mice shows a segregation between microbiota of the early and late time points (**Figure 29**). However, the segregation due to the time point is more pronounced than that between different FMTs. The plot suggests a subtle segregation between the microbiota of the control mice and mice inoculated with the control FMT from those inoculated with the diabetic or the cancer microbiota.

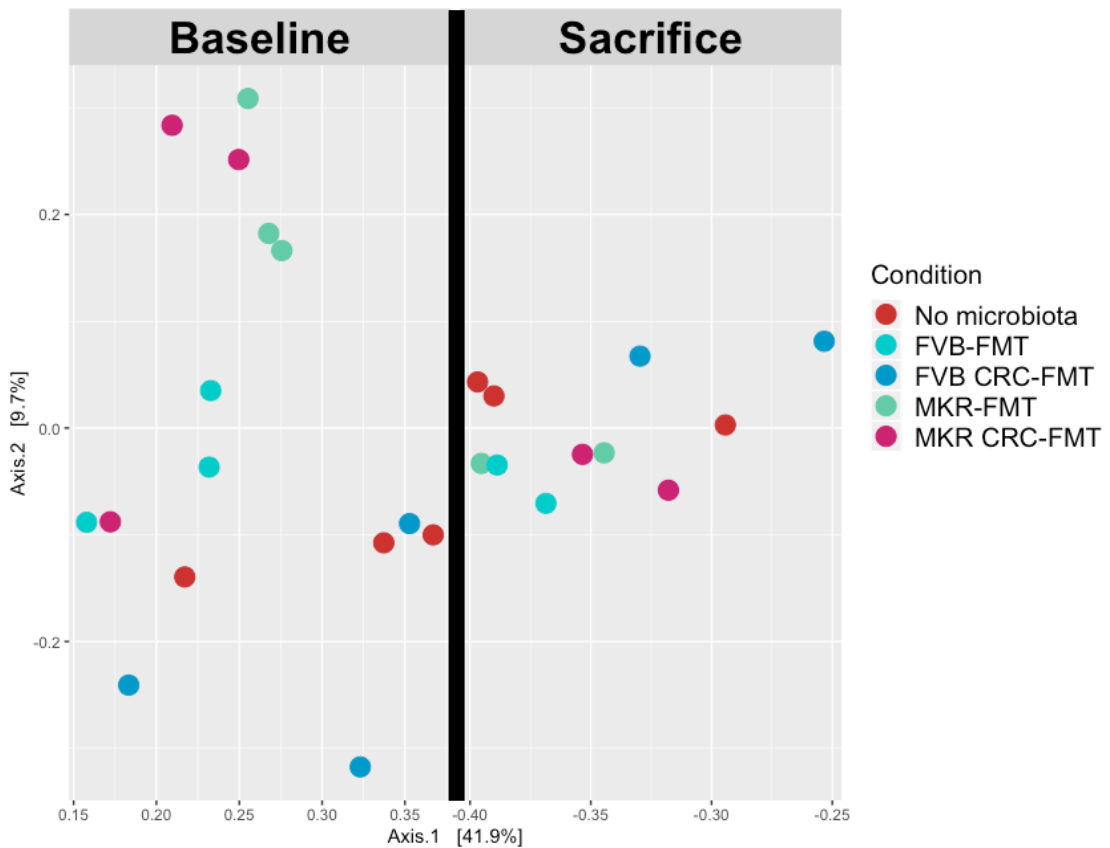


Figure 29: The principal coordinate analysis (PCoA) plot for the antibiotic-treated mice at early and late time points.

Since we suspected that the huge difference between microbiota of mice at early and late time points may have masked the differences between microbiota of mice inoculated with different FMTs, we repeated the PCoA on the samples of the late time points alone (**Figure 30**). Fortuitously, mice inoculated with the control microbiota were clustered the farthest from all other samples suggesting that microbiota of these mice are different from that of other groups. Mice inoculated with diabetic FMT were also clustered with each other while mice in other groups were scattered with overlap with each other.

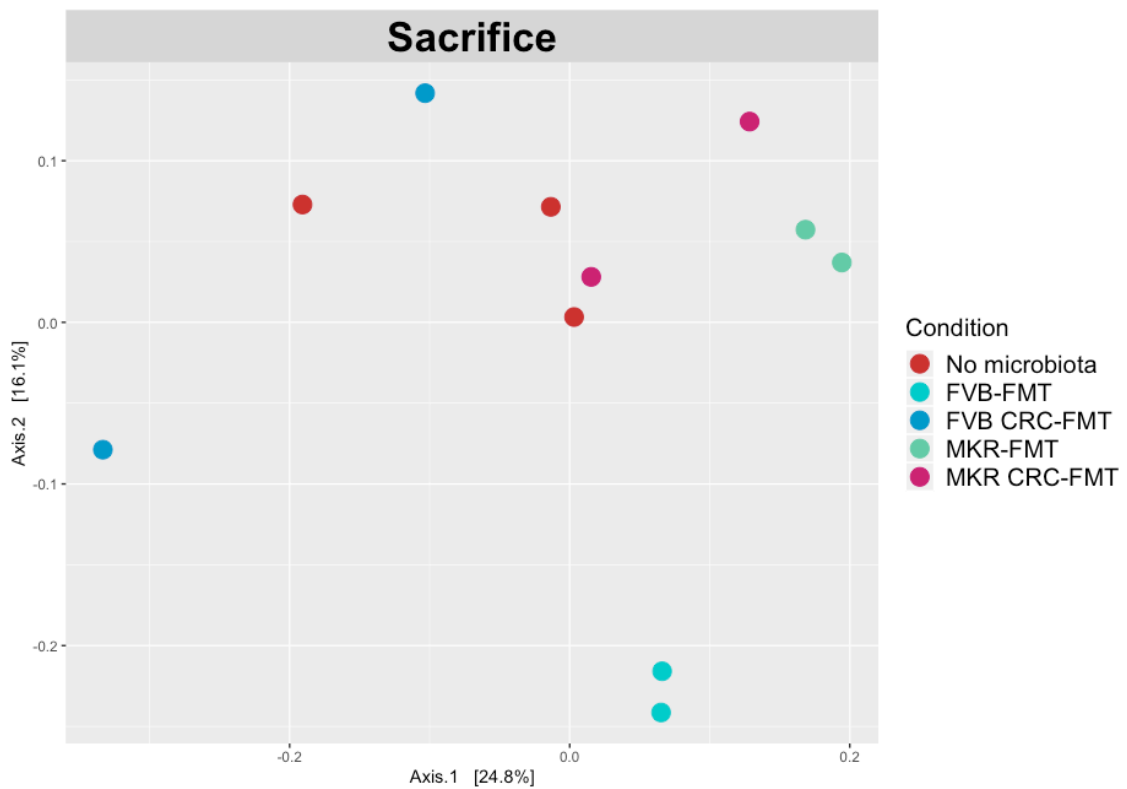


Figure 30: The principal coordinate analysis (PCoA) plot for the antibiotic-treated mice at late time point.

Finally, we performed PCoA on the probiotics-treated mice (**Figure 31**). Our results show that at the late time point, the probiotics-treated mice tend to move away from the diabetic mice cluster which suggests that probiotics succeeded in changing the diabetic microbiota to a certain extent and the new microbiota is stabilized. **Figure 32** shows the plot for the late samples alone for better resolution of clustering.

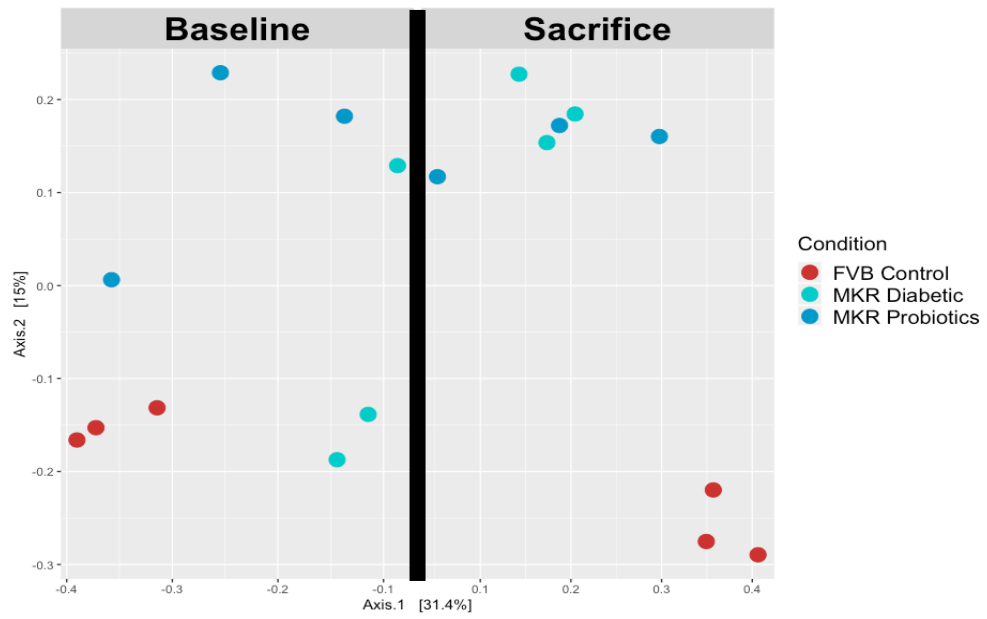


Figure 31: The principal coordinate analysis (PCoA) plot for the probiotics-treated mice at early and late time point. Note: the point for one of the late diabetic samples (1-diabetic) is plotted over another one making them appear as a single point.

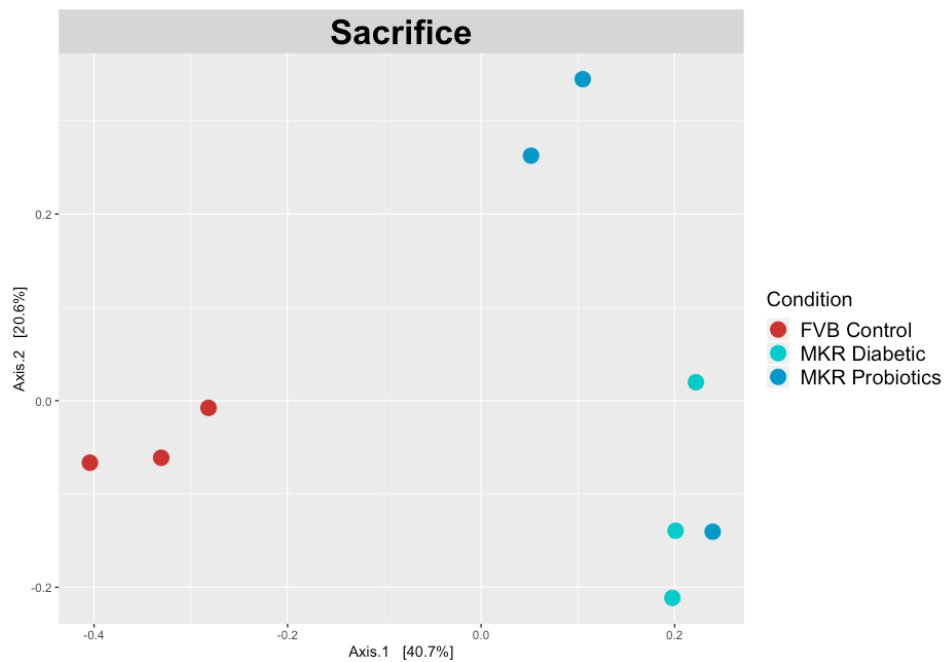


Figure 32: The principal coordinate analysis (PCoA) plot for the probiotics-treated mice at late time point.

4.7.4. Microbiota composition in control, diabetic and colorectal cancer mice

To identify the shared microbiota composition of the control, diabetic and CRC groups, we grouped the samples of each group at the late time point and performed taxonomic analysis on each group features. The most significant difference was observed in the phylum Porphyromonadaceae where the microbiota composition for the control group (**Figure 33**) is composed of 57% Porphyromonadaceae (unclassified) which is significantly higher than the 41% in *MKR* mice (**Figure 34**) or the 49% in mice with colorectal cancer (**Figure 35**). Noteworthy, the phylum Porphyromonadaceae contains many butyrate-forming bacteria ¹⁷⁴.

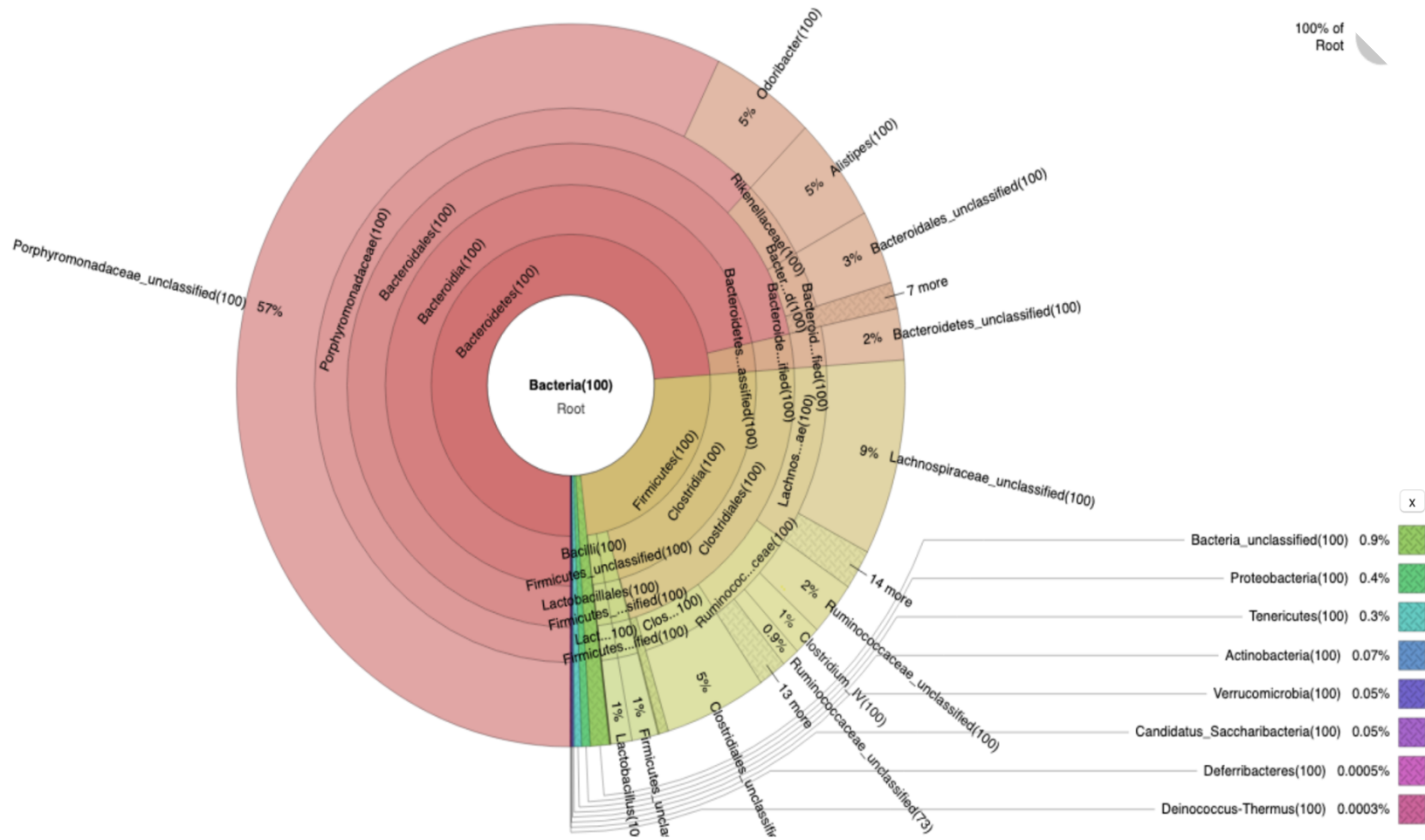


Figure 33: Microbiota composition of control *FVB-NJ* mice.



Figure 34: Microbiota composition of diabetic *MKR* mice.

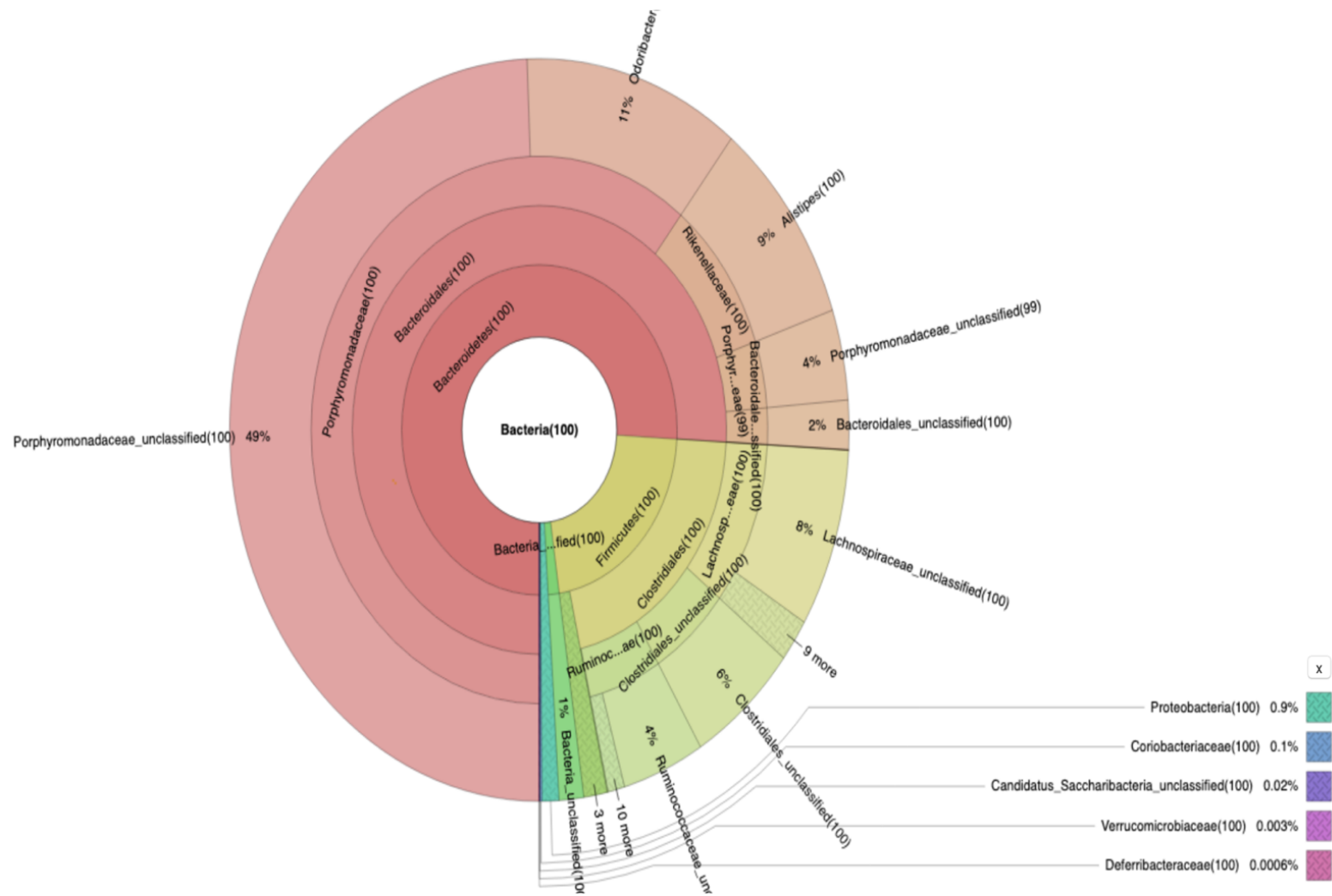


Figure 35: Microbiota composition of colorectal cancer mice.

4.7.5. Tests of significances

We used the permutational multivariate analysis of variances (PERMANOVA) test and AMOVA test to test for significance between different groups. Our results show that there is a significant difference between all the early and late time points ($p < 0.001$) suggesting that microbiota varies with age. There was also a significant difference between control, *MKR*, CRC and diabetic mice with CRC at different time points (Table 3).

Table 3: Analysis of molecular variances (AMOVA) results for significance testing between control, diabetic and colorectal cancer mice. Significant p-values are in bold

First group	Second group	p-value
All groups		0.001
Early <i>FVB</i> Control	Advanced <i>FVB</i> Control	0.005
Advanced <i>FVB</i> CRC	Advanced <i>MKR</i> Diabetic	0.014
Advanced <i>MKR</i> Diabetic	Advanced <i>MKR</i> CRC	0.022
Advanced <i>FVB</i> CRC	Early <i>MKR</i> CRC	0.024
Early <i>FVB</i> Control	Early <i>MKR</i> Diabetic	0.025
Advanced <i>FVB</i> Control	Advanced <i>MKR</i> Diabetic	0.025
Early <i>FVB</i> Control	Early <i>MKR</i> CRC	0.028
Early <i>MKR</i> Diabetic	Early <i>MKR</i> CRC	0.030
Early <i>FVB</i> CRC	Early <i>FVB</i> Control	0.033
Early <i>FVB</i> CRC	Advanced <i>FVB</i> CRC	0.051
Early <i>FVB</i> CRC	Early <i>MKR</i> Diabetic	0.056
Early <i>MKR</i> Diabetic	Advanced <i>MKR</i> Diabetic	0.059
Advanced <i>FVB</i> Control	Advanced <i>FVB</i> CRC	0.095
Advanced <i>FVB</i> Control	Advanced <i>MKR</i> CRC	0.099
Advanced <i>FVB</i> CRC	Advanced <i>MKR</i> CRC	0.106

Concerning the antibiotic-treated mice, although there was a significant difference between the early and late time points, there was no significant difference for the collective microbial signature between different groups. This finding is most probably due to the short duration of the FMT experiment which succeeded in changing the microbiota but not to the extent that can be detected by AMOVA stringent test.

Finally, in the probiotics-treated mice, there was a significant difference in the probiotics-treated group and the diabetic group at the late time point ($p < 0.003$). Similar to the previous 2 experiments, there was a significant difference between the microbiota at the early and late time points.

4.7.6. Analysis of composition of microbiome (ANCOM)

We used the ANCOM tool to identify the phyla that are responsible for the significant differences between groups. We chose ANCOM because it can reduce false discoveries in detecting differentially abundant taxa by accounting for compositional constraints while maintaining high statistical power²⁰⁴. Our analysis shows that Verrucomicrobia is the most significant phylum responsible for the segregation of control, diabetic and cancer groups at early and late time points (**Figure 36**).

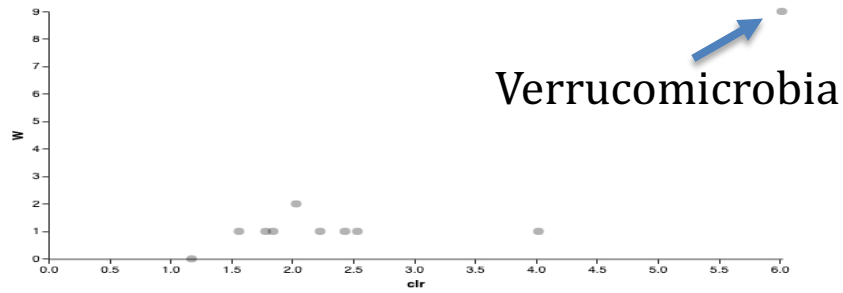


Figure 36: Volcano blot of analysis of microbial composition of control, diabetic and colorectal cancer mice.

The volcano blot for the ANCOM of the antibiotic-treated mice showed that Proteobacteria, Verrucomicrobia and Cyanobacteria are the most responsible phyla for the differentiation between FMT inoculated groups (**Figure 37**).

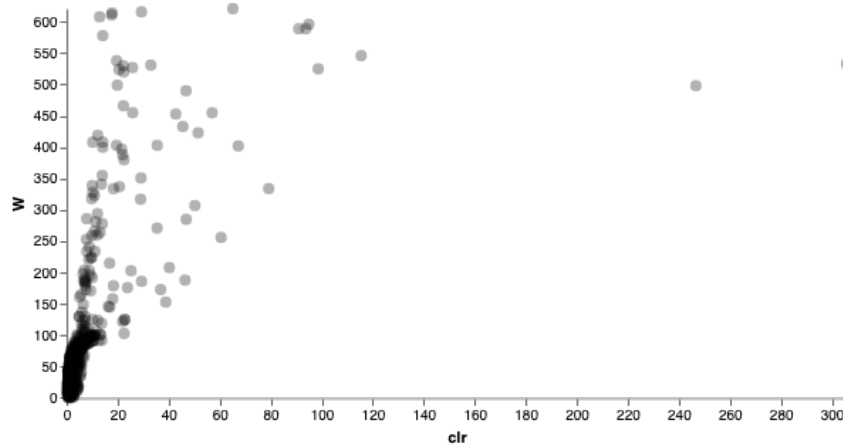


Figure 37: Volcano blot of analysis of microbial composition of antibiotic-treated mice.

For the probiotics-treated mice, once again Verrucomicrobia and Proteobacteria are the most significant phyla dissociating control, diabetic and probiotics-treated groups at early and late time points (**Figure 38**).

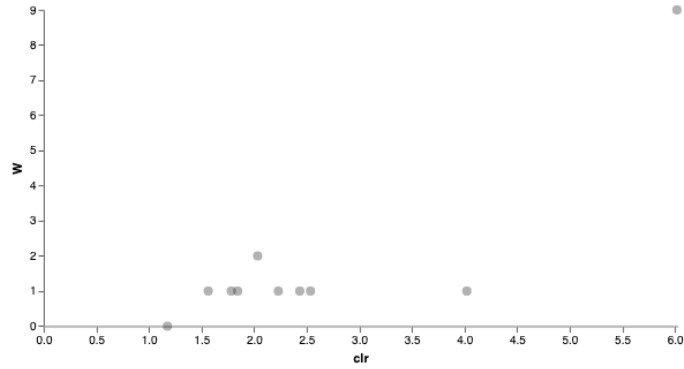


Figure 38: Volcano blot of analysis of microbial composition of control, diabetic and probiotics-treated mice.

4.7.7. Significantly characteristic bacteria in each group

We used the LEfSe (Linear discriminant analysis effect size) tool ²⁰⁵ to find the significantly characteristic bacteria for each group on the species level. **Table 4** includes the top 3 most characteristic bacteria in each group that distinguishes it from other groups.

Table 4: Significantly characteristic bacteria in each mice group.

A. Characteristic bacteria per group in control, diabetic, colorectal cancer mice at early time point.		
Group	pValue	Taxonomy
Control	0.00623	Bacteria(100);Firmicutes(100);Clostridia(100);Clostridia_unclassified(100);Clostridia_unclassified(100);Clostridia_unclassified(100);
	0.006409	Bacteria(100);Bacteroidetes(100);Bacteroidia(100);Bacteroidales(100);Porphyromonadaceae(100);Porphyromonadaceae_unclassified(100);
	0.007927	Bacteria(100);Bacteroidetes(100);Bacteroidetes_unclassified(100);Bacteroidetes_unclassified(100);Bacteroidetes_unclassified(100);Bacteroidetes_unclassified(100);
Colorectal cancer	0.003523	Bacteria(100);Firmicutes(100);Clostridia(100);Clostridiales(100);Lachnospiraceae(100);Lachnospiraceae_unclassified(100);

	0.003523	Bacteria(100);Firmicutes(100);Firmicutes_unclassified(100);Firmicutes_unclassified(100);Firmicutes_unclassified(100);Firmicutes_unclassified(100);
	0.015094	Bacteria(100);Firmicutes(100);Clostridia(100);Clostridiales(100);Clostridiales_unclassified(94);Clostridiales_unclassified(94);
Diabetic	0.003197	Bacteria(100);Firmicutes(100);Firmicutes_unclassified(100);Firmicutes_unclassified(100);Firmicutes_unclassified(100);Firmicutes_unclassified(100);
	0.00543	Bacteria(100);Firmicutes(100);Clostridia(100);Clostridiales(100);Clostridiales_unclassified(100);Clostridiales_unclassified(100);
	0.005882	Bacteria(100);Firmicutes(100);Clostridia(100);Clostridiales(100);Clostridiales_unclassified(100);Clostridiales_unclassified(100);
Diabetic and colorectal cancer	0.006605	Bacteria(100);Bacteroidetes(100);Bacteroidia(100);Bacteroidales(100);Porphyromonadaceae(100);Porphyromonadaceae_unclassified(100);
	0.008063	Bacteria(100);Bacteroidetes(100);Bacteroidia(100);Bacteroidales(100);Rikenellaceae(100);Alistipes(100);
	0.008653	Bacteria(100);Bacteroidetes(100);Bacteroidia(100);Bacteroidales(100);Porphyromonadaceae(100);Porphyromonadaceae_unclassified(100);
B. Characteristic bacteria per group in control, diabetic, colorectal cancer mice at late time point.		
Group	pValue	Taxonomy
Control	0.017414	Bacteria(100);Bacteroidetes(100);Bacteroidia(100);Bacteroidales(100);Porphyromonadaceae(100);Porphyromonadaceae_unclassified(100);
	0.019453	Bacteria(100);Bacteroidetes(100);Bacteroidia(100);Bacteroidales(100);Porphyromonadaceae(100);Porphyromonadaceae_unclassified(100);
	0.020628	Bacteria(100);Firmicutes(100);Clostridia(100);Clostridiales(100);Clostridiales_unclassified(100);Clostridiales_unclassified(100);
Colorectal cancer	0.007677	Bacteria(100);Firmicutes(100);Clostridia(100);Clostridiales(100);Clostridiales_unclassified(100);Clostridiales_unclassified(100);
	0.007677	Bacteria(100);Firmicutes(100);Clostridia(100);Clostridiales(100);Ruminococcaceae(100);Ruminococcaceae_unclassified(100);

	0.030339	Bacteria(100);Firmicutes(100);Clostridia(100);Clostridiales(100);Ruminococcaceae(100);Ruminococcaceae_unclassified(100);
Diabetic	0.024927	Bacteria(100);Firmicutes(100);Clostridia(100);Clostridiales(100);Clostridiales_unclassified(100);Clostridiales_unclassified(100);
	0.033717	Bacteria(100);Firmicutes(100);Bacilli(100);Lactobacillales(100);Lactobacillaceae(100);Lactobacillus(100);
	0.038058	Bacteria(100);Firmicutes(100);Clostridia(100);Clostridiales(100);Clostridiales_unclassified(100);Clostridiales_unclassified(100);
Diabetic and colorectal cancer	0.008037	Bacteria(100);Firmicutes(100);Clostridia(100);Clostridiales(100);Lachnospiraceae(100);Dorea(100);
	0.008261	Bacteria(100);Bacteroidetes(100);Bacteroidia(100);Bacteroidales(100);Porphyromonadaceae(100);Porphyromonadaceae_unclassified(100);
	0.008261	Bacteria(100);Firmicutes(100);Clostridia(100);Clostridiales(100);Ruminococcaceae(100);Ruminococcaceae_unclassified(100);
C. Characteristic bacteria per group in antibiotic-treated mice at early time point.		
Group	pValue	Taxonomy
Control FMT	0.01129	Bacteria(100);Firmicutes(100);Firmicutes_unclassified(100);Firmicutes_unclassified(100);Firmicutes_unclassified(100);Firmicutes_unclassified(100);
	0.018433	Bacteria(100);Firmicutes(100);Firmicutes_unclassified(100);Firmicutes_unclassified(100);Firmicutes_unclassified(100);Firmicutes_unclassified(100);
	0.033752	Bacteria(100);Firmicutes(100);Clostridia(100);Clostridiales(100);Clostridiales_unclassified(100);Clostridiales_unclassified(100);
Diabetic FMT	0.014335	Bacteria(100);Bacteria_unclassified(100);Bacteria_unclassified(100);Bacteria_unclassified(100);Bacteria_unclassified(100);
	0.02001	Bacteria(100);Bacteria_unclassified(100);Bacteria_unclassified(100);Bacteria_unclassified(100);Bacteria_unclassified(100);
	0.021061	Bacteria(100);Firmicutes(100);Firmicutes_unclassified(100);Firmicutes_unclassified(100);Firmicutes_unclassified(100);Firmicutes_unclassified(100);
Diabetic and	0.016267	Bacteria(100);Firmicutes(100);Clostridia(100);Clostridiales(100);Lachnospiraceae(100);Lachnospiraceae_unclassified(100);

cancer FMT	0.020608	Bacteria(100);Firmicutes(100);Clostridia(100);Clostridiales(100);Ruminococcaceae(100);Ruminococcaceae_unclassified(100);
	0.04177	Bacteria(100);Firmicutes(100);Bacilli(100);Lactobacillales(100);Lactobacillaceae(100);Lactobacillus(100);
D. Characteristic bacteria per group in antibiotic-treated mice at late time point.		
Group	pValue	Taxonomy
Control FMT	0.01129	Bacteria(100);Firmicutes(100);Firmicutes_unclassified(100);Firmicutes_unclassified(100);Firmicutes_unclassified(100);Firmicutes_unclassified(100);
	0.018433	Bacteria(100);Firmicutes(100);Firmicutes_unclassified(100);Firmicutes_unclassified(100);Firmicutes_unclassified(100);Firmicutes_unclassified(100);
	0.033752	Bacteria(100);Firmicutes(100);Clostridia(100);Clostridiales(100);Clostridiales_unclassified(100);Clostridiales_unclassified(100);
Diabetic FMT	0.014335	Bacteria(100);Bacteria_unclassified(100);Bacteria_unclassified(100);Bacteria_unclassified(100);Bacteria_unclassified(100);
	0.02001	Bacteria(100);Bacteria_unclassified(100);Bacteria_unclassified(100);Bacteria_unclassified(100);Bacteria_unclassified(100);
	0.021061	Bacteria(100);Firmicutes(100);Firmicutes_unclassified(100);Firmicutes_unclassified(100);Firmicutes_unclassified(100);Firmicutes_unclassified(100);
Diabetic and cancer FMT	0.016267	Bacteria(100);Firmicutes(100);Clostridia(100);Clostridiales(100);Lachnospiraceae(100);Lachnospiraceae_unclassified(100);
	0.020608	Bacteria(100);Firmicutes(100);Clostridia(100);Clostridiales(100);Ruminococcaceae(100);Ruminococcaceae_unclassified(100);
	0.04177	Bacteria(100);Firmicutes(100);Bacilli(100);Lactobacillales(100);Lactobacillaceae(100);Lactobacillus(100);
E. Characteristic bacteria per group in probiotics-treated mice at early time point.		
Group	pValue	Taxonomy
Control	0.008261	Bacteria(100);Bacteria_unclassified(100);Bacteria_unclassified(100);Bacteria_unclassified(100);Bacteria_unclassified(100);
	0.008261	Bacteria(100);Bacteroidetes(100);Bacteroidia(100);Bacteroidales(100);Porphyromonadaceae(100);Porphyromonadaceae_unclassified(100);

	0.008261	Bacteria(100);Bacteroidetes(100);Bacteroidia(100);Bacteroidales(100);Bacteroidales_unclassified(100);Bacteroidales_unclassified(100);
Diabetic	0.020777	Bacteria(100);Bacteroidetes(100);Bacteroidia(100);Bacteroidales(100);Bacteroidaceae(100);Bacteroides(100);
	0.027288	Bacteria(100);Firmicutes(100);Clostridia(100);Clostridiales(100);Lachnospiraceae(100);Lachnospiraceae_unclassified(100);
	0.03157	Bacteria(100);Bacteria_unclassified(100);Bacteria_unclassified(100);Bacteria_unclassified(100);Bacteria_unclassified(100);
Probiotics-treated	0.024902	Bacteria(100);Firmicutes(100);Clostridia(100);Clostridiales(100);Ruminococcaceae(100);Ruminococcaceae_unclassified(99);
	0.046942	Bacteria(100);Bacteroidetes(100);Bacteroidia(100);Bacteroidales(100);Porphyromonadaceae(100);Porphyromonadaceae_unclassified(100);
F. Characteristic bacteria per group in probiotics-treated mice at late time point.		
Group	pValue	Taxonomy
Control	0.022125	Bacteria(100);Bacteroidetes(100);Bacteroidia(100);Bacteroidales(100);Bacteroidaceae(100);Bacteroides(100);
	0.027324	Bacteria(100);Bacteroidetes(100);Bacteroidia(100);Bacteroidales(100);Bacteroidales_unclassified(100);Bacteroidales_unclassified(100);
	0.033576	Bacteria(100);Firmicutes(100);Clostridia(100);Clostridiales(100);Clostridiales_unclassified(70);Clostridiales_unclassified(70);
Diabetic	0.022125	Bacteria(100);Bacteroidetes(100);Bacteroidia(100);Bacteroidales(100);Porphyromonadaceae(100);Porphyromonadaceae_unclassified(100);
	0.022125	Bacteria(100);Bacteroidetes(100);Bacteroidia(100);Bacteroidales(100);Rikenellaceae(100);Alistipes(100);
	0.024134	Bacteria(100);Bacteroidetes(100);Bacteroidetes_unclassified(100);Bacteroidetes_unclassified(100);Bacteroidetes_unclassified(100);
Probiotics-treated	0.022125	Bacteria(100);Firmicutes(100);Bacilli(100);Lactobacillales(100);Lactobacillaceae(100);Lactobacillus(100);
	0.022125	Bacteria(100);Bacteroidetes(100);Bacteroidia(100);Bacteroidales(100);Rikenellaceae(100);Alistipes(100);

	0.024134	Bacteria(100);Bacteroidetes(100);Bacteroidia(100);Bacteroidales(100);Porphyromonadaceae(100);Porphyromonadaceae_unclassified(100);
--	----------	--

4.8. Diabetes is coupled to a decrease in Cecal and fecal butyrate content, a higher activity of the colon HDAC3 and alteration of inflammatory cytokines

Since T2DM is correlated with less abundance of butyrate-forming bacterial population, we measured the cecal and fecal butyrate contents of *MKR* and *FVB-NJ* control mice. Both cecal and fecal butyrate contents were significantly lower in *MKR* mice (**Figure 39a**), correlating with their reduced content of the butyrate-forming bacteria.

One of the main biological actions of butyrate is its role as an HDAC inhibitor. As *MKR* diabetic mice showed less abundance of butyrate, we assessed the activity of HDAC3 in colon tissues. As expected, *MKR* mice had higher HDAC3 activity compared to their control littermates (**Figure 39b**). Likewise, we assessed the activity of HAT, and our results show no significant differences between the activities of HAT of *MKR* mice when compared to that of their control littermates suggesting that butyrate affects HDAC3 without inhibiting HAT (**Figure 39b**).

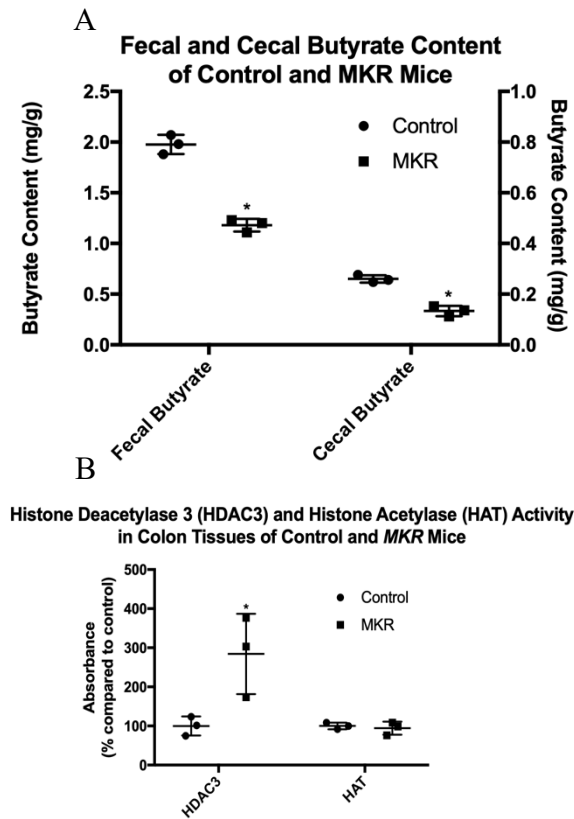


Figure 39: Butyrate content and its downstream molecular effects in *MKR* and control mice (n=3). Data are expressed as mean \pm standard deviation (SD). * statistically significant at $p < 0.05$ vs control.

4.9. Diabetes causes alteration of inflammatory cytokines and increases expression of IL-1 β

It is thought that dysbiosis in DM plays a key role in the alteration of the inflammatory state^{43,206,207}. Likewise, butyrate-forming bacteria, showed to be altered in our diabetic model, may affect the host immunity and the inflammatory state. For that, we assessed the levels of circulatory cytokines in plasma of *MKR* and control mice. Our results show that the levels of the anti-inflammatory cytokine IL-10 and the pro-inflammatory IL-17 α are significantly lower in *MKR* mice when compared to their control littermates (**Figure 40a**). Moreover, the plasma levels of IL-12, TNF- α and G-

CSF did not show any significant difference between the two groups (**Figure 40a**). In parallel, the protein expression of IL-1 β , which is the major cytokine involved in diabetic pathogenesis and diabetic complications²⁰⁸⁻²¹² in colon tissue of *MKR* mice was significantly upregulated when compared to control mice. Of interest, treatment with sodium butyrate restored back the homeostatic levels of IL-1 β (**Figure 40b**). Taken together, these results highlight the implication of the butyrate-forming bacteria in the diabetes-induced inflammatory state modification.

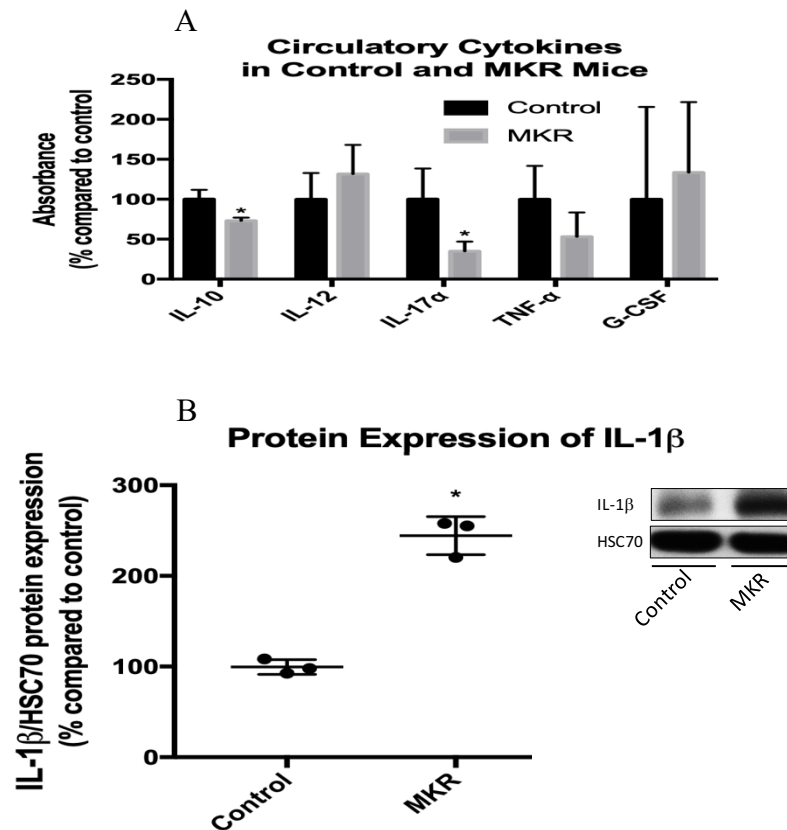


Figure 40: Diabetes causes alteration of inflammatory cytokines and increases expression of IL-1 β (n=3). Data are expressed as mean \pm standard deviation (SD). * statistically significant at $p < 0.05$ vs control.

4.10. Butyrate treatment reverse diabetes-induced ROS production and NADPH oxidase 4 protein expression

Diabetes is described to be associated with increased NADPH oxidases-induced reactive oxygen species production^{128–130,188,213}. As expected, ROS levels were increased in the colon of the *MKR* mice, and this was correlated with increased NOX4 protein expression (**Figure 41a,b**). Importantly, treatment with butyrate reversed the increase in ROS production and reduces NOX4 protein expression (**Figure 41**). Taken together, these results suggest that diabetes-induce dysbiosis is associated with an alteration in ROS production through an upregulation of NOX4 in colon tissue.

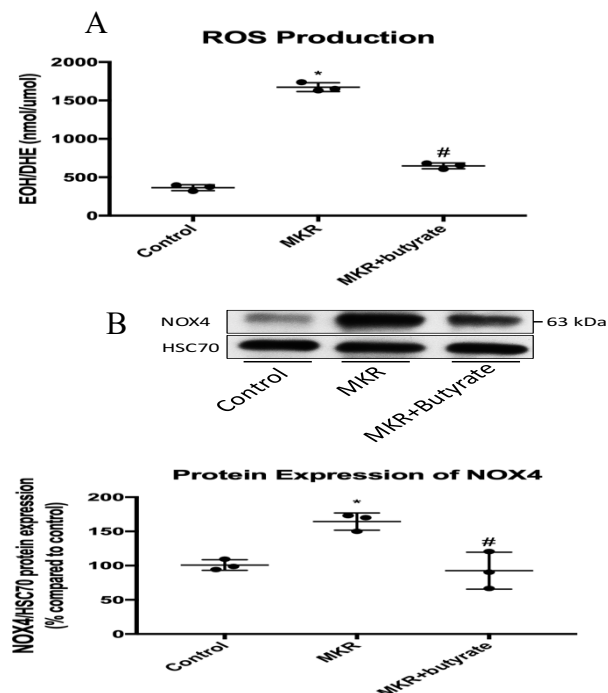


Figure 41: Reactive oxygen species (ROS) production and protein expression of NADPH oxidase (NOX4) in *MKR* and control mice groups (n=3). Data are expressed as mean \pm standard deviation (SD). * statistically significant at $p < 0.05$ vs control. # statistically significant at $p < 0.05$ vs *MKR* diabetic mice. NOX: NADPH oxidase.

4.11. Diabetes and colorectal cancer increase the expression of IL-1 β and NOX4

We measured the protein expression of both IL-1 β and NOX4 in colon tissues of control, diabetic, CRC mice and diabetic mice with CRC. We found that the expressions of both proteins were increased due to cancer and diabetes compared to those of control mice (**Figure 42 and Figure 43**). Of note, there were no significant differences between the expression of both proteins between the cancer and diabetic groups.

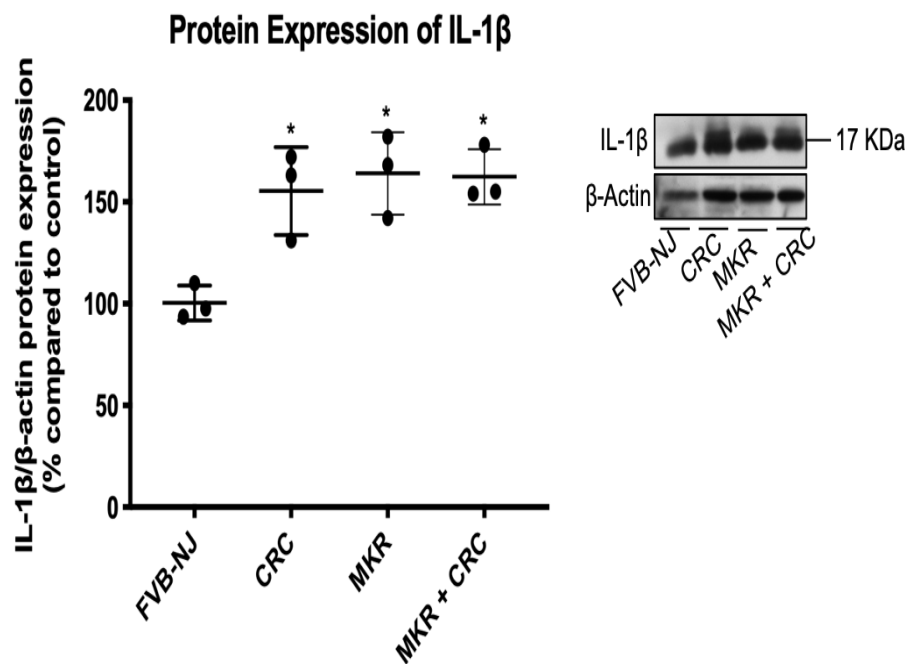


Figure 42: Protein expression of IL-1 β in colorectal cancer (CRC), *MKR* and control mice groups (n=3). Data are expressed as mean \pm standard deviation (SD). * statistically significant at $p < 0.05$ vs control. CRC: colorectal cancer.

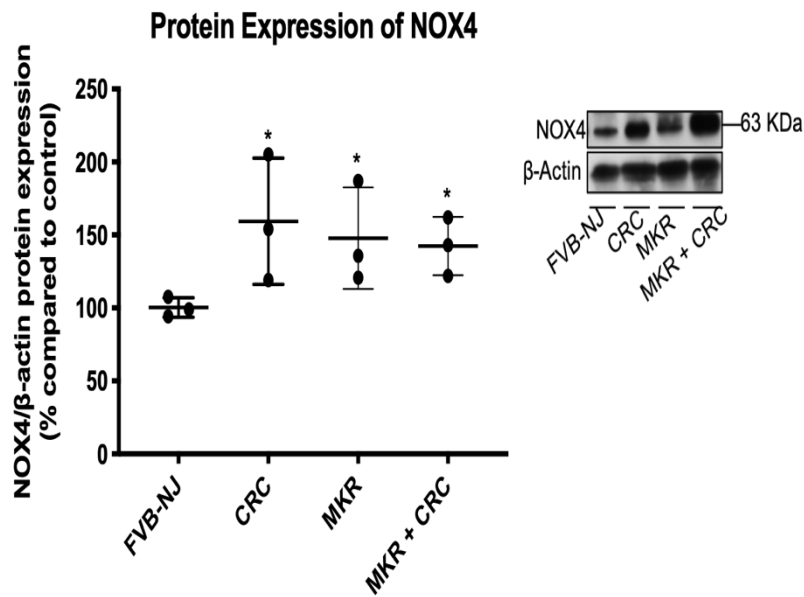


Figure 43: Protein expression of NADPH oxidase (NOX4) in colorectal cancer (CRC), *MKR* and control mice groups (n=3). Data are expressed as mean \pm standard deviation (SD). * statistically significant at $p < 0.05$ vs control. CRC: colorectal cancer, NOX: NADPH oxidase.

4.12. Effect of FMT on the expression of IL-1 β and NOX4

We investigated the effect of different fecal microbial transplants on the expression levels of both IL-1 β and NOX4 proteins. Our results show that the expressions of IL-1 β (**Figure 44**) or NOX4 (**Figure 45**) were not significantly different between the different groups. We owe this finding to the fact that CRC was chemically induced in all these animals following the FMT. The co-occurrence of CRC may have masked the effects of FMT on the expression levels of IL-1 β or NOX4.

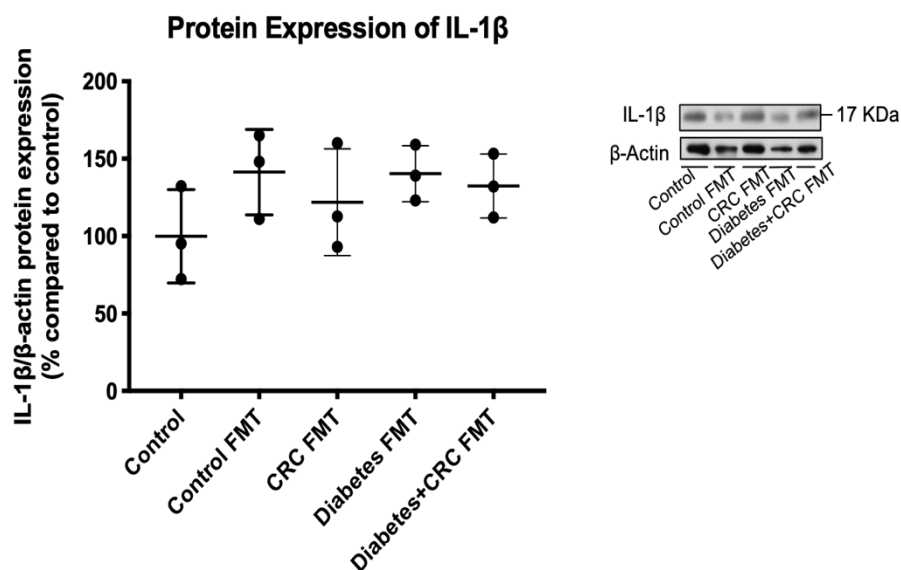


Figure 44: Protein expression of IL-1 β in mice groups inoculated with fecal microbial transplants (n=3). Data are expressed as mean \pm standard deviation (SD). CRC: colorectal cancer, FMT: fecal microbial transplant.

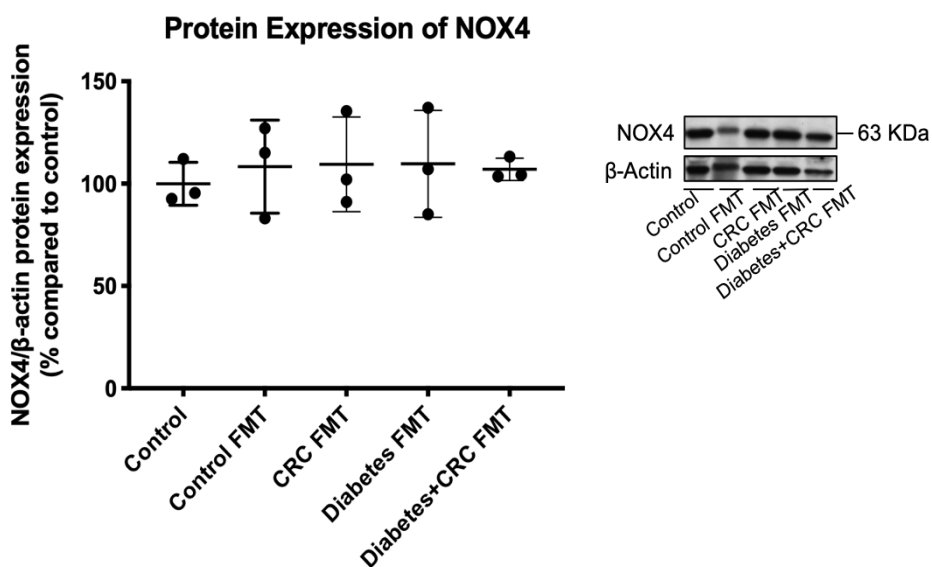


Figure 45: Protein expression of NOX4 in mice groups inoculated with fecal microbial transplants (n=3). Data are expressed as mean \pm standard deviation (SD). CRC: colorectal cancer, FMT: fecal microbial transplant.

4.13. NADPH oxidase 4 protein expression is under control of HDAC 3

Previous data from the literature suggests that the expression of NOX4 is under strong epigenetic regulation by HDAC3²¹⁴. To investigate if the reduction of NOX4 protein expression observed with butyrate treatment was the result of HDAC3 inhibition, primary cultures of colon tissues extracted from the control mice were incubated with either normal glucose NG (5 mM), high glucose (25 mM) in the presence or absence of sodium butyrate (4 mM), high glucose with the presence or absence of TSA (an HDAC specific inhibitor; 0.5 μ M), or with high glucose with the presence or absence of a combination of butyrate and TSA. After 48 hours of incubation, our results show that cells exposed to high glucose had an increased expression of NOX4, mimicking the observed upregulation of NOX4 in the diabetic mice. Importantly, NOX4 overexpression was reversed when the incubated cells with high glucose were treated with butyrate or TSA. Of interest, the combination of TSA and butyrate did not show any additive effect on NOX4 expression when compared to the monotherapy treatment. These results suggest that butyrate effect is mediated by HDAC inhibition (**Figure 46**).

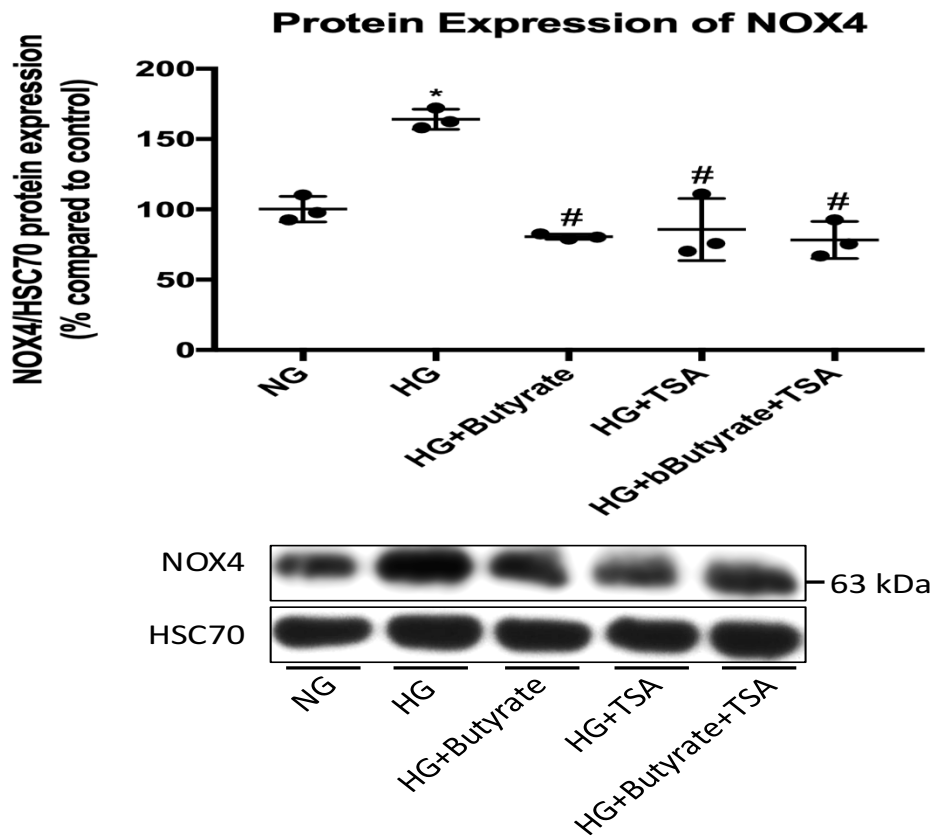


Figure 46: protein expression of NADPH oxidase (NOX4) in primary culture of colon tissue. Data are expressed as mean \pm standard deviation (SD). * statistically significant at $p < 0.05$ vs control. # statistically significant at $p < 0.05$ vs HG. HG: high glucose, NG: normal glucose, NOX: NADPH oxidase, TSA: Trichostatin A.

4.14. Butyrate reverses GI disturbance and molecular changes observed in diabetes

To investigate the beneficial effect of butyrate in reversing the GI changes observed in diabetes, we treated a subset of *MKR* with 20 mg/kg IP butyrate for 8 weeks. Butyrate treatment had no effect on body weight, blood glucose levels or HbA_{1c}% (**Figure 47a-c**) while it preserved a normal colon length in treated mice compared to the untreated littermates (**Figure 47d**).

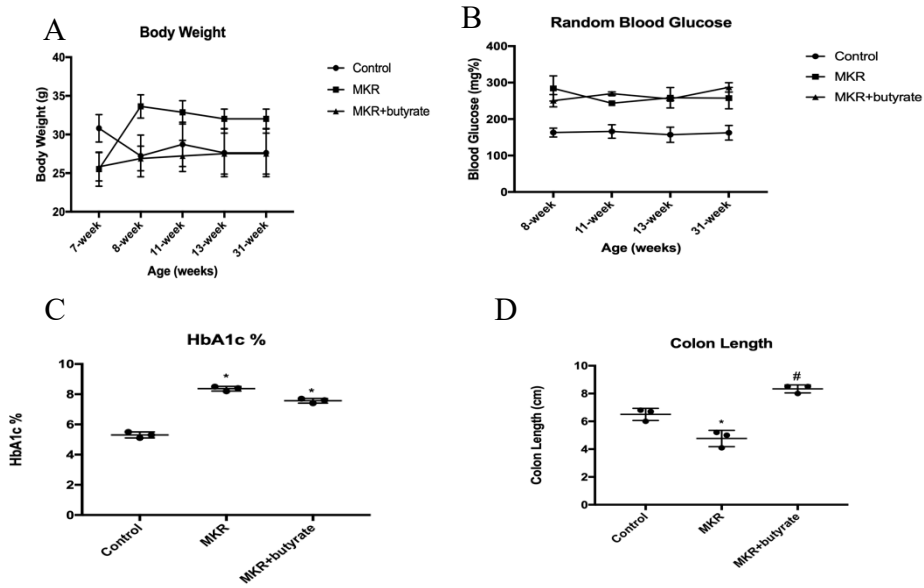


Figure 47: Body weight, random blood glucose, HbA_{1c}% and colon lengths of *MKR* and control mice (n≥3). A subset of *MKR* diabetic mice were treated with butyrate (20 mg/kg) interperitoneally for 8 weeks (from week 23 till week 31). Data are expressed as mean ± standard deviation (SD). * statistically significant at p<0.05 vs control. # statistically significant at p<0.05 vs *MKR* diabetic mice.

Additionally, butyrate prevented the overexpression of IL-1β (**Figure 48**) and NOX4 and resulted in lower ROS production (**Figure 41a,b**).

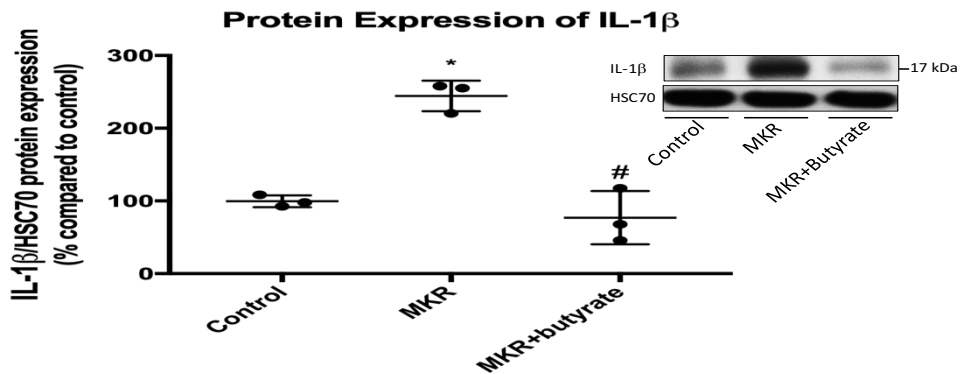


Figure 48: Butyrate rectifies the overexpression of IL-1β due to diabetes (n=3). Data are expressed as mean ± standard deviation (SD). * statistically significant at p<0.05 vs control. # statistically significant at p<0.05 vs *MKR* diabetic mice.

4.15. Probiotics reverses GI disturbance and molecular changes observed in diabetes and ameliorates CRC

To investigate the beneficial effect of probiotics in reversing the GI changes observed in diabetes, we treated a subset of *MKR* with once daily dose of 5 mg/kg of ProbioLife probiotics given by oral gavage for 8 weeks. Probiotics preserved a normal colon length in treated mice compared to the untreated littermates (**Figure 49a**). Furthermore, probiotics treatment decreased the production of ROS in *MKR* mice (**Figure 49b**).

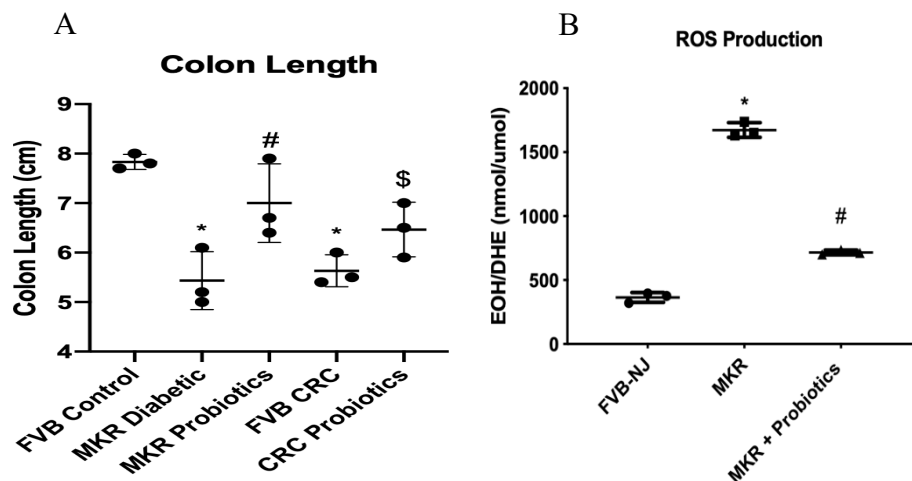


Figure 49: Colon Lengths and ROS production in colon tissues. Results are expressed as mean + SEM. * significantly different from *FVB-NJ* control mice at $p < 0.05$. # Significantly different from *MKR* mice at $p < 0.05$. \$ statistically significant at $p < 0.05$ vs *FVB CRC*.

Moreover, probiotics protected *MKR* mice from the overexpression of IL-1 β (**Figure 50**) and NOX4 proteins (**Figure 52**). Likewise, *FVB CRC* mice treated with probiotics had lower protein expression of both IL-1 β (**Figure 51**) and NOX4 proteins (**Figure 53**).

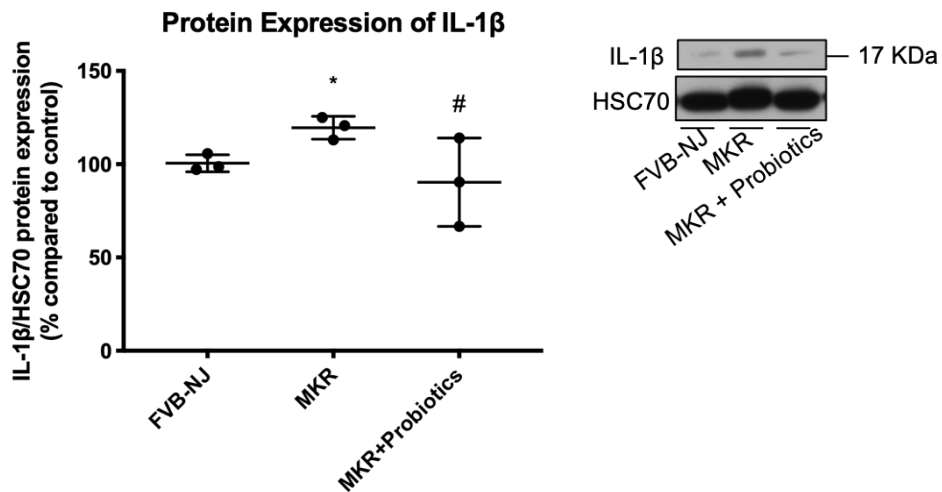


Figure 50: Probiotics protects against the overexpression of IL-1 β caused by diabetes (n=3). Data are expressed as mean \pm standard deviation (SD). * statistically significant at $p < 0.05$ vs control. # statistically significant at $p < 0.05$ vs *MKR* diabetic mice.

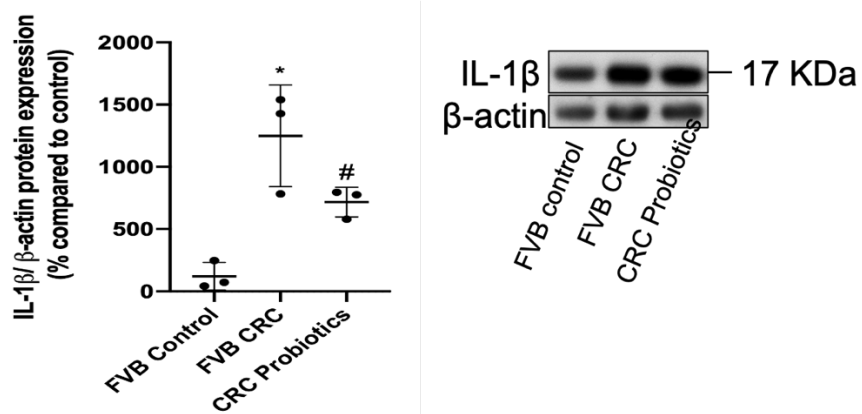


Figure 51: Probiotics protects against the overexpression of IL-1 β caused by colorectal cancer (n=3). Data are expressed as mean \pm standard deviation (SD). * statistically significant at $p < 0.05$ vs control. # statistically significant at $p < 0.05$ vs *FVB CRC* mice.

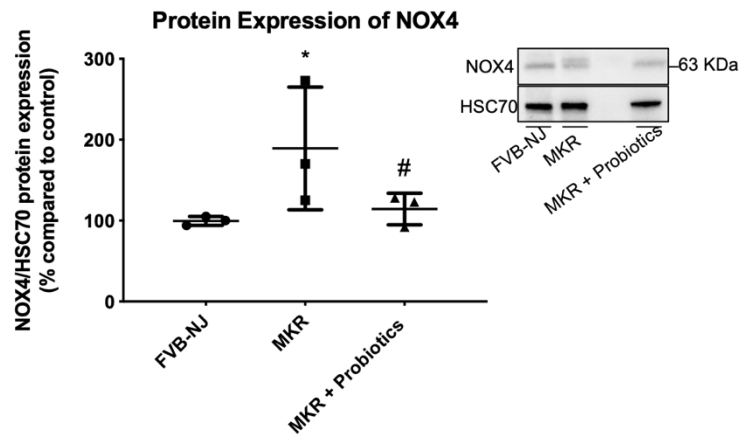


Figure 52: Probiotics protects against the overexpression of NOX4 caused by diabetes (n=3). Data are expressed as mean \pm standard deviation (SD). * statistically significant at $p < 0.05$ vs control. # statistically significant at $p < 0.05$ vs *MKR* diabetic mice.

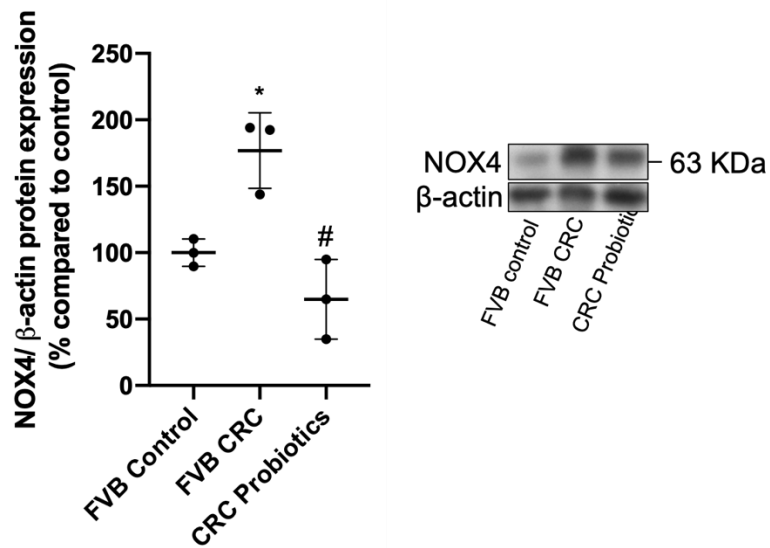


Figure 53: Probiotics protects against the overexpression of NOX4 caused by colorectal cancer (n=3). Data are expressed as mean \pm standard deviation (SD). * statistically significant at $p < 0.05$ vs control. # statistically significant at $p < 0.05$ vs *MKR* diabetic mice.

CHAPTER 5

DISCUSSION

We embarked on this project to investigate the role of microbiota in diabetes-associated colorectal cancer. The central hypothesis is that diabetes induces dysbiosis characterized by reduced amount of butyrate forming bacteria leading to less production of butyrate resulting in activation of HDAC3 which in turn leads to overexpression of NOX4 and IL-1 β . The overexpression of NOX4 and IL-1 β lead to the deleterious hyperproduction of ROS and exaggerated inflammatory immune which predisposes GI dysfunction and contribute to the oncogenic transformation of colon epithelial cells.

Type 2 DM is associated with disturbance of gut microbiota that contributes to its pathogenesis and the development of its complications. Noteworthy, all the association studies between gut microbiota and DM that included obese patients with T2DM could not differentiate if the reported microbial signature is associated with diabetes, obesity or to both co-morbidities. The bias of obesity was actually previously introduced in both mice and human studies ^{52,53,206,215–218}. ***This current study was performed to establish a microbial signature unique to the hyperglycemia associated with T2DM without the obesity component and to elucidate the molecular mechanisms by which microbiota, and its secreted butyrate, contribute to the diabetic pathogenesis and complications.***

We used *MKR* mice models which are non-obese mice that develop T2DM in adulthood due to a mutation in the insulin receptor in their muscles ¹⁶⁹. During the whole period of the study, these mice had high levels of blood glucose and HbA_{1c}% and similar body weights (**Figure 13**) when compared to their control littermates confirming

the non-obese insulin-resistant diabetic phenotype. Additionally, *MKR* mice suffered from impaired glucose utilization compared to their control littermates (**Figure 14**). Food consumption was monitored weekly and the mean food intake per group was calculated. Our data show that the *MKR* mice consumed more amount of food per mouse compared to their control littermates. The increase in food consumption by the diabetic *MKR* may explain why the diabetic mice did not lose weight due to diabetes.

MKR mice had shorter colons compared to the control group (**Figure 13**) which reflects gastrointestinal complications and colitis due to diabetes. Shortening of colons is considered a hallmark of gastrointestinal complications ^{219,220}.

Colorectal cancer was induced chemically using the azoxymethane/DSS protocol. Mice with CRC showed colon polyps with different numbers and sizes. The CRC mice also suffered from symptoms related to cancer such as rectal bleeding, inflamed colons, colon bleeding and fecal impaction (**Figure 15**). Dextran sulfate sodium is the sodium salt of dextran sulfate polymer. It is available in different molecular weights that differ in their ability to induce colitis in mice ²²¹. While the medium molecular weight DSS (35-50 kDa) is proven to induce the most severe colitis, the high molecular weight DSS (500 kDa) does not induce colitis in mice ²²¹. This fact gives an insight about the mechanism of action of DSS. Absorption of DSS is essential to mediate its effect. While the medium molecular weight DSS can form liposomes and consequently absorbed from the colon eliciting innate immune reaction that can precipitate colitis ²²², the high molecular weight DSS lacks this feature. DSS can induce acute, chronic or relapsing models of colitis and CRC when it is combined with azoxymethane. This can be achieved using variable concentrations of DSS and/or changing number of DSS and spacing between cycles ²²³. This model has been validated to mimic human CRC and is widely

used to study this disorder and its treatment ²²⁴.

Noteworthy, the *MKR* diabetic mice suffered from more aggressive cancer and had greater number of polyps compared to the *FVB-NJ* CRC mice (**Figure 15**). Previous work by our group has shown that type 1 diabetic mice exhibit more aggressive cancer phenotype than the control mice in a transgenic *C57BL/6-Apc^{tm1Tyj}/J* (*APC*) mice that spontaneously develop CRC ¹³¹. Similarly, Hata *et al.* reported a higher incidence and multiplicity of intestinal adenoma in *db/db* mice with *Apc* mutation compared to that in non-diabetic mice with the same mutation ²²⁵.

To test the effect of diabetic and cancer microbiota on the progression of CRC, we depleted the microbiota of *FVB-NJ* control mice using an antibiotic cocktail. We tried several antibiotic protocols from literature that are guaranteed to deplete the mice microbiota and we optimized our final protocol accordingly. After several trials, we found out that mice at 3 weeks of age cannot handle this high dose of antibiotics daily and we had high number of deaths among mice, so we resorted to give it in drinking water every other day. **Table 5** shows the comparison between our antibiotic protocol and other documented protocols from the literature.

Table 5: Comparison between the antibiotic protocol used in this study and other protocols from literature.

Antibiotic (mg/ml)	Ours	Desbonne <i>et al.</i> , 2015	Deshmukh <i>et al.</i> , 2014	Winek <i>et al.</i> , 2016	Heimesaat <i>et al.</i> , 2006	Li <i>et al.</i> , 2017
Reference		226	227	228	229	230
Starting age	3 Weeks	3 Weeks	In utero then after weaning	8 Weeks	10 Weeks	3 Weeks
Duration	4 Weeks	3 Weeks	3 Weeks	8 Weeks	6-8 Weeks	3 Weeks

Ampicillin (or Amoxicillin)	1	1	1	1	1	
Vancomycin	5	5	1	0.5	0.5	0.05
Metronidazole	1	10	1	1	1	0.1
Amphotricin B	0.05	0.1				
Neomycin	0	10	1			0.1
Streptomycin	0.05					0.05
Penicillin	50 U					100U
Ciprofloxacin	0.125			0.2	0.2	0.125
Gentamycin			1			0.17
Imipenem				0.25	0.25	
Bacitracin						0.001
Ceftazidime						0.1

After the depletion of microbiota, these mice were inoculated with FMT from control, diabetic and CRC mice as detailed in the methods section. Interestingly, mice inoculated with FMT from diabetic or CRC mice exhibited more aggressive CRC development and greater number of polyps compared to those who were inoculated by the control microbiota or those left without FMT (**Figure 16**). These results confirm the active role of microbiota in the development and progression of CRC. ***To our knowledge, our study is the first to describe this role through a controlled FMT experiment.***

Concerning the differential microbial population signature, our initial rt-PCR results show that *B. fragilis* and butyrate-forming bacteria were reduced in mice with T2DM when compared to their control littermates. Both *MKR* mice and their control littermates had similar abundance of *Akkermansia muciniphila*, Bacteroidaceae, Enterobacteriaceae, *Faecalibacterium prausnitzii*, Lachnospiraceae and Ruminococcaceae. The reduction of *B. fragilis* in the microbiota of patients with T2DM was recently reported by Navab-Moghadam *et al.*⁵⁰. Many studies focused on the reduction of *F. prausnitzii* and other butyrate-forming bacteria in obesity and T2DM

^{215,231}, here we report similar reduction for butyrate-forming bacteria with same abundance of *F. prausnitzii*. Although an association was previously reported between an increase of Bacteroidaceae ²³¹, reduction of *A. muciniphila* and T2DM mellitus ^{194,195}, ***our non-obese MKR mice did not show similar signature suggesting that the previous reported associations may have been due to obesity rather than T2DM.***

As for the Lachnospiraceae and Ruminococcaceae, both phyla contain butyrate-forming species. Our results show that the abundance of these 2 families was comparable between *MKR* and control mice while *MKR* mice show lower abundance of butyrate-forming bacteria. This may have been due to an increased abundance of butyrate non-forming bacteria in both phyla that compensated for the observed reduction of the butyrate-forming proportion.

Furthermore, performing a deeper analysis of the butyrate-forming bacterial species, confirmed these results where the *MKR* mice had lower abundance of *Butyricoccus spp* (from Ruminococcaceae family) and *Butyrivibrio spp*, *Coprococcus comes*, *Eubacterium hallii*, *Eubacterium rectale*, *Eubacterium ventriosum*, and *Roseburia intestinalis* (from the Lachnospiraceae family) compared to that of their control littermates. These findings are in accordance with other previous studies.

A large metagenome-wide study was previously conducted to identify the microbial signature of T2DM ⁷⁶. The authors reported some remarkable associations between gut microbiota and clinical findings of patients with T2DM. The most significant difference was related to the butyrate-forming bacteria such as Clostridiales sp. SS3/4, *E. rectale*, *F. prausnitzii*, and *Roseburia intestinalis* ⁷⁶. Patients with T2DM had lower abundance of these type of bacteria compared to healthy subjects. The microbiota of patients with T2DM also showed a marked abundance of opportunistic

pathogens such as *Bacteroides caccae*, various Clostridiales, *Escherichia coli* and the sulfate-reducing species *Desulfovibrio*⁷⁶. Differences in gut microbiota were regressed against functional associations in T2DM and it was found that microbiota has a role in membrane transport of sugars, ***oxidative stress responses***, branched chain amino acid transport, sulfate reduction and ***decreased butyrate biosynthesis***⁷⁶. On average, there was about 3% difference in the gut microbial genes between patients with T2DM and healthy subjects⁷⁶. The findings by Qin *et al.* were confirmed in a follow-up study that included Scandinavian postmenopausal women²³². This study also reported a reduction in the butyrate-forming bacteria associated with T2DM such as *R. intestinalis* and *F. prausnitzii*²³². Additionally, it was found that patients with T2DM or impaired glucose tolerance has more abundance of *Lactobacillus* species^{76,232}.

To identify the microbiota associated with diabetes and CRC in more depth, we performed 16S rRNA analysis which is considered the gold standard for all microbiome studies. The rarefaction analysis confirmed that all our samples were sequenced deep enough to discover all the underlying features or OTUs (**Figure 23**). The rarefaction curves for the antibiotic-treated mice hinted towards a lower OTU abundance in samples of the early time point compared to those of the late time point (**Figure 23**). The lower number of OTUs in the antibiotic-treated mice is expected as antibiotics depleted the microbiota in these mice which was restored at the late time point after FMT and conventionalization.

Alpha diversity analysis of our samples showed that there is a diversity in the richness of our samples with the lowest richness recorded at the early time point for the antibiotic-treated mice (**Figure 22**). *FVB-NJ* mice tend to have similar degree of richness while *MKR* samples tend to have different richness degrees. This finding

confirms that the diabetic microbiota is more diverse than the control microbiota and diabetic animals may have inconsistent microbiota from each other even when they share the same diet and same cage.

After assigning taxonomy to the discovered features, we found that samples collected from control, diabetic and CRC mice at late time point had higher abundance of Verrucomicrobia compared to the early time point. Diabetic mice have more bacteria belonging to phylum Firmicutes compared to their control littermates. The higher percentage of Firmicutes resulted in lower percentage of Bacteroidetes in *MKR* mice compared to their control littermates (**Figure 25**).

Concerning the antibiotic-treated mice, the microbiota of all mice at the early time point had significant proportion of Verrucomicrobia which indicates the resistance of these bacteria to antibiotic depletion and its opportunistic behavior. Consistent with our results, the increase in abundance of Verrucomicrobia has been previously reported in patients receiving broad-spectrum antibiotics²³³. Of interest, this increase was not associated with any intestinal disorders²³³ suggesting that the opportunistic members of Verrucomicrobia are not pathogenic. The high abundance of Verrucomicrobia was replaced by Bacteroidetes and Firmicutes at the late time point (**Figure 26**). We have also observed an increase in the abundance of Proteobacteria at the early time point which significantly decreased at the late time point. Cyanobacteria were of significant proportions only in the late time point in mice inoculated with the diabetic or the diabetic and CRC microbiota but not in the other groups.

Noteworthy, probiotics treatment increased the abundance of Bacteroidetes while it decreased the abundance of Cyanobacteria at the late time point (**Figure 27**). Cyanobacteria secrete LPS and other immunologic toxins that increases intestinal

inflammation²³⁴. Reduction of the abundance of Cyanobacteria is believed to be protective against GI inflammation.

The beta diversity analysis for the samples show that the principal coordinates separated the early and late time points very efficiently. This separation indicates that microbiota differs considerably due to ageing. PCoA also clustered *FVB-NJ* mice away from the *MKR* mice indicating that diabetes has a distinct microbial signature that differs from that of the control mice. Although the CRC mice were not fully separated from other groups in the PCoA plot, the high alpha diversity of samples at late time point made clustering difficult indicating that the ageing microbiota is becoming deleterious for the gut health and may contribute to colon inflammation (**Figure 28**).

For the antibiotic-treated mice, mice inoculated with diabetic or diabetic and CRC microbiota were distinctively clustered away from other groups even in the early time point showing a distinctive signature and early colonization compared to other FMT (**Figure 29**). At the late time point, mice inoculated with control or diabetic microbiota formed separate clusters from each other and from those inoculated with CRC microbiota (**Figure 30**). However, samples at the late time point for the antibiotic-treated mice were of low quality and only 2 mice per group passed the quality control procedure. Further studies with higher sample size are warranted to confirm and validate our obtained pilot results.

Probiotics succeeded in changing the microbiota of the diabetic mice and could form a separate cluster from the diabetic mice in the late time point (**Figure 32**) indicating that the beneficial effects of probiotics treatment are mediated mainly through changing the microbiota.

Analyzing the microbial composition of the control, diabetic and CRC mice showed that the control mice had significant proportion of bacteria belonging to phylum Porphyromonadaceae (**Figure 33**) which is documented to include many butyrate-forming bacteria ¹⁷⁴. These results indicate that microbiota of diabetic and CRC mice is characterized by less abundance of butyrate-forming bacteria corroborating our previous results.

Both PERMANOVA and AMOVA tests for multivariate and molecular significance showed that the microbiota in control mice were significantly different from that of the diabetic or the CRC mice (**Table 3**). It also showed a strong significant difference between the early and the late time points. In the same essence, the microbiota of the probiotics-treated mice was significantly different from that of the diabetic mice.

The phylum Verrucomicrobia was the most significant phylum accounting for differences between various groups and between the early and late time points (**Figure 36**). Additionally, the Proteobacteria and Cyanobacteria also accounted for differences between the groups of antibiotic-treated mice that were inoculated with different FMT (**Figure 37**). Probiotics affected the abundance of bacteria belonging to both Verrucomicrobia and Proteobacteria as shown through ANCOM analysis (**Figure 38**).

The phylum Verrucomicrobia include many important bacteria such as *Akkermansia muciniphila* which is a mucin-degrading bacterium. *A. muciniphila* has beneficial effects on the health of the host and glucose homeostasis ^{235,236}. It can represent up to 5% of the microbiota and it is a resident of the intestinal mucosa ^{215,237}. It has been shown that its abundance is inversely proportional to the body mass ^{195,199,238}. It can also protect mice on HFD from gaining weight and adiposity ¹⁹⁶.

The observed reduction in butyrate-forming bacteria resulted in reduced secretion of butyrate in cecal and fecal contents. The reduction of butyrate may be responsible for some of the pathological findings in T2DM due to HDAC3 activation^{94,95}. As an anti-inflammatory, butyrate inhibits HDAC3 which restores the peroxisome proliferation activated receptor (PPAR)- γ and liver-X receptor (LXR) function in obese rats²³⁹. Additionally, butyrate can bind to free fatty acid receptors (FFA) 1 and 2, which modulate immune responses²⁴⁰. Whether these effects are solely due to HDAC inhibition or histone acetylation or non-histone targets is still unknown^{241,242}. Our diabetic *MKR* mice also showed enhanced HDAC3 activity in colon tissues compared to the control group. The correlation between T2DM and increased HDAC3 activity was reported previously by Sathishkumar *et al.* without explaining the underlying cause⁹⁸. ***In our study, we potentially fill the missing link by showing that the correlation between T2DM and the increase in HDAC3 activity is due to the reduction of gut butyrate production.***

Another confirmation for this regulation was shown when the inhibition of HDACs by TSA, β -hydroxybutyrate or SAHA reduced the expression of NOX4 in endothelial cells, spinal cord tissues and human aortic smooth muscles cells^{214,243,244}. Our results confirm this observation, where TSA attenuates diabetes induced NOX4 protein expression. Moreover, our results are in line with the finding of Chen *et al.* where chromatin immunoprecipitation (ChIP) and luciferase promoter assays showed that the expression of NOXs are under direct control of HDAC in immune cells²⁴⁵.

HDAC3 epigenetically regulates inflammation and metabolic pathways related to diabetic pathogenesis⁹⁷. Genome-wide ChIP studies showed that HDAC inhibition can result in anti-inflammatory responses²⁴⁶. Many studies emphasized that inhibition

of HDAC3 attenuates diet-induced metabolic dysfunction²⁴⁷ and hyperglycemia by regulating the transcriptional activity of FoxO1²⁴⁸. In adult β -cells, deletion of HDAC3 increases the secretion of insulin and improves glucose tolerance²⁴⁹ and prevents cytokine-induced (mainly IL-1 β) apoptosis²⁵⁰. However, data from the literature showed that depletion of HDAC3 can induce glucose intolerance and increase susceptibility for insulin resistance in islet beta cells^{251,252}. These findings suggest that although partial inhibition of HDAC3 is beneficial in T2DM, its total depletion can impact the glucose metabolism profoundly. The work on HDAC3 inhibitors has been culminated with the virtual screening and *in vitro* testing of novel inhibitors that can be used as anti-diabetic drugs²⁵³. Moreover, a selective HDAC3 inhibitor, LW3 has been recently discovered confirming the druggability of this important epigenetic regulator²⁵⁴.

In our study, we show that the protein expression of IL-1 β significantly increased as a result of T2DM. Increased IL-1 β have been previously correlated with specific commensal bacterial abundance such as *Streptococcus*, *Prevotella*, *Haemophilus* and *Veillonella* spp.²⁵⁵ in inflammatory bowel syndrome. High plasma levels of IL-1 are associated with many auto-immune diseases including T1DM and blockage of IL-1 pathway was shown to be beneficial in both T1DM and T2DM^{208,209}.

Likewise, CRC mice showed an overexpression of IL-1 β (**Figure 42**). The role of IL-1 β in intestinal inflammation and colitis has been described before^{114,115}. However, there has been some contradictory reports that IL-1 β -deficient mice may be more susceptible to colitis than wild-type mice²⁵⁶. This contradiction has been attributed to, at least partially, to differences in the composition of baseline microbiota²⁵⁷. A finding that underscores the role of microbiota in the secretion of IL-1 β and the

activation of its downstream signaling leading to precipitation of colonic inflammation and eventually CRC. CRC is promoted by the activation of Wnt/ β -catenin signaling pathway²⁵⁸. This signaling pathway is believed to be potentiated by IL-1 β manifesting the role of this cytokine in CRC²⁵⁹. Many studies have associated the overexpression of IL-1 β with CRC (reviewed in²⁶⁰).

Besides, butyrate and PSA (produced by *B. fragilis*) are important for the maturation of T-cells that produce anti-inflammatory IL-10 and pro-inflammatory IL-17^{261,262}. ***Since we have observed a reduction of B. fragilis and butyrate-forming bacterial population together with reduced production of cecal and fecal butyrate, we found that circulatory levels of IL-10 and IL-17 are decreased in comparison to the controls.*** IL-10 is protective against progression of DM as per Robert *et al.* who reported that delivery of IL-10 can actually reverses DM in NOD mice²⁶³. The role of IL-17 in DM is paradoxical. Although it is a pro-inflammatory marker, its reduced plasma levels were associated with diabetic nephropathy and retinopathy and were negatively correlated with body mass index, T2DM duration and glycated haemoglobin^{264,265}.

In parallel, we investigated the protein expression of NOX4 that is involved in key pathways of diabetic complications^{128–130,188,213}. We found that their protein expressions were higher in *MKR* diabetic mice when compared to the controls. This is concomitant with other studies on DM^{149,188,266,267}. ***This is the first study to molecularly correlate the elevated expression of NOXs to increased activity of HDAC3 due to the reduction of butyrate production.***

NOX4 was also overexpressed in colon tissues of CRC mice (**Figure 43**). We have previously exposed the role of NOX4 in diabetes-associated CRC¹³¹ after

inducing T1DM in *Apc* mice. The sole function for NOX4 is the production of ROS which are beneficial for the cell in moderate amounts. Dysregulation in the expression of NOX4 can lead to excessive production of ROS which can damage the cell or induce mutations that can contribute to the cell oncogenic transformation ¹³¹.

We tested if microbiota is responsible for the induction of the expression of IL-1 β and NOX4 seen in case of diabetes and CRC. Our results show that the diabetic or CRC FMT did not significantly alter the expression of IL-1 β (**Figure 44**) and NOX4 (**Figure 45**). Noteworthy, CRC was induced chemically in all of these mice which may have had a direct effect on the levels of both proteins which led to confounding of the results. Therefore, we cannot rule out a role for microbiota in inducing the expression of both proteins. Further studies are warranted to investigate and explain the causal effect for diabetic and cancer microbiota on the expression of IL-1 β and NOX4.

After showing that diabetes-associated dysbiosis is characterized by a reduction of the butyrate-forming bacteria leading to inadequate butyrate secretion, we supplied the mice with IP sodium butyrate to compensate for this loss without affecting the gut microbiota. Our results show that butyrate treatment protected against diabetes-associated gastrointestinal complications and shortening of the colons as a result of inflammation (**Figure 47**). Additionally, butyrate supplement protected colon tissue from oxidative stress and ROS production due to over-expression of NOX4 and it decreased the expression of the pro-inflammatory cytokine IL-1 β (**Figure 48**). Taken together, these findings emphasize the beneficial effects of butyrate supplements on the gut health without affecting the gut microbiota composition. These results are concomitant with other studies that presented that butyrate, through acting as an HDAC inhibitor and anti-inflammatory agent, could impart protection against colon

inflammation and gastrointestinal complications^{84,268–270}. In the context of diabetes, butyrate supplementation was shown to increase insulin sensitivity and delaying diabetic complications^{44,93,271}.

Similarly, probiotics treatments had beneficial effect on the GI health. Although it did not affect the blood glucose levels or HbA_{1c}%, it succeeded in improving GI health which was reflected by longer colons compared to that of untreated *MKR* mice (**Figure 49**). Probiotics also protected against the over expression of NOX4 and IL-1 β and the ensuing hyperproduction of ROS (**Figure 50, Figure 51, Figure 52 and Figure 53**). These findings underscore the advantageous outcomes of probiotics treatment. They also confirm that rectifying the microbiota or compensating for the reduced production of butyrate can be beneficial in diabetes. However, probiotics should be used in combination with an antidiabetic drug as they have no effect on the hyperglycemia.

One of the theories for the probiotics action is revolving around SCFAs. SCFAs are believed to bind to specific G-protein coupled receptors in the gut leading to manipulation of the enteroendocrine system^{272,273}. This will in turn lead to the upregulation of gut hormones such as proglucagon²⁷⁴, glucagon-like peptide-1 (GLP-1)²⁷⁵, GLP-2, gastric inhibitory peptide (GIP)²⁷⁶ and leptin²⁷⁷ as well as downregulating ghrelin²⁷⁸. These hormones affects intestinal permeability, satiety, gastric emptying and food intake²⁷⁹. These findings stress on the interplay between probiotics and butyrate in maintaining a healthy microbiome which endorses a healthy metabolism.

To our knowledge, this study is the first to describe a microbial signature that is unique to the hyperglycemia component of T2DM without the obesity component. The novelty of this work is represented in underscoring the role of microbiota in

mediating GI complications of T2DM and aggravating CRC. The results obtained from this work pave the way for better understanding of the mechanisms by which T2DM is precipitating GI complications and potentiating CRC with focus on inflammation and ROS production pathways.

Our study suffered from some limitations that should be tackled in future studies mainly the low sample size which prevented the deduction of significance in some experiments, the short duration of the FMT experiment and the introduction of CRC in all the groups which masked the differences in protein expressions of NOX4 and IL-1 β , the complexity of the probiotics mixture used in the treatment and the lack of probiotics-treated CRC group. Our future plans include the replication of the FMT experiment with higher number of animals and non-cancer controls, including a probiotics as a prophylactic for T2DM and CRC, *in vivo* experiments that investigate different treatments with specific bacterial species for CRC and T2DM, assessment of the activity of other HDAC enzymes in colon tissues, the use of the specific HDAC3 inhibitor, LW3 in *in vivo* and *in vitro* experiments that involve animals with CRC and T2DM, assessment of plasma butyrate concentration in diabetes and CRC and finally investigating the involvement of other mechanistic pathways such as the mTOR (mechanistic target of rapamycin) in the development of diabetes-associated CRC.

CHAPTER 6

CONCLUSION

In conclusion, our study show that T2DM is associated with a unique microbial signature that is characterized by reduction of *B. fragilis* and butyrate-forming bacteria. Both bacterial populations secrete metabolites that contribute to the inflammatory state observed with DM. Consequently, mice with T2DM have less butyrate production which impacts its beneficial function as an HDAC inhibitor. Less butyrate resulted in increased activity of HDAC3, which regulates inflammatory pathways and NOX4 expression and results in development of diabetic complications (**Figure 7**). Targeting this pathway by probiotics, butyrate supplements, HDAC3 inhibitor, or NOX4 inhibitors represents a potential novel, specific and promising therapeutic approach for the management of T2DM and protecting against CRC.

BIBLIOGRAPHY

1. IDF. International Diabetes Federation Atlas 2019. *accessed on 20/4/2020*
<http://www.diabetesatlas.org> (2019).
2. Rimm, A. A., Werner, L. H., Yserloo, B. V & Bernstein, R. A. Relationship of obesity and disease in 73,532 weight-conscious women. *Public Health Rep.* **90**, 44 (1975).
3. Wilson, E. B. & Maher, H. C. Cancer and tuberculosis with some comments on cancer and other diseases. *Am. J. Cancer* **16**, 227–250 (1932).
4. Simon, D. & Balkau, B. Diabetes mellitus, hyperglycaemia and cancer. *Diabetes Metab.* **36**, 182–191 (2010).
5. Szablewski, L. Diabetes mellitus: influences on cancer risk. *Diabetes. Metab. Res. Rev.* **30**, 543–553 (2014).
6. Vigneri, P., Frasca, F., Sciacca, L., Pandini, G. & Vigneri, R. Diabetes and cancer. *Endocr. Relat. Cancer* **16**, 1103–1123 (2009).
7. Barone, B. B. *et al.* Long-term all-cause mortality in cancer patients with preexisting diabetes mellitus: a systematic review and meta-analysis. *Jama* **300**, 2754–2764 (2008).
8. Elwing, J. E., Gao, F., Davidson, N. O. & Early, D. S. Type 2 diabetes mellitus: the impact on colorectal adenoma risk in women. *Am. J. Gastroenterol.* **101**, 1866 (2006).
9. Chowdhury, T. A. Diabetes and cancer. *QJM An Int. J. Med.* **103**, 905–915 (2010).
10. Coughlin, S. S., Calle, E. E., Teras, L. R., Petrelli, J. & Thun, M. J. Diabetes mellitus as a predictor of cancer mortality in a large cohort of US adults. *Am. J.*

- Epidemiol.* **159**, 1160–1167 (2004).
11. Jurjus, A. *et al.* Inflammatory bowel disease, colorectal cancer and type 2 diabetes mellitus: The links. *BBA Clin.* **5**, 16–24 (2016).
 12. Parkin, D. M., Bray, F., Ferlay, J. & Pisani, P. Global cancer statistics, 2002. *CA. Cancer J. Clin.* **55**, 74–108 (2005).
 13. Marshall, J. R. Prevention of colorectal cancer: diet, chemoprevention, and lifestyle. *Gastroenterol. Clin. North Am.* **37**, 73–82 (2008).
 14. Arvanitakis, C. & Tozun, N. Mediterranean Diet-Health and Culture. *Int. J. Anthropol.* **28**, (2013).
 15. Estruch, R. *et al.* Primary prevention of cardiovascular disease with a Mediterranean diet. *N. Engl. J. Med.* **368**, 1279–1290 (2013).
 16. Chan, A. T. & Giovannucci, E. L. Primary prevention of colorectal cancer. *Gastroenterology* **138**, 2029–2043 (2010).
 17. Jo, W.-S. & Chung, D. C. Genetics of hereditary colorectal cancer. in *Seminars in oncology* vol. 32 11–23 (Elsevier, 2005).
 18. Fearon, E. R. & Vogelstein, B. A genetic model for colorectal tumorigenesis. *Cell* **61**, 759–767 (1990).
 19. Network, C. G. A. Comprehensive molecular characterization of human colon and rectal cancer. *Nature* **487**, 330 (2012).
 20. Vetrano, S. & Danese, S. Colitis, microbiota, and colon cancer: an infernal triangle. *Gastroenterology* **144**, 461–463 (2013).
 21. Hu, B. *et al.* Microbiota-induced activation of epithelial IL-6 signaling links inflammasome-driven inflammation with transmissible cancer. *Proc. Natl. Acad. Sci.* **110**, 9862–9867 (2013).

22. Abreu, M. T. & Peek Jr, R. M. Gastrointestinal malignancy and the microbiome. *Gastroenterology* **146**, 1534–1546 (2014).
23. Sears, C. L. & Garrett, W. S. Microbes, microbiota, and colon cancer. *Cell Host Microbe* **15**, 317–328 (2014).
24. Song, X. *et al.* Alterations in the microbiota drive interleukin-17C production from intestinal epithelial cells to promote tumorigenesis. *Immunity* **40**, 140–152 (2014).
25. Singh, N. *et al.* Activation of Gpr109a, receptor for niacin and the commensal metabolite butyrate, suppresses colonic inflammation and carcinogenesis. *Immunity* **40**, 128–139 (2014).
26. McCarthy, K., Pearson, K., Fulton, R. & Hewitt, J. Pre-operative chemoradiation for non-metastatic locally advanced rectal cancer. *Cochrane database Syst. Rev.* (2012).
27. André, T. *et al.* Oxaliplatin, fluorouracil, and leucovorin as adjuvant treatment for colon cancer. *N. Engl. J. Med.* **350**, 2343–2351 (2004).
28. Therkildsen, C., Bergmann, T. K., Henrichsen-Schnack, T., Ladelund, S. & Nilbert, M. The predictive value of KRAS, NRAS, BRAF, PIK3CA and PTEN for anti-EGFR treatment in metastatic colorectal cancer: A systematic review and meta-analysis. *Acta Oncol. (Madr)*. **53**, 852–864 (2014).
29. Eckburg, P. B. *et al.* Diversity of the human intestinal microbial flora. *Science* (80-.). **308**, 1635–1638 (2005).
30. Damman, C. J., Miller, S. I., Surawicz, C. M. & Zisman, T. L. The microbiome and inflammatory bowel disease: is there a therapeutic role for fecal microbiota transplantation? *Am. J. Gastroenterol.* **107**, 1452–1459 (2012).

31. Sokol, H. *et al.* Faecalibacterium prausnitzii is an anti-inflammatory commensal bacterium identified by gut microbiota analysis of Crohn disease patients. *Proc. Natl. Acad. Sci.* **105**, 16731–16736 (2008).
32. Veerappan, G. R., Betteridge, J. & Young, P. E. Probiotics for the treatment of inflammatory bowel disease. *Curr. Gastroenterol. Rep.* **14**, 324–333 (2012).
33. Tirandaz, H. & Mohammadi, E. Efficient tumor targeting by anaerobic butyrate-producing bacteria. *Med. Hypotheses* **80**, 675–678 (2013).
34. Guinane, C. M. & Cotter, P. D. Role of the gut microbiota in health and chronic gastrointestinal disease: understanding a hidden metabolic organ. *Therap. Adv. Gastroenterol.* **6**, 295–308 (2013).
35. Korecka, A. & Arulampalam, V. The gut microbiome: scourge, sentinel or spectator? *J. Oral Microbiol.* **4**, 9367 (2012).
36. Shanahan, F. The gut microbiota—a clinical perspective on lessons learned. *Nat. Rev. Gastroenterol. Hepatol.* **9**, 609–614 (2012).
37. Tomasello, G. *et al.* The fingerprint of the human gastrointestinal tract microbiota: a hypothesis of molecular mapping. *J Biol Regul Homeost Agents* **31**, 245–249 (2017).
38. Tennyson, C. A. & Friedman, G. Microecology, obesity, and probiotics. *Curr. Opin. Endocrinol. Diabetes Obes.* **15**, 422–427 (2008).
39. Akin, H. & Tözün, N. Diet, microbiota, and colorectal cancer. *J. Clin. Gastroenterol.* **48**, S67–S69 (2014).
40. Mejía-León, M. E. & Barca, A. M. Diet, microbiota and immune system in type 1 diabetes development and evolution. *Nutrients* **7**, 9171–9184 (2015).
41. Haro, C. *et al.* Two healthy diets modulate gut microbial community improving

- insulin sensitivity in a human obese population. *J. Clin. Endocrinol.* **101**, 233–242 (2016).
42. Blandino, G., Inturri, R., Lazzara, F., Di Rosa, M. & Malaguarnera, L. Impact of gut microbiota on diabetes mellitus. *Diabetes Metab.* **42**, 303–315 (2016).
 43. Cani, P. D. *et al.* Metabolic endotoxemia initiates obesity and insulin resistance. *Diabetes* **56**, 1761–1772 (2007).
 44. Gao, Z. *et al.* Butyrate improves insulin sensitivity and increases energy expenditure in mice. *Diabetes* (2009).
 45. Donohoe, D. R. *et al.* The Warburg effect dictates the mechanism of butyrate-mediated histone acetylation and cell proliferation. *Mol. Cell* **48**, 612–626 (2012).
 46. Li, N. *et al.* Butyrate and type 1 diabetes mellitus: can we fix the intestinal leak? *J. Pediatr. Gastroenterol. Nutr.* **51**, 414–417 (2010).
 47. Canani, R. B. *et al.* Potential beneficial effects of butyrate in intestinal and extraintestinal diseases. *World J. Gastroenterol. WJG* **17**, 1519 (2011).
 48. Goicoa, S., Álvarez, S., Ricordi, C., Inverardi, L. & Domínguez-Bendala, J. Sodium butyrate activates genes of early pancreatic development in embryonic stem cells. *Cloning Stem Cells* **8**, 140–149 (2006).
 49. Anderson, J. W. *et al.* Health benefits of dietary fiber. *Nutr. Rev.* **67**, 188–205 (2009).
 50. Navab-Moghadam, F. *et al.* The association of type II diabetes with gut microbiota composition. *Microb. Pathog.* **110**, 630–636 (2017).
 51. Ahmad, A. *et al.* Analysis of gut microbiota of obese individuals with type 2 diabetes and healthy individuals. *PLoS One* **14**, (2019).

52. Esteve, E., Ricart, W. & Fernandez-Real, J.-M. Gut microbiota interactions with obesity, insulin resistance and type 2 diabetes: did gut microbiote co-evolve with insulin resistance? *Curr. Opin. Clin. Nutr. Metab. Care* **14**, 483–490 (2011).
53. Musso, G., Gambino, R. & Cassader, M. Obesity, diabetes, and gut microbiota: the hygiene hypothesis expanded? *Diabetes Care* **33**, 2277–2284 (2010).
54. Manco, M., Putignani, L. & Bottazzo, G. F. Gut microbiota, lipopolysaccharides, and innate immunity in the pathogenesis of obesity and cardiovascular risk. *Endocr. Rev.* **31**, 817–844 (2010).
55. Patterson, E. E. *et al.* Gut microbiota, obesity and diabetes. *Postgraduate Medical Journal* (2016) doi:10.1136/postgradmedj-2015-133285.
56. Johnson, A. M. F. & Olefsky, J. M. The origins and drivers of insulin resistance. *Cell* **152**, 673–684 (2013).
57. Pussinen, P. J., Havulinna, A. S., Lehto, M., Sundvall, J. & Salomaa, V. Endotoxemia is associated with an increased risk of incident diabetes. *Diabetes Care* **34**, 392–397 (2011).
58. Lassenius, M. I. *et al.* Bacterial endotoxin activity in human serum is associated with dyslipidemia, insulin resistance, obesity, and chronic inflammation. *Diabetes Care* **34**, 1809–1815 (2011).
59. Serino, M. *et al.* Metabolic adaptation to a high-fat diet is associated with a change in the gut microbiota. *Gut* **61**, 543–553 (2012).
60. Amar, J. *et al.* Intestinal mucosal adherence and translocation of commensal bacteria at the early onset of type 2 diabetes: molecular mechanisms and probiotic treatment. *EMBO Mol. Med.* **3**, 559–572 (2011).
61. Amar, J. *et al.* Involvement of tissue bacteria in the onset of diabetes in humans:

- evidence for a concept. *Diabetologia* **54**, 3055–3061 (2011).
62. McCoy, W. C. & Mason 3rd, J. M. Enterococcal endocarditis associated with carcinoma of the sigmoid; report of a case. *J. Med. Assoc. State Ala.* **21**, 162–166 (1951).
 63. Azcárate-Peril, M. A., Sikes, M. & Bruno-Bárcena, J. M. The intestinal microbiota, gastrointestinal environment and colorectal cancer: a putative role for probiotics in prevention of colorectal cancer? *Am. J. Physiol. Liver Physiol.* **301**, G401–G424 (2011).
 64. Tjalsma, H., Boleij, A., Marchesi, J. R. & Dutilh, B. E. A bacterial driver-passenger model for colorectal cancer: beyond the usual suspects. *Nat. Rev. Microbiol.* **10**, 575 (2012).
 65. Sobhani, I. *et al.* Microbial dysbiosis and colon carcinogenesis: could colon cancer be considered a bacteria-related disease? *Therap. Adv. Gastroenterol.* **6**, 215–229 (2013).
 66. Moore, W. E. & Moore, L. H. Intestinal floras of populations that have a high risk of colon cancer. *Appl. Environ. Microbiol.* **61**, 3202–3207 (1995).
 67. Scanlan, P. D., Shanahan, F. & Marchesi, J. R. Culture-independent analysis of desulfovibrios in the human distal colon of healthy, colorectal cancer and polypectomized individuals. *FEMS Microbiol. Ecol.* **69**, 213–221 (2009).
 68. Marchesi, J. R. *et al.* Towards the human colorectal cancer microbiome. *PLoS One* **6**, (2011).
 69. Scanlan, P. D. *et al.* Culture-independent analysis of the gut microbiota in colorectal cancer and polyposis. *Environ. Microbiol.* **10**, 789–798 (2008).
 70. Zeller, G. *et al.* Potential of fecal microbiota for early-stage detection of

- colorectal cancer. *Mol. Syst. Biol.* **10**, (2014).
71. Elinav, E. *et al.* NLRP6 inflammasome regulates colonic microbial ecology and risk for colitis. *Cell* (2011) doi:10.1016/j.cell.2011.04.022.
 72. Chen, G. Y., Liu, M., Wang, F., Bertin, J. & Núñez, G. A functional role for Nlrp6 in intestinal inflammation and tumorigenesis. *J. Immunol.* **186**, 7187–7194 (2011).
 73. González, N. *et al.* 2017 update on the relationship between diabetes and colorectal cancer: epidemiology, potential molecular mechanisms and therapeutic implications. *Oncotarget* **8**, 18456 (2017).
 74. Henao-Mejia, J. *et al.* Inflammasome-mediated dysbiosis regulates progression of NAFLD and obesity. *Nature* (2012) doi:10.1038/nature10809.
 75. Proctor, L. M. *et al.* The Integrative Human Microbiome Project. *Nature* (2019) doi:10.1038/s41586-019-1238-8.
 76. Wang, J. *et al.* A metagenome-wide association study of gut microbiota in type 2 diabetes. *Nature* (2012) doi:10.1038/nature11450.
 77. Cook, S. I. & Sellin, J. H. Short chain fatty acids in health and disease. *Aliment. Pharmacol. Ther.* **12**, 499–507 (1998).
 78. Cummings, J. H. Colonic absorption: the importance of short chain fatty acids in man. *Scand. J. Gastroenterol. Suppl.* **93**, 89–99 (1983).
 79. Ruemmele, F. M. *et al.* Butyrate mediates Caco-2 cell apoptosis via up-regulation of pro-apoptotic BAK and inducing caspase-3 mediated cleavage of poly-(ADP-ribose) polymerase(PARP). *Cell Death Differ.* **6**, 729–735 (1999).
 80. Trock, B., Lanza, E. & Greenwald, P. Dietary fiber, vegetables, and colon cancer: critical review and meta-analyses of the epidemiologic evidence. *JNCI J. Natl.*

- Cancer Inst.* **82**, 650–661 (1990).
81. Hague, A., Elder, D. J. E., Hicks, D. J. & Paraskeva, C. Apoptosis in colorectal tumour cells: induction by the short chain fatty acids butyrate, propionate and acetate and by the bile salt deoxycholate. *Int. J. Cancer* **60**, 400–406 (1995).
 82. Hamer, H. M. *et al.* The role of butyrate on colonic function. *Aliment. Pharmacol. Ther.* **27**, 104–119 (2008).
 83. Canfora, E. E., Jocken, J. W. & Blaak, E. E. Short-chain fatty acids in control of body weight and insulin sensitivity. *Nat. Rev. Endocrinol.* **11**, 577–591 (2015).
 84. Scharlau, D. *et al.* Mechanisms of primary cancer prevention by butyrate and other products formed during gut flora-mediated fermentation of dietary fibre. *Mutat. Res. Mutat. Res.* **682**, 39–53 (2009).
 85. Hovhannisyan, G., Aroutiounian, R. & Gleib, M. Butyrate reduces the frequency of micronuclei in human colon carcinoma cells in vitro. *Toxicol. Vitro.* **23**, 1028–1033 (2009).
 86. Suzuki, T., Yoshida, S. & Hara, H. Physiological concentrations of short-chain fatty acids immediately suppress colonic epithelial permeability. *Br. J. Nutr.* **100**, 297–305 (2008).
 87. Hu, S. *et al.* The microbe-derived short chain fatty acid butyrate targets miRNA-dependent p21 gene expression in human colon cancer. *PLoS One* **6**, (2011).
 88. Winter, J. *et al.* Inhibition by resistant starch of red meat–induced promutagenic adducts in mouse colon. *Cancer Prev. Res.* **4**, 1920–1928 (2011).
 89. Worthley, D. L. *et al.* DNA methylation in the rectal mucosa is associated with crypt proliferation and fecal short-chain fatty acids. *Dig. Dis. Sci.* **56**, 387–396 (2011).

90. Rosignoli, P. *et al.* Protective activity of butyrate on hydrogen peroxide-induced DNA damage in isolated human colonocytes and HT29 tumour cells. *Carcinogenesis* **22**, 1675–1680 (2001).
91. Zhang, J. *et al.* Sodium butyrate induces endoplasmic reticulum stress and autophagy in colorectal cells: implications for apoptosis. *PLoS One* **11**, e0147218 (2016).
92. Canani, R. B., Di Costanzo, M. & Leone, L. The epigenetic effects of butyrate: potential therapeutic implications for clinical practice. *Clin. Epigenetics* **4**, 4 (2012).
93. Khan, S. & Jena, G. The role of butyrate, a histone deacetylase inhibitor in diabetes mellitus: experimental evidence for therapeutic intervention. *Epigenomics* **7**, 669–680 (2015).
94. Furusawa, Y. *et al.* Commensal microbe-derived butyrate induces the differentiation of colonic regulatory T cells. *Nature* **504**, 446 (2013).
95. Khan, S. & Jena, G. Sodium butyrate, a HDAC inhibitor ameliorates eNOS, iNOS and TGF- β 1-induced fibrogenesis, apoptosis and DNA damage in the kidney of juvenile diabetic rats. *Food Chem. Toxicol.* **73**, 127–139 (2014).
96. Dirice, E. *et al.* Isoform-selective inhibitor of histone deacetylase 3 (HDAC3) limits pancreatic islet infiltration and protects female nonobese diabetic mice from diabetes. *J. Biol. Chem.* jbc-M117 (2017).
97. Meier, B. C. & Wagner, B. K. Inhibition of HDAC3 as a strategy for developing novel diabetes therapeutics. *Epigenomics* **6**, 209–214 (2014).
98. Sathishkumar, C. *et al.* Augmentation of histone deacetylase 3 (HDAC3) epigenetic signature at the interface of proinflammation and insulin resistance in

- patients with type 2 diabetes. *Clin. Epigenetics* **8**, 125 (2016).
99. Xu, Z. *et al.* Inhibition of HDAC3 prevents diabetic cardiomyopathy in OVE26 mice via epigenetic regulation of DUSP5-ERK1/2 pathway. *Clin. Sci.* CS20170064 (2017).
 100. Zhang, J. *et al.* HDAC3 inhibition in diabetic mice may activate Nrf2 preventing diabetes-induced liver damage and FGF21 synthesis and secretion leading to aortic protection. *Am. J. Physiol. Metab.* (2018).
 101. Lundh, M., Galbo, T., Poulsen, S. S. & Mandrup-Poulsen, T. Histone deacetylase 3 inhibition improves glycaemia and insulin secretion in obese diabetic rats. *Diabetes, Obes. Metab.* **17**, 703–707 (2015).
 102. Lotz, M. *et al.* Postnatal acquisition of endotoxin tolerance in intestinal epithelial cells. *J. Exp. Med.* **203**, 973–984 (2006).
 103. Smythies, L. E. *et al.* Human intestinal macrophages display profound inflammatory anergy despite avid phagocytic and bacteriocidal activity. *J. Clin. Invest.* **115**, 66–75 (2005).
 104. Kamada, N. & Núñez, G. Regulation of the immune system by the resident intestinal bacteria. *Gastroenterology* **146**, 1477–1488 (2014).
 105. Garrett, W. S. *et al.* Communicable ulcerative colitis induced by T-bet deficiency in the innate immune system. *Cell* **131**, 33–45 (2007).
 106. Kirkland, D. *et al.* B cell-intrinsic MyD88 signaling prevents the lethal dissemination of commensal bacteria during colonic damage. *Immunity* **36**, 228–238 (2012).
 107. Kitajima, S., Morimoto, M., Sagara, E., SHIMIZU, C. & IKEDA, Y. Dextran sodium sulfate-induced colitis in germ-free IQI/Jic mice. *Exp. Anim.* **50**, 387–395

- (2001).
108. Hudcovic, T., Štěpánková, R., Cebra, J. & Tlaskalova-Hogenova, H. The role of microflora in the development of intestinal inflammation: acute and chronic colitis induced by dextran sulfate in germ-free and conventionally reared immunocompetent and immunodeficient mice. *Folia Microbiol. (Praha)*. **46**, 565–572 (2001).
 109. Bloom, S. M. *et al.* Commensal *Bacteroides* species induce colitis in host-genotype-specific fashion in a mouse model of inflammatory bowel disease. *Cell Host Microbe* **9**, 390–403 (2011).
 110. Garrett, W. S. *et al.* Enterobacteriaceae act in concert with the gut microbiota to induce spontaneous and maternally transmitted colitis. *Cell Host Microbe* **8**, 292–300 (2010).
 111. Schroder, K. & Tschopp, J. The inflammasomes. *Cell* **140**, 821–832 (2010).
 112. Franchi, L., Muñoz-Planillo, R. & Núñez, G. Sensing and reacting to microbes through the inflammasomes. *Nat. Immunol.* **13**, 325 (2012).
 113. Seo, S.-U. *et al.* Distinct commensals induce interleukin-1 β via NLRP3 inflammasome in inflammatory monocytes to promote intestinal inflammation in response to injury. *Immunity* **42**, 744–755 (2015).
 114. Coccia, M. *et al.* IL-1 β mediates chronic intestinal inflammation by promoting the accumulation of IL-17A secreting innate lymphoid cells and CD4⁺ Th17 cells. *J. Exp. Med.* **209**, 1595–1609 (2012).
 115. Saitoh, T. *et al.* Loss of the autophagy protein Atg16L1 enhances endotoxin-induced IL-1 β production. *Nature* **456**, 264–268 (2008).
 116. Dinarello, C. A., Donath, M. Y. & Mandrup-Poulsen, T. Role of IL-1 β in type 2

- diabetes. *Curr. Opin. Endocrinol. Diabetes Obes.* **17**, 314–321 (2010).
117. Mantovani, A. Cancer: Inflaming metastasis. *Nature* (2009)
doi:10.1038/457036b.
118. Germano, G., Allavena, P. & Mantovani, A. Cytokines as a key component of cancer-related inflammation. *Cytokine* (2008) doi:10.1016/j.cyto.2008.07.014.
119. Apte, R. N. & Voronov, E. Interleukin-1 - A major pleiotropic cytokine in tumor-host interactions. *Semin. Cancer Biol.* (2002) doi:10.1016/S1044-579X(02)00014-7.
120. Colasante, A. *et al.* Transforming growth factor β 1, interleukin-8 and interleukin-1, in non- small-cell lung tumors. *Am. J. Respir. Crit. Care Med.* (1997)
doi:10.1164/ajrccm.156.3.9701122.
121. Kaler, P., Godasi, B. N., Augenlicht, L. & Klampfer, L. The NF- κ B/AKT-dependent induction of Wnt signaling in colon cancer cells by macrophages and IL-1 β . *Cancer Microenviron.* (2009) doi:10.1007/s12307-009-0030-y.
122. Bessler, H. & Djaldetti, M. Role of the equilibrium between colon cancer and mononuclear cells in cytokine production. *Biomed. Pharmacother.* (2010)
doi:10.1016/j.biopha.2010.08.006.
123. Kaler, P., Augenlicht, L. & Klampfer, L. Macrophage-derived IL-1 β stimulates Wnt signaling and growth of colon cancer cells: A crosstalk interrupted by vitamin D³. *Oncogene* (2009) doi:10.1038/onc.2009.247.
124. Jedinak, A., Dudhgaonkar, S. & Sliva, D. Activated macrophages induce metastatic behavior of colon cancer cells. *Immunobiology* (2010)
doi:10.1016/j.imbio.2009.03.004.
125. Lagosz, K. B. *et al.* HDAC3 regulates gingival fibroblast inflammatory responses

- in periodontitis. *J. Dent. Res.* **99**, 98–106 (2020).
126. Brownlee, M. The pathobiology of diabetic complications: a unifying mechanism. *Diabetes* **54**, 1615–1625 (2005).
 127. Carini, F. *et al.* Colorectal carcinogenesis: Role of oxidative stress and antioxidants. *Anticancer Res.* **37**, 4759–4766 (2017).
 128. Fitzgerald, J. P. *et al.* Nox4 mediates renal cell carcinoma cell invasion through hypoxia-induced interleukin 6-and 8-production. *PLoS One* **7**, e30712 (2012).
 129. Maalouf, R. M. *et al.* Nox4-derived reactive oxygen species mediate cardiomyocyte injury in early type 1 diabetes. *Am. J. Physiol. Physiol.* **302**, C597–C604 (2011).
 130. Eid, A. A. *et al.* mTOR regulates Nox4-mediated podocyte depletion in diabetic renal injury. *Diabetes* DB_121504 (2013).
 131. Mroueh, F. M. *et al.* Unmasking the interplay between mTOR and Nox4: novel insights into the mechanism connecting diabetes and cancer. *FASEB J.* **33**, 14051–14066 (2019).
 132. Altenhöfer, S. *et al.* The NOX toolbox: validating the role of NADPH oxidases in physiology and disease. *Cell. Mol. Life Sci.* **69**, 2327–2343 (2012).
 133. Tomasello, G. *et al.* Nutrition, oxidative stress and intestinal dysbiosis: Influence of diet on gut microbiota in inflammatory bowel diseases. *Biomed Pap Med Fac Univ Palacky Olomouc Czech Repub* **160**, 461–466 (2016).
 134. Mazzola, M. *et al.* INFLAMMATORY BOWEL DISEASE AND COLORECTAL CANCER, NUTRACEUTICAL ASPECTS. *Euromediterranean Biomed. J.* **11**, (2016).
 135. Kleniewska, P., Piechota, A., Skibska, B. & Gorąca, A. The NADPH oxidase

- family and its inhibitors. *Arch. Immunol. Ther. Exp. (Warsz)*. **60**, 277–294 (2012).
136. Eid, A. A. *et al.* Mammalian target of rapamycin regulates Nox4-mediated podocyte depletion in diabetic renal injury. *Diabetes* **62**, 2935–2947 (2013).
137. Juhasz, A. *et al.* Expression of NADPH oxidase homologues and accessory genes in human cancer cell lines, tumours and adjacent normal tissues. *Free Radic. Res.* **43**, 523–532 (2009).
138. Mitsushita, J., Lambeth, J. D. & Kamata, T. The superoxide-generating oxidase Nox1 is functionally required for Ras oncogene transformation. *Cancer Res.* **64**, 3580–3585 (2004).
139. Brar, S. S. *et al.* NOX5 NAD (P) H oxidase regulates growth and apoptosis in DU 145 prostate cancer cells. *Am. J. Physiol. Physiol.* **285**, C353–C369 (2003).
140. Kumar, B., Koul, S., Khandrika, L., Meacham, R. B. & Koul, H. K. Oxidative stress is inherent in prostate cancer cells and is required for aggressive phenotype. *Cancer Res.* **68**, 1777–1785 (2008).
141. Hsieh, C.-H. *et al.* NADPH oxidase subunit 4 mediates cycling hypoxia-promoted radiation resistance in glioblastoma multiforme. *Free Radic. Biol. Med.* **53**, 649–658 (2012).
142. Crosas-Molist, E. *et al.* The NADPH oxidase NOX4 inhibits hepatocyte proliferation and liver cancer progression. *Free Radic. Biol. Med.* **69**, 338–347 (2014).
143. Kim, H. J. *et al.* Ubiquitin C-terminal hydrolase-L1 increases cancer cell invasion by modulating hydrogen peroxide generated via NADPH oxidase 4. *Oncotarget* **6**, 16287 (2015).

144. Lin, X.-L. *et al.* Overexpression of NOX4 predicts poor prognosis and promotes tumor progression in human colorectal cancer. *Oncotarget* **8**, 33586 (2017).
145. Nisimoto, Y., Jackson, H. M., Ogawa, H., Kawahara, T. & Lambeth, J. D. Constitutive NADPH-dependent electron transferase activity of the Nox4 dehydrogenase domain. *Biochemistry* **49**, 2433–2442 (2010).
146. Pandey, D. *et al.* SUMO1 negatively regulates reactive oxygen species production from NADPH oxidases. *Arterioscler. Thromb. Vasc. Biol.* **31**, 1634–1642 (2011).
147. Hilenski, L. L., Clempus, R. E., Quinn, M. T., Lambeth, J. D. & Griendling, K. K. Distinct subcellular localizations of Nox1 and Nox4 in vascular smooth muscle cells. *Arterioscler. Thromb. Vasc. Biol.* **24**, 677–683 (2004).
148. Chen, F., Haigh, S., Barman, S. A. & Fulton, D. From form to function: the role of Nox4 in the cardiovascular system. *Front. Physiol.* **3**, 412 (2012).
149. Siuda, D. *et al.* Transcriptional regulation of Nox4 by histone deacetylases in human endothelial cells. *Basic Res. Cardiol.* **107**, 283 (2012).
150. Tremaroli, V. & Bäckhed, F. Functional interactions between the gut microbiota and host metabolism. *Nature* **489**, 242 (2012).
151. Hill, C. *et al.* Expert consensus document: The international scientific association for probiotics and prebiotics consensus statement on the scope and appropriate use of the term probiotic. *Nat. Rev. Gastroenterol. Hepatol.* (2014) doi:10.1038/nrgastro.2014.66.
152. Yadav, H., Jain, S. & Sinha, P. R. Antidiabetic effect of probiotic dahi containing *Lactobacillus acidophilus* and *Lactobacillus casei* in high fructose fed rats. *Nutrition* (2007) doi:10.1016/j.nut.2006.09.002.

153. Yun, S. I., Park, H. O. & Kang, J. H. Effect of *Lactobacillus gasseri* BNR17 on blood glucose levels and body weight in a mouse model of type 2 diabetes. *J. Appl. Microbiol.* (2009) doi:10.1111/j.1365-2672.2009.04350.x.
154. Ejtahed, H. S. *et al.* Probiotic yogurt improves antioxidant status in type 2 diabetic patients. *Nutrition* (2012) doi:10.1016/j.nut.2011.08.013.
155. Asemi, Z., Zare, Z., Shakeri, H., Sabihi, S. S. & Esmailzadeh, A. Effect of multispecies probiotic supplements on metabolic profiles, hs-CRP, and oxidative stress in patients with type 2 diabetes. *Ann. Nutr. Metab.* (2013) doi:10.1159/000349922.
156. Cani, P. D., Geurts, L., Matamoros, S., Plovier, H. & Duparc, T. Glucose metabolism: Focus on gut microbiota, the endocannabinoid system and beyond. *Diabetes and Metabolism* (2014) doi:10.1016/j.diabet.2014.02.004.
157. Molska, M. & Reguła, J. Potential mechanisms of probiotics action in the prevention and treatment of colorectal cancer. *Nutrients* **11**, 2453 (2019).
158. Hendler, R. & Zhang, Y. Probiotics in the Treatment of Colorectal Cancer. *Medicines* (2018) doi:10.3390/medicines5030101.
159. Rafter, J. *et al.* Dietary synbiotics reduce cancer risk factors in polypectomized and colon cancer patients. *Am. J. Clin. Nutr.* (2007) doi:10.1093/ajcn/85.2.488.
160. Ishikawa, H. *et al.* Randomized trial of dietary fiber and *Lactobacillus casei* administration for prevention of colorectal tumors. *Int. J. Cancer* (2005) doi:10.1002/ijc.21115.
161. Pala, V. *et al.* Yogurt consumption and risk of colorectal cancer in the Italian European prospective investigation into cancer and nutrition cohort. *Int. J. Cancer* (2011) doi:10.1002/ijc.26193.

162. Mego, M. *et al.* Prevention of irinotecan induced diarrhea by probiotics: A randomized double blind, placebo controlled pilot study. *Complement. Ther. Med.* (2015) doi:10.1016/j.ctim.2015.03.008.
163. Österlund, P. *et al.* Lactobacillus supplementation for diarrhoea related to chemotherapy of colorectal cancer: A randomised study. *Br. J. Cancer* (2007) doi:10.1038/sj.bjc.6603990.
164. Fuccio, L. *et al.* Effects of probiotics for the prevention and treatment of radiation-induced diarrhea. *Journal of Clinical Gastroenterology* (2009) doi:10.1097/MCG.0b013e3181a1f59c.
165. Kotzampassi, K. *et al.* A Four-Probiotics Regimen Reduces Postoperative Complications after Colorectal Surgery: A Randomized, Double-Blind, Placebo-Controlled Study. *World J. Surg.* (2015) doi:10.1007/s00268-015-3071-z.
166. Krebs, B. Prebiotic and Synbiotic Treatment before Colorectal Surgery-- Randomised Double Blind Trial. *Coll. Antropol.* (2016).
167. Geagea, A. G. *et al.* A novel therapeutic approach to colorectal cancer in diabetes: role of metformin and rapamycin. *Oncotarget* **10**, 1284 (2019).
168. Kattar, S. Al *et al.* Metformin and Probiotics in the Crosstalk between Colitis-Associated Colorectal Cancer and Diabetes in Mice. *Cancers (Basel)*. **12**, 1857 (2020).
169. Fernández, A. M. *et al.* Functional inactivation of the IGF-I and insulin receptors in skeletal muscle causes type 2 diabetes. *Genes Dev.* **15**, 1926–1934 (2001).
170. Nishitsuji, K. *et al.* Analysis of the gut microbiome and plasma short-chain fatty acid profiles in a spontaneous mouse model of metabolic syndrome. *Sci. Rep.* **7**, 15876 (2017).

171. Thaker, A. I., Shaker, A., Rao, M. S. & Ciorba, M. A. Modeling colitis-associated cancer with azoxymethane (AOM) and dextran sulfate sodium (DSS). *J. Vis. Exp. JoVE* (2012).
172. Schloss, P. D. *et al.* Introducing mothur: open-source, platform-independent, community-supported software for describing and comparing microbial communities. *Appl. Environ. Microbiol.* **75**, 7537–7541 (2009).
173. Schloss, P. D. *et al.* Stabilization of the murine gut microbiome following weaning. *Gut Microbes* **3**, 383–393 (2012).
174. Vital, M., Karch, A. & Pieper, D. H. Colonic butyrate-producing communities in humans: an overview using omics data. *Msystems* **2**, e00130-17 (2017).
175. Schneeberger, M. *et al.* Akkermansia muciniphila inversely correlates with the onset of inflammation, altered adipose tissue metabolism and metabolic disorders during obesity in mice. *Sci. Rep.* **5**, 16643 (2015).
176. Roager, H. M., Licht, T. R., Poulsen, S. K., Larsen, T. M. & Bahl, M. I. Microbial enterotypes, inferred by the prevotella-to-bacteroides ratio, remained stable during a 6-month randomized controlled diet intervention with the new nordic diet. *Appl. Environ. Microbiol.* **80**, 1142–1149 (2014).
177. Chia, L. W. *et al.* Deciphering the trophic interaction between Akkermansia muciniphila and the butyrogenic gut commensal Anaerostipes caccae using a metatranscriptomic approach. *Antonie Van Leeuwenhoek* **111**, 859–873 (2018).
178. Kennedy, N. A. *et al.* The impact of different DNA extraction kits and laboratories upon the assessment of human gut microbiota composition by 16S rRNA gene sequencing. *PLoS One* **9**, e88982 (2014).
179. Sánchez, E., Laparra, J. M. & Sanz, Y. Discerning the role of Bacteroides fragilis

- in celiac disease pathogenesis. *Appl. Environ. Microbiol.* **78**, 6507–6515 (2012).
180. Yadav, H., Lee, J.-H., Lloyd, J., Walter, P. & Rane, S. G. Beneficial metabolic effects of a probiotic via butyrate-induced GLP-1 hormone secretion. *J. Biol. Chem.* **288**, 25088–25097 (2013).
181. Eeckhaut, V. *et al.* Butyricococcus pullicaecorum in inflammatory bowel disease. *Gut* **62**, 1745–1752 (2013).
182. Kurakawa, T. *et al.* Diversity of intestinal Clostridium coccoides group in the Japanese population, as demonstrated by reverse transcription-quantitative PCR. *PLoS One* **10**, e0126226 (2015).
183. Ramirez-Farias, C. *et al.* Effect of inulin on the human gut microbiota: stimulation of Bifidobacterium adolescentis and Faecalibacterium prausnitzii. *Br. J. Nutr.* **101**, 541–550 (2008).
184. Kageyama, A. & Benno, Y. Rapid detection of human fecal Eubacterium species and related genera by nested PCR method. *Microbiol. Immunol.* **45**, 315–318 (2001).
185. Lopez-Siles, M. *et al.* Mucosa-associated Faecalibacterium prausnitzii phylotype richness is reduced in patients with inflammatory bowel disease. *Appl. Environ. Microbiol.* **81**, 7582–7592 (2015).
186. Tong, J., Liu, C., Summanen, P., Xu, H. & Finegold, S. M. Application of quantitative real-time PCR for rapid identification of Bacteroides fragilis group and related organisms in human wound samples. *Anaerobe* **17**, 64–68 (2011).
187. Walker, A. W. *et al.* Dominant and diet-responsive groups of bacteria within the human colonic microbiota. *ISME J.* **5**, 220 (2011).
188. Eid, S. *et al.* mTORC2 signaling regulates Nox4-induced podocyte depletion in

- diabetes. *Antioxid. Redox Signal.* **25**, 703–719 (2016).
189. Parise, R. A., Shawaqfeh, M., Egorin, M. J. & Beumer, J. H. Liquid chromatography–mass spectrometric assay for the quantitation in human plasma of ABT-888, an orally available, small molecule inhibitor of poly (ADP-ribose) polymerase. *J. Chromatogr. B* **872**, 141–147 (2008).
190. Udden, S. M. N., Waliullah, S., Harris, M. & Zaki, H. The ex vivo colon organ culture and its use in antimicrobial host defense studies. *JoVE (Journal Vis. Exp.)* e55347 (2017).
191. Peterson, G. L. A simplification of the protein assay method of Lowry et al. which is more generally applicable. *Anal. Biochem.* **83**, 346–356 (1977).
192. Motulsky, H. *Analyzing data with GraphPad prism.* (GraphPad Software Incorporated, 1999).
193. Li, J. V *et al.* Metabolic surgery profoundly influences gut microbial–host metabolic cross-talk. *Gut* **60**, 1214–1223 (2011).
194. Shin, N.-R. *et al.* An increase in the Akkermansia spp. population induced by metformin treatment improves glucose homeostasis in diet-induced obese mice. *Gut* **63**, 727–735 (2014).
195. Everard, A. *et al.* Cross-talk between Akkermansia muciniphila and intestinal epithelium controls diet-induced obesity. *Proc. Natl. Acad. Sci.* **110**, 9066–9071 (2013).
196. Lukovac, S. *et al.* Differential modulation by Akkermansia muciniphila and Faecalibacterium prausnitzii of host peripheral lipid metabolism and histone acetylation in mouse gut organoids. *MBio* **5**, e01438-14 (2014).
197. Roopchand, D. E. *et al.* Dietary polyphenols promote growth of the gut

- bacterium *Akkermansia muciniphila* and attenuate high-fat diet-induced metabolic syndrome. *Diabetes* **64**, 2847–2858 (2015).
198. Plovier, H. *et al.* A purified membrane protein from *Akkermansia muciniphila* or the pasteurized bacterium improves metabolism in obese and diabetic mice. *Nat. Med.* **23**, 107 (2017).
199. Dao, M. C. *et al.* *Akkermansia muciniphila* and improved metabolic health during a dietary intervention in obesity: relationship with gut microbiome richness and ecology. *Gut* **65**, 426–436 (2016).
200. Kameyama, K. & Itoh, K. Intestinal colonization by a Lachnospiraceae bacterium contributes to the development of diabetes in obese mice. *Microbes Environ. ME14054* (2014).
201. Lippert, K. *et al.* Gut microbiota dysbiosis associated with glucose metabolism disorders and the metabolic syndrome in older adults. *Benef. Microbes* **8**, 545–556 (2017).
202. Peet, R. K. Relative diversity indices. *Ecology* **56**, 496–498 (1975).
203. Lozupone, C. & Knight, R. UniFrac: a new phylogenetic method for comparing microbial communities. *Appl. Environ. Microbiol.* **71**, 8228–8235 (2005).
204. Mandal, S. *et al.* Analysis of composition of microbiomes: a novel method for studying microbial composition. *Microb. Ecol. Health Dis.* **26**, 27663 (2015).
205. Segata, N. *et al.* Metagenomic biomarker discovery and explanation. *Genome Biol.* **12**, R60 (2011).
206. Everard, A. & Cani, P. D. Diabetes, obesity and gut microbiota. *Best Pract. Res. Clin. Gastroenterol.* **27**, 73–83 (2013).
207. Cani, P. D., Osto, M., Geurts, L. & Everard, A. Involvement of gut microbiota in

- the development of low-grade inflammation and type 2 diabetes associated with obesity. *Gut Microbes* **3**, 279–288 (2012).
208. Mandrup-Poulsen, T., Pickersgill, L. & Donath, M. Y. Blockade of interleukin 1 in type 1 diabetes mellitus. *Nat. Rev. Endocrinol.* **6**, 158 (2010).
209. Larsen, C. M. *et al.* Interleukin-1–receptor antagonist in type 2 diabetes mellitus. *N. Engl. J. Med.* **356**, 1517–1526 (2007).
210. Blakemore, A. I. F. *et al.* Interleukin-1 receptor antagonist allele (ILIRN* 2) associated with nephropathy in diabetes mellitus. *Hum. Genet.* **97**, 369–374 (1996).
211. Hasegawa, G. *et al.* Possible role of tumor necrosis factor and interleukin-1 in the development of diabetic nephropathy. *Kidney Int.* **40**, 1007–1012 (1991).
212. Banerjee, M. & Saxena, M. Interleukin-1 (IL-1) family of cytokines: role in type 2 diabetes. *Clin. Chim. acta* **413**, 1163–1170 (2012).
213. Eid, A. A., Lee, D.-Y., Roman, L. J., Khazim, K. & Gorin, Y. Sestrin 2 and AMPK connect hyperglycemia to Nox4-dependent eNOS uncoupling and matrix protein expression. *Mol. Cell. Biol.* MCB-00217 (2013).
214. Hakami, N. Y., Dusting, G. J. & Peshavariya, H. M. Trichostatin A, a histone deacetylase inhibitor suppresses NADPH Oxidase 4-Derived Redox Signalling and Angiogenesis. *J. Cell. Mol. Med.* **20**, 1932–1944 (2016).
215. Karlsson, C. L. J. *et al.* The microbiota of the gut in preschool children with normal and excessive body weight. *Obesity* **20**, 2257–2261 (2012).
216. Grasset, E. *et al.* A specific gut microbiota dysbiosis of type 2 diabetic mice induces GLP-1 resistance through an enteric NO-dependent and gut-brain axis mechanism. *Cell Metab.* **25**, 1075–1090 (2017).

217. Ellekilde, M. *et al.* Characterization of the gut microbiota in leptin deficient obese mice–Correlation to inflammatory and diabetic parameters. *Res. Vet. Sci.* **96**, 241–250 (2014).
218. Vijay-Kumar, M. *et al.* Metabolic syndrome and altered gut microbiota in mice lacking Toll-like receptor 5. *Science (80-.)*. **328**, 228–231 (2010).
219. Ko, S.-J. *et al.* Protective effect of *Laminaria japonica* with probiotics on murine colitis. *Mediators Inflamm.* **2014**, (2014).
220. Chassaing, B., Aitken, J. D., Malleshappa, M. & Vijay-Kumar, M. Dextran sulfate sodium (DSS)-induced colitis in mice. *Curr. Protoc. Immunol.* **104**, 15–25 (2014).
221. Kitajima, S., Takuma, S. & Morimoto, M. Histological analysis of murine colitis induced by dextran sulfate sodium of different molecular weights. *Exp. Anim.* **49**, 9–15 (2000).
222. Laroui, H. *et al.* Dextran sodium sulfate (DSS) induces colitis in mice by forming nano-lipocomplexes with medium-chain-length fatty acids in the colon. *PLoS One* **7**, e32084 (2012).
223. Perše, M. & Cerar, A. Dextran sodium sulphate colitis mouse model: traps and tricks. *Biomed Res. Int.* **2012**, (2012).
224. Melgar, S. *et al.* Validation of murine dextran sulfate sodium-induced colitis using four therapeutic agents for human inflammatory bowel disease. *Int. Immunopharmacol.* **8**, 836–844 (2008).
225. Hata, K. *et al.* C57BL/KsJ-db/db-ApcMin/+ mice exhibit an increased incidence of intestinal neoplasms. *Int. J. Mol. Sci.* **12**, 8133–8145 (2011).
226. Desbonnet, L. *et al.* Gut microbiota depletion from early adolescence in mice:

- Implications for brain and behaviour. *Brain. Behav. Immun.* **48**, 165–173 (2015).
227. Deshmukh, H. S. *et al.* The microbiota regulates neutrophil homeostasis and host resistance to *Escherichia coli* K1 sepsis in neonatal mice. *Nat. Med.* **20**, 524 (2014).
228. Winek, K. *et al.* Depletion of cultivatable gut microbiota by broad-spectrum antibiotic pretreatment worsens outcome after murine stroke. *Stroke* **47**, 1354–1363 (2016).
229. Heimesaat, M. M. *et al.* Gram-negative bacteria aggravate murine small intestinal Th1-type immunopathology following oral infection with *Toxoplasma gondii*. *J. Immunol.* **177**, 8785–8795 (2006).
230. Li, G. *et al.* Intermittent fasting promotes white adipose browning and decreases obesity by shaping the gut microbiota. *Cell Metab.* **26**, 672–685 (2017).
231. Lau, K. *et al.* Inhibition of type 1 diabetes correlated to a *Lactobacillus johnsonii* N6. 2-mediated Th17 bias. *J. Immunol.* 1001864 (2011).
232. Karlsson, F. H. *et al.* Gut metagenome in European women with normal, impaired and diabetic glucose control. *Nature* **498**, 99–103 (2013).
233. Dubourg, G. *et al.* High-level colonisation of the human gut by Verrucomicrobia following broad-spectrum antibiotic treatment. *Int. J. Antimicrob. Agents* **41**, 149–155 (2013).
234. Kubickova, B., Babica, P., Hilscherová, K. & Šindlerová, L. Effects of cyanobacterial toxins on the human gastrointestinal tract and the mucosal innate immune system. *Environ. Sci. Eur.* **31**, 31 (2019).
235. Belzer, C. & De Vos, W. M. Microbes inside—from diversity to function: the case of *Akkermansia*. *ISME J.* **6**, 1449–1458 (2012).

236. Johansson, M. E. V, Larsson, J. M. H. & Hansson, G. C. The two mucus layers of colon are organized by the MUC2 mucin, whereas the outer layer is a legislator of host–microbial interactions. *Proc. Natl. Acad. Sci.* **108**, 4659–4665 (2011).
237. Santacruz, A. *et al.* Gut microbiota composition is associated with body weight, weight gain and biochemical parameters in pregnant women. *Br. J. Nutr.* **104**, 83–92 (2010).
238. Everard, A. *et al.* Responses of gut microbiota and glucose and lipid metabolism to prebiotics in genetic obese and diet-induced leptin-resistant mice. *Diabetes* **60**, 2775–2786 (2011).
239. Li, D. *et al.* High expression of liver histone deacetylase 3 contributes to high-fat-diet-induced metabolic syndrome by suppressing the PPAR- γ and LXR- α -pathways in E3 rats. *Mol. Cell. Endocrinol.* **344**, 69–80 (2011).
240. Masui, R. *et al.* G protein-coupled receptor 43 moderates gut inflammation through cytokine regulation from mononuclear cells. *Inflamm. Bowel Dis.* **19**, 2848–2856 (2013).
241. Remely, M. *et al.* Effects of short chain fatty acid producing bacteria on epigenetic regulation of FFAR3 in type 2 diabetes and obesity. *Gene* **537**, 85–92 (2014).
242. Kaji, I., Karaki, S. & Kuwahara, A. Short-chain fatty acid receptor and its contribution to glucagon-like peptide-1 release. *Digestion* **89**, 31–36 (2014).
243. Kong, G. *et al.* The ketone metabolite β -hydroxybutyrate attenuates oxidative stress in spinal cord injury by suppression of class I histone deacetylases. *J. Neurotrauma* **34**, 2645–2655 (2017).

244. Manea, S.-A. *et al.* Epigenetic regulation of vascular NADPH oxidase expression and reactive oxygen species production by histone deacetylase-dependent mechanisms in experimental diabetes. *Redox Biol.* **16**, 332–343 (2018).
245. Chen, F. *et al.* Inhibition of histone deacetylase reduces transcription of NADPH oxidases and ROS production and ameliorates pulmonary arterial hypertension. *Free Radic. Biol. Med.* **99**, 167–178 (2016).
246. Rafehi, H. *et al.* Vascular histone deacetylation by pharmacological HDAC inhibition. *Genome Res.* **24**, 1271–1284 (2014).
247. McGee-Lawrence, M. E., White, T. A., LeBrasseur, N. K. & Westendorf, J. J. Conditional deletion of Hdac3 in osteoprogenitor cells attenuates diet-induced systemic metabolic dysfunction. *Mol. Cell. Endocrinol.* **410**, 42–51 (2015).
248. Cho, H., Seok, Y., Lee, H., Song, M. & Kim, I. Repression of Transcriptional Activity of Forkhead Box O1 by Histone Deacetylase Inhibitors Ameliorates Hyperglycemia in Type 2 Diabetic Rats. *Int. J. Mol. Sci.* **19**, 3539 (2018).
249. Remsberg, J. R. *et al.* Deletion of histone deacetylase 3 in adult beta cells improves glucose tolerance via increased insulin secretion. *Mol. Metab.* **6**, 30–37 (2017).
250. Larsen, L. *et al.* Inhibition of histone deacetylases prevents cytokine-induced toxicity in beta cells. *Diabetologia* **50**, 779–789 (2007).
251. Chen, W.-B. *et al.* Conditional ablation of HDAC3 in islet beta cells results in glucose intolerance and enhanced susceptibility to STZ-induced diabetes. *Oncotarget* **7**, 57485 (2016).
252. Hong, S. *et al.* Dissociation of muscle insulin sensitivity from exercise endurance in mice by HDAC3 depletion. *Nat. Med.* **23**, 223 (2017).

253. Xia, J., Hu, H., Xue, W., Wang, X. S. & Wu, S. The discovery of novel HDAC3 inhibitors via virtual screening and in vitro bioassay. *J. Enzyme Inhib. Med. Chem.* **33**, 525–535 (2018).
254. Gryder, B. E. *et al.* Chemical genomics reveals histone deacetylases are required for core regulatory transcription. *Nat. Commun.* **10**, 3004 (2019).
255. Said, H. S. *et al.* Dysbiosis of salivary microbiota in inflammatory bowel disease and its association with oral immunological biomarkers. *DNA Res.* **21**, 15–25 (2013).
256. Bersudsky, M. *et al.* Non-redundant properties of IL-1 α and IL-1 β during acute colon inflammation in mice. *Gut* **63**, 598–609 (2014).
257. Bauer, C., Duewell, P., Lehr, H.-A., Endres, S. & Schnurr, M. Protective and aggravating effects of Nlrp3 inflammasome activation in IBD models: influence of genetic and environmental factors. *Dig. Dis.* **30**, 82–90 (2012).
258. Westbrook, A. M., Wei, B., Braun, J. & Schiestl, R. H. Intestinal mucosal inflammation leads to systemic genotoxicity in mice. *Cancer Res.* (2009) doi:10.1158/0008-5472.CAN-08-4416.
259. Katsurano, M. *et al.* Early-stage formation of an epigenetic field defect in a mouse colitis model, and non-essential roles of T- and B-cells in DNA methylation induction. *Oncogene* (2012) doi:10.1038/onc.2011.241.
260. Voronov, E. & Apte, R. N. IL-1 in Colon Inflammation, Colon Carcinogenesis and Invasiveness of Colon Cancer. *Cancer Microenviron.* (2015) doi:10.1007/s12307-015-0177-7.
261. Park, J. *et al.* Short chain fatty acids induce both effector and regulatory T cells by suppression of histone deacetylases and regulation of the mTOR-S6K

- pathway. *Mucosal Immunol.* **8**, 80 (2015).
262. Bereswill, S. *et al.* Novel murine infection models provide deep insights into the “menage a trois” of *Campylobacter jejuni*, microbiota and host innate immunity. *PLoS One* **6**, e20953 (2011).
263. Robert, S. *et al.* Oral delivery of glutamic acid decarboxylase (GAD)-65 and IL10 by *Lactococcus lactis* reverses diabetes in recent-onset NOD mice. *Diabetes* DB_131236 (2014).
264. Galvan, D. L. & Danesh, F. R. Paradoxical role of IL-17 in progression of diabetic nephropathy. (2016).
265. Chen, H., Ren, X., Liao, N. & Wen, F. Th17 cell frequency and IL-17A concentrations in peripheral blood mononuclear cells and vitreous fluid from patients with diabetic retinopathy. *J. Int. Med. Res.* **44**, 1403–1413 (2016).
266. Thallas-Bonke, V., Jandeleit-Dahm, K. A. M. & Cooper, M. E. Nox-4 and progressive kidney disease. *Curr. Opin. Nephrol. Hypertens.* **24**, 74–80 (2015).
267. Gray, S. P. *et al.* Nox1 plays a key role in diabetes accelerated atherosclerosis. *Circulation* CIRCULATIONAHA-112 (2013).
268. Vieira, E. L. M. *et al.* Oral administration of sodium butyrate attenuates inflammation and mucosal lesion in experimental acute ulcerative colitis. *J. Nutr. Biochem.* **23**, 430–436 (2012).
269. Davie, J. R. Inhibition of histone deacetylase activity by butyrate. *J. Nutr.* **133**, 2485S-2493S (2003).
270. Ye, J. & Gao, Z. Metabolic Benefits to Butyrate as a Chronic Diet Supplement. (2013).
271. Roshanravan, N. *et al.* Effect of butyrate and inulin supplementation on glycemic

- status, lipid profile and glucagon-like peptide 1 level in patients with type 2 diabetes: A randomized double-blind, placebo-controlled trial. *Horm. Metab. Res.* **49**, 886–891 (2017).
272. Kimura, I. *et al.* The gut microbiota suppresses insulin-mediated fat accumulation via the short-chain fatty acid receptor GPR43. *Nat. Commun.* **4**, 1829 (2013).
273. Tazoe, H. *et al.* Roles of short-chain fatty acids receptors, GPR41 and GPR43 on colonic functions. in *Journal of Physiology and Pharmacology* (2008).
274. Tappenden, K. A., Thomson, A. B. R., Wild, G. E. & Mcburney, M. I. Short-chain fatty acids increase proglucagon and ornithine decarboxylase messenger RNAs after intestinal resection in rats. *J. Parenter. Enter. Nutr.* (1996) doi:10.1177/0148607196020005357.
275. Tolhurst, G. *et al.* Short-chain fatty acids stimulate glucagon-like peptide-1 secretion via the G-protein-coupled receptor FFAR2. *Diabetes* (2012) doi:10.2337/db11-1019.
276. Nøhr, M. K. *et al.* GPR41/FFAR3 and GPR43/FFAR2 as cosensors for short-chain fatty acids in enteroendocrine cells vs FFAR3 in enteric neurons and FFAR2 in enteric leukocytes. *Endocrinology* (2013) doi:10.1210/en.2013-1142.
277. Zaibi, M. S. *et al.* Roles of GPR41 and GPR43 in leptin secretory responses of murine adipocytes to short chain fatty acids. *FEBS Lett.* (2010) doi:10.1016/j.febslet.2010.04.027.
278. Lin, H. V. *et al.* Butyrate and propionate protect against diet-induced obesity and regulate gut hormones via free fatty acid receptor 3-independent mechanisms. *PLoS One* (2012) doi:10.1371/journal.pone.0035240.

279. Lovshin, J. A. & Drucker, D. J. Incretin-based therapies for type 2 diabetes mellitus. *Nature Reviews Endocrinology* (2009) doi:10.1038/nrendo.2009.48.

APPENDIX 1

Publications related to the thesis

- **Noureldein, Mohamed H.**, Sara Bitar, Natalie Youssef, Sami Azar, and Assaad A. Eid. "Butyrate modulates diabetes-linked gut dysbiosis: epigenetic and mechanistic modifications." *Journal of molecular endocrinology* 64, no. 1 (2020): 29-42.
- Youssef, Natalie, **Mohamed Noureldein**, Georges Daoud, and Assaad A. Eid. "Immune Checkpoint Inhibitors and Diabetes: Mechanisms and Predictors." *Diabetes & Metabolism* (2020).
- **Noureldein, Mohamed H.**, Batoul A. Dia, Ali I. Nabbouh, and Assaad A. Eid. "Promising anti-diabetic effect of dextran sulfate sodium: Is it its clinical come back?" *Diabetes Research and Clinical Practice* 159 (2020): 107661.
- Mroueh, Fatima Mohsen, **Mohamed Noureldein**, Youssef H. Zeidan, Suzan Boutary, Sara Abou Merhi Irani, Stéphanie Eid, Mary Haddad *et al.* "Unmasking the interplay between mTOR and Nox4: novel insights into the mechanism connecting diabetes and cancer." *The FASEB Journal* 33, no. 12 (2019): 14051-14066.
- **Noureldein, Mohamed H.**, and Assaad A. Eid. "Gut microbiota and mTOR signaling: insight on a new pathophysiological interaction." *Microbial pathogenesis* 118 (2018): 98-104.

Submitted Articles

- **Noureldein, Mohamed H.**, Sara Bitar, Rashad Nawfal, Lama Ammar, and Assaad A. Eid. "Role Of Microbiota In Diabetes-Associated Colorectal Cancer." *Gastroenterology*. Submitted October 2020.

Conferences

- Oral presentation “Role of gut microbiota on mediating diabetic complications: Epigenomics perspective” at the Gordon Research Conference on Epigenomics of Diabetes and Other Metabolic Diseases held May 27, 2018 - June 01, 2018 at Regal Riverside Hotel in Hong Kong, China.
- Poster presentation “Role of microbiota in diabetes-associated colorectal cancer” at for the American Diabetes Association's 80th Scientific Sessions, June 12 - 16, 2020, in Chicago, IL. Abstract published in Diabetes journal:
NOURELDEIN, MOHAMED H., and ASSAAD A. EID. "1646-P: Role Of Microbiota In Diabetes-Associated Colorectal Cancer." (2020).

APPENDIX 2

Analysis of microbiota using mothur

```
set.dir(input=~/Desktop/MOE/Moe_seq_data/1/2, output=~/Desktop/MOE/out
put)
make.contigs(file=.files, processors=32)
screen.seqs(fasta=current, group=current, maxambig=0, maxlength=275)
unique.seqs(fasta=current)
count.seqs(name=current, group=current)
summary.seqs(count=current)
align.seqs(fasta= current, reference=silva.nr_v132.pcr.align)
summary.seqs(fasta= current, count= current)
screen.seqs(fasta=current, count=current, summary=current, start=1968,
end=11550, maxhomop=8)
summary.seqs(fasta= current, count= current)
filter.seqs(fasta=current, vertical=T, trump=.)
unique.seqs(fasta=current, count=current)
pre.cluster(fasta=current, count=current, diffs=2)
chimera.vsearch(fasta=current, count=current, dereplicate=t)
remove.seqs(fasta=current, accnos=current)
summary.seqs(fasta=current, count=current)
classify.seqs(fasta=current, count=current, reference= trainset16_0220
16.rdp.fasta, taxonomy= trainset16_022016.rdp.tax, cutoff=80)
remove.lineage(fasta=current, count=current, taxonomy=current, taxon=C
hloroplast-Mitochondria-unknown-Archaea-Eukaryota)
summary.tax(taxonomy=current, count=current)
dist.seqs(fasta=current, cutoff=0.03)
cluster(column=current, count=current)
make.shared(list=current, count=current, label=0.03)
rarefaction.single(shared=current)
dist.seqs(fasta=current, cutoff=0.03)
cluster(column=current, count=current)
cluster.split(fasta=current, count=current, taxonomy=current, splitmet
hod=classify, taxlevel=4, cutoff=0.03)
make.shared(list=current, count=current, label=0.03)
```

```

classify.otu(list=current, count=current, taxonomy=current, label=0.03
)
phylotype(taxonomy=current)
make.shared(list=current, count=current, label=1)
classify.otu(list=current, count=current, taxonomy=current, label=1)
dist.seqs(fasta=current, output=lt, processors=8)
clearcut(phylip=current)

rename.file(taxonomy=.trim.contigs.good.unique.good.filter.unique.prec
luster.pick.pick.opti_mcc.0.03.cons.taxonomy, shared= .trim.contigs.go
od.unique.good.filter.unique.precluster.pick.pick.opti_mcc.shared)
count.groups(shared=.opti_mcc.shared)

sub.sample(shared= current, size= least number of sequences in sample)
rarefaction.single(shared=current, calc=sobs, freq=100)

summary.single(shared=current, calc=nseqs-coverage-sobs-invsimpson, su
bsample=T)

dist.shared(shared=current, calc=thetayc-jclass, subsample=t)

pcoa(phylip=current)
nmds(phylip=current)
nmds(phylip=current, mindim=3, maxdim=3)
amova(phylip=current, design=.design)
homova(phylip=current, design=current)

corr.axes(axes=.opti_mcc.0.03.subsample.jclass.0.03.lt.ave.nmds.axes,
shared=current, method=spearman, numaxes=3)

get.communitytype(shared=current)

metastats(shared=current, design=current)

lefse(shared=current, design=current)

phylo.diversity(tree=.trim.contigs.good.unique.good.filter.unique.prec
luster.pick.pick.phylip.tre, count=.denovo.vsearch.pick.pick.count_tab
le, rarefy=T)

unifrac.unweighted(tree=current, count=current, distance=lt, processor
s=2, random=F, subsample=t)

unifrac.weighted(tree=current, count=current, distance=lt, processors=
2, random=F, subsample=t)

make.biom(shared= exp1.opti_mcc.0.03.subsample.shared, constaxonomy= e
xp1.taxonomy, metadata=.metadata file)

```

Analysis and visualization on R

```

# Install the following packages (Phyloseq, vegan, ggplot2).
install.packages("ggplot2")

```

```

install.packages("vegan")
if (!requireNamespace("BiocManager", quietly = TRUE))
  install.packages("BiocManager")
BiocManager::install("phyloseq")

# Load the installed packages
library("phyloseq")
library("ggplot2")
library("vegan")

ps <- import_biom("MKR-table.w_omd.biom", treefilename="tree.nwk")
map <- import_qiime_sample_data("MKR-metadata.tsv")
ps <- merge_phyloseq(ps, map)

#Plot core graphs (rarefaction, family, species)
rarecurve(t(otu_table(ps)), step=50, cex=0.5)
plot_bar(ps, fill="Rank2") + facet_wrap(~condition, scales = "free_x",
nrow = 1)
plot_richness(ps, x="condition", color="condition", measures=c("Observed"))
plot_richness(ps, x="condition", measures=c("Observed", "Shannon")) +
geom_boxplot()

#Plot PCoA
sample_data(ps)[ , 2] <- sample_data(ps)[ ,1]
my.PCoA2 <- ordinate(ps, "PCoA", "bray")
plot_ordination(ps, my.PCoA2, type = "samples", color = "condition")+
geom_point(size=3)

# PCoA plot using the unweighted UniFrac as distance
wunifrac_dist = phyloseq::distance(ps, method="unifrac", weighted=F)
ordination = ordinate(ps, method="PCoA", distance=wunifrac_dist)
plot_ordination(ps, ordination, color="condition") + theme(aspect.ratio=1)+
  ggtitle("PCoA: unweigthed Unifrac")+geom_point(size=3)

#Plot PCoA (another method)
wunifrac_dist = phyloseq::distance(ps, method="unifrac", weighted=T)

```

```

ordUF = ordinate(ps, method="PCoA", distance=wunifrac_dist)
plot_ordination(ps, ordUF, color = "condition") +
  ggtitle("PCoA: unweigthed Unifrac")+geom_point(size=3)

# PCoA plot using the unweighted UniFrac as distance
wunifrac_dist = phyloseq::distance(ps, method="unifrac", weighted=F)
ordination = ordinate(ps, method="PCoA", distance=wunifrac_dist)
plot_ordination(ps, ordination, color="condition") + theme(aspect.ratio=1)

plot_heatmap(ps)
plot_bar(ps, fill="Genus")
plot_bar(ps, x="condition", fill="l6")
plot_tree(ps, color="condition", label.tips="taxa_names", ladderize="left", plot.margin=0.3)

#Plot each phyllum alone
prevelancedf = apply(X = otu_table(ps),
  MARGIN = 1,
  FUN = function(x){sum(x > 0)})
# Add taxonomy and total read counts to this data.frame
prevelancedf = data.frame(Prevalence = prevelancedf,
  TotalAbundance = taxa_sums(ps),
  tax_table(ps))
prevelancedf[1:10,]

prevelancedf1 = subset(prevelancedf, Phylum %in% get_taxa_unique(ps, taxonomic.rank = "Phylum"))
ggplot(prevelancedf1, aes(TotalAbundance, Prevalence / nsamples(ps), color=Phylum)) +
  # Include a guess for parameter
  geom_hline(yintercept = 0.05, alpha = 0.5, linetype = 2) + geom_point(size = 2, alpha = 0.7) +
  scale_x_log10() + xlab("Total Abundance") + ylab("Prevalence [Frac. Samples]") +
  facet_wrap(~Phylum) + theme(legend.position="none")

```

Analysis of microbiota using qiime2

Activate qiime2 environment

```
conda activate /opt/miniconda3/envs/qiime2-2020.2
```

Import Data

```
qiime tools import \  
  --type 'SampleData[PairedEndSequencesWithQuality]' \  
  --input-path microbiota \  
  --input-format CasavaOneEightSingleLanePerSampleDirFmt \  
  --output-path demux-paired-end.qza
```

Obtain a summary of the demultiplexed data

```
qiime demux summarize \  
  --i-data demux-paired-end.qza \  
  --o-visualization demux.qzv  
qiime tools view demux.qzv
```

Quality control and feature table construction

```
qiime dada2 denoise-single \  
  --i-demultiplexed-seqs demux-paired-end.qza \  
  --p-trim-left 0 \  
  --p-trunc-len 120 \  
  --o-representative-sequences rep-seqs.qza \  
  --o-table table.qza \  
  --o-denoising-stats stats.qza  
  
qiime metadata tabulate \  
  --m-input-file stats.qza \  
  --o-visualization stats.qzv  
  
qiime tools view stats.qzv  
  
qiime feature-table tabulate-seqs \  
  --i-table table.qza \  
  --o-feature-table feature-table.qza
```

```
--i-data rep-seqs.qza \  
--o-visualization rep-seqs.qzv  
qiime tools view rep-seqs.qzv
```

Classification

```
qiime feature-classifier classify-sklearn \  
--i-classifier gg-13-8-99-515-806-nb-classifier.qza \  
--i-reads rep-seqs.qza \  
--o-classification taxonomy.qza  
  
qiime metadata tabulate \  
--m-input-file taxonomy.qza \  
--o-visualization taxonomy.qzv
```

Generate a tree for phylogenetic diversity analyses

```
qiime phylogeny align-to-tree-mafft-fasttree \  
--i-sequences rep-seqs.qza \  
--o-alignment aligned-rep-seqs.qza \  
--o-masked-alignment masked-aligned-rep-seqs.qza \  
--o-tree unrooted-tree.qza \  
--o-rooted-tree rooted-tree.qza
```

Filter data by experiment

```
qiime feature-table filter-samples \  
--i-table table.qza \  
--m-metadata-file lexp2-metadata.tsv \  
--o-filtered-table lexp2-table.qza  
qiime feature-table summarize \  
--i-table lexp2-table.qza \  
--o-visualization lexp2-table.qzv \  
--m-sample-metadata-file lexp2-metadata.tsv
```

Alpha and beta diversity

```
qiime diversity core-metrics-phylogenetic \  

```

```

--i-phylogeny rooted-tree.qza \
--i-table lexp2-table.qza \
--p-sampling-depth 26993 \
--m-metadata-file lexp2-metadata.tsv \
--output-dir lexp2-core-metrics-results

qiime diversity alpha-group-significance \
  --i-alpha-diversity lexp2-core-metrics-results/faith_pd_vector.qza \
  --m-metadata-file lexp2-metadata.tsv \
  --o-visualization lexp2-core-metrics-results/faith-pd-group-significance.qzv

qiime diversity alpha-group-significance \
  --i-alpha-diversity lexp2-core-metrics-results/evenness_vector.qza \
  --m-metadata-file lexp2-metadata.tsv \
  --o-visualization lexp2-core-metrics-results/evenness-group-significance.qzv

qiime diversity beta-group-significance \
  --i-distance-matrix lexp2-core-metrics-results/unweighted_unifrac_distance_matrix.qza \
  --m-metadata-file lexp2-metadata.tsv \
  --m-metadata-column condition \
  --o-visualization lexp2-core-metrics-results/unweighted-unifrac-condition-significance.qzv \
  --p-pairwise

qiime diversity beta-group-significance \
  --i-distance-matrix lexp2-core-metrics-results/unweighted_unifrac_distance_matrix.qza \
  --m-metadata-file lexp2-metadata.tsv \
  --m-metadata-column time point \
  --o-visualization lexp2-core-metrics-results/unweighted-unifrac-time-point-significance.qzv \
  --p-pairwise

qiime emperor plot \

```

```

--i-pcoa lexp2-core-metrics-results/unweighted_unifrac_pcoa_results.
qza \
--m-metadata-file lexp2-metadata.tsv \
--o-visualization lexp2-core-metrics-results/unweighted-unifrac-empe
ror.qzv

qiime emperor plot \
--i-pcoa lexp2-core-metrics-results/bray_curtis_pcoa_results.qza \
--m-metadata-file lexp2-metadata.tsv \
--o-visualization lexp2-core-metrics-results/bray-curtis-emperor.qzv

qiime diversity alpha-rarefaction \
--i-table lexp2-table.qza \
--i-phylogeny rooted-tree.qza \
--p-max-depth 4000 \
--m-metadata-file lexp2-metadata.tsv \
--o-visualization lexp2-alpha-rarefaction.qzv

qiime taxa barplot \
--i-table lexp2-table.qza \
--i-taxonomy taxonomy.qza \
--m-metadata-file lexp2-metadata.tsv \
--o-visualization lexp2-taxa-bar-plots.qzv

```

Differential abundance testing with ANCOM

```

qiime composition add-pseudocount \
--i-table lexp2-table.qza \
--o-composition-table comp-lexp2-table.qza

qiime composition ancom \
--i-table comp-lexp2-table.qza \
--m-metadata-file lexp2-metadata.tsv \
--m-metadata-column condition \
--o-visualization ancom-lexp2.qzv

```

Performing a differential abundance test at a specific taxonomic level.


```

qiime taxa collapse \
  --i-table lexp2-table.qza \
  --i-taxonomy taxonomy.qza \
  --p-level 2 \
  --o-collapsed-table lexp2-table-l2.qza

qiime composition add-pseudocount \
  --i-table lexp2-table-l2.qza \
  --o-composition-table comp-lexp2-table-l2.qza

qiime composition ancom \
  --i-table comp-lexp2-table-l2.qza \
  --m-metadata-file lexp2-metadata.tsv \
  --m-metadata-column condition \
  --o-visualization ancom-lexp2-table-l2.qzv

qiime gneiss correlation-clustering \
  --i-table lexp2-table.qza \
  --o-clustering lexp2-hierarchy.qza

qiime gneiss dendrogram-heatmap \
  --i-table lexp2-table.qza \
  --i-tree lexp2-hierarchy.qza \
  --m-metadata-file lexp2-metadata.tsv \
  --m-metadata-column condition \
  --p-color-map seismic \
  --o-visualization lexp2-heatmap.qzv

```

Export to biom hdf5

```

qiime tools export \
  --input-path taxonomy.qza \
  --output-path taxonomy.biom

qiime tools export \
  --input-path lexp2-table.qza \

```

```
--output-path lexp2-table.biom

#append taxonomy classification to feature table and convert to biom format

biom add-metadata -i lexp2-table.biom/feature-table.biom -o lexp2-table.w_omd.biom --observation-metadata-fp taxonomy.biom/taxonomy.tsv --observation-header OTUID,taxonomy --sc-separated taxonomy
```

Visualization

```
qiime tools view taxonomy.qzv
qiime tools view lexp2-table.qzv
qiime tools view lexp2-core-metrics-results/unweighted_unifrac_emperor.qzv
qiime tools view lexp2-core-metrics-results/faith-pd-group-significance.qzv
qiime tools view lexp2-core-metrics-results/evenness-group-significance.qzv
qiime tools view lexp2-core-metrics-results/unweighted-unifrac-condition-significance.qzv
qiime tools view lexp2-core-metrics-results/unweighted-unifrac-time-point-significance.qzv
qiime tools view lexp2-core-metrics-results/bray-curtis-emperor.qzv
qiime tools view lexp2-core-metrics-results/unweighted-unifrac-emperor.qzv
qiime tools view lexp2-alpha-rarefaction.qzv
qiime tools view lexp2-taxa-bar-plots.qzv
qiime tools view ancom-lexp2.qzv
qiime tools view ancom-lexp2-table-l2.qzv
qiime tools view lexp2-heatmap.qzv
```

Export the following files to be used in R-phyloseq

```
feature table in biom format
taxonomy (export as tsv)
re_seq_file.fasta
tree.nwk
metadata.tsv
```

APPENDIX 3

Supplementary Figures

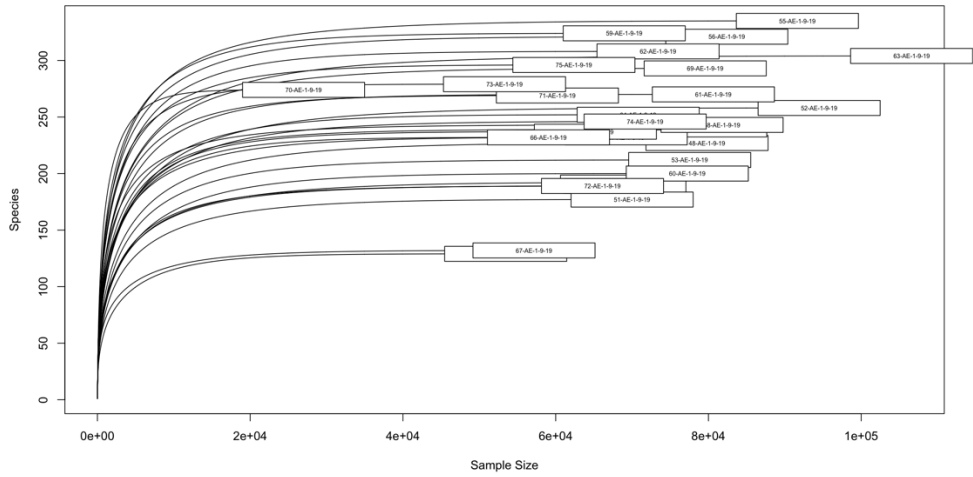


Figure 1: Rarefaction curve of samples of control, diabetic and colorectal cancer mice.

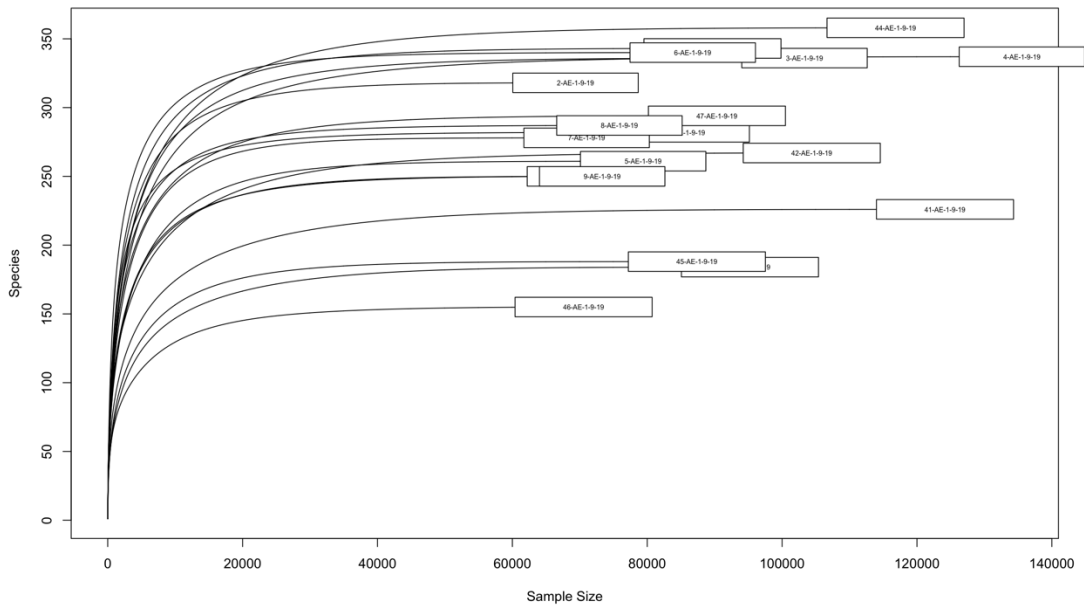


Figure 2: Rarefaction curve of samples of the control, diabetic and probiotics-treated mice.

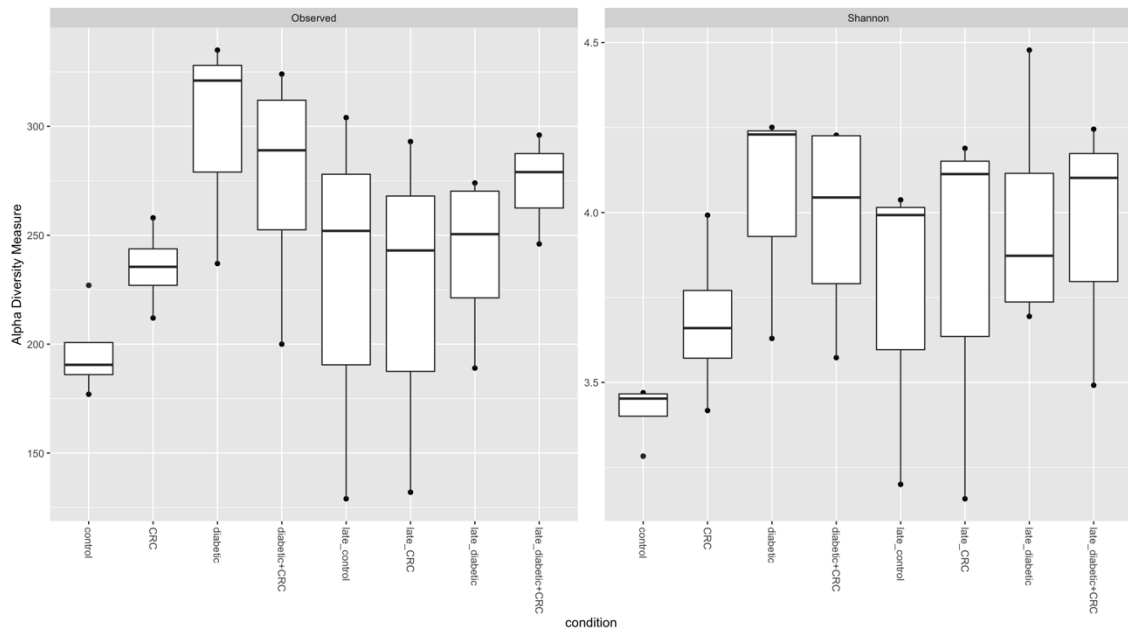


Figure 3: Alpha diversity per sample in control, diabetic, colorectal cancer mice.

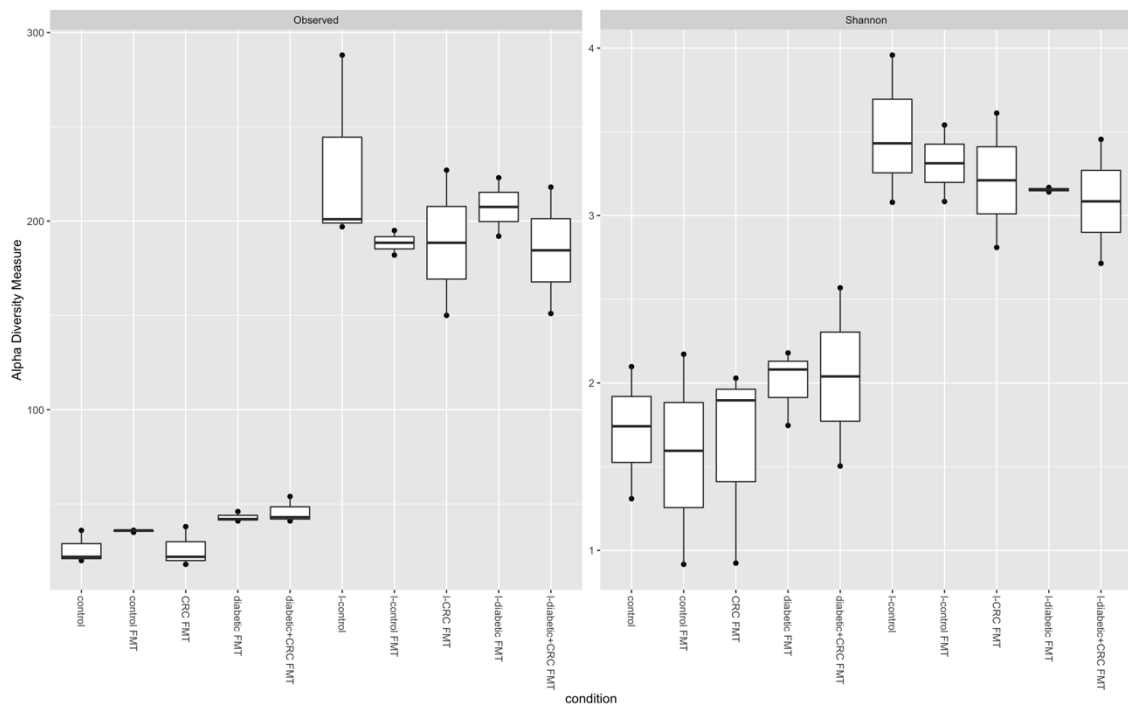


Figure 4: Alpha diversity per sample in antibiotic-treated mice.

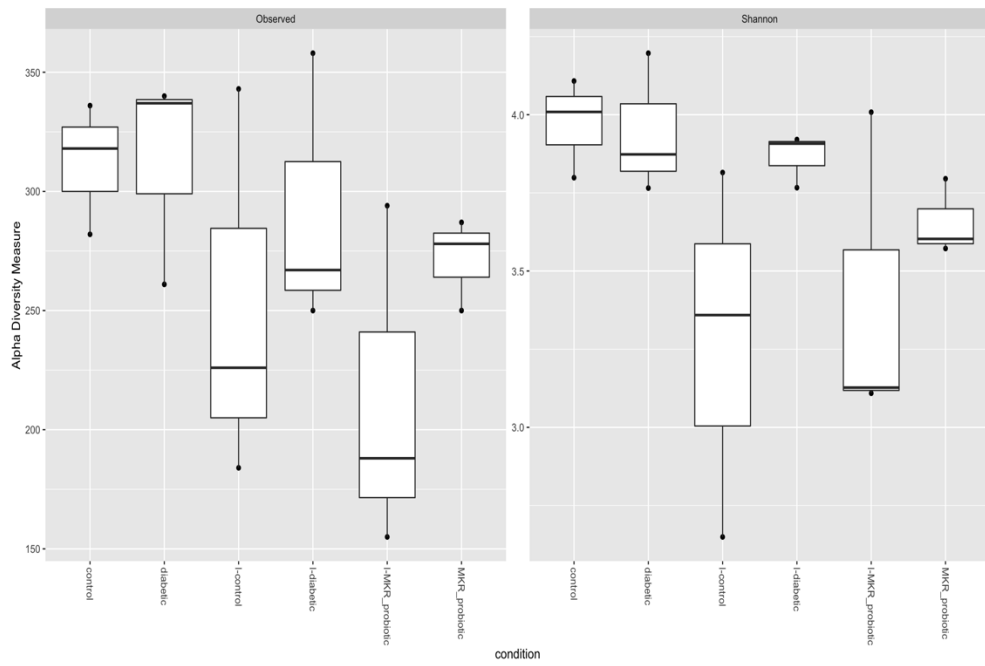


Figure 5: Alpha diversity per sample in control, diabetic and probiotics-treated mice.

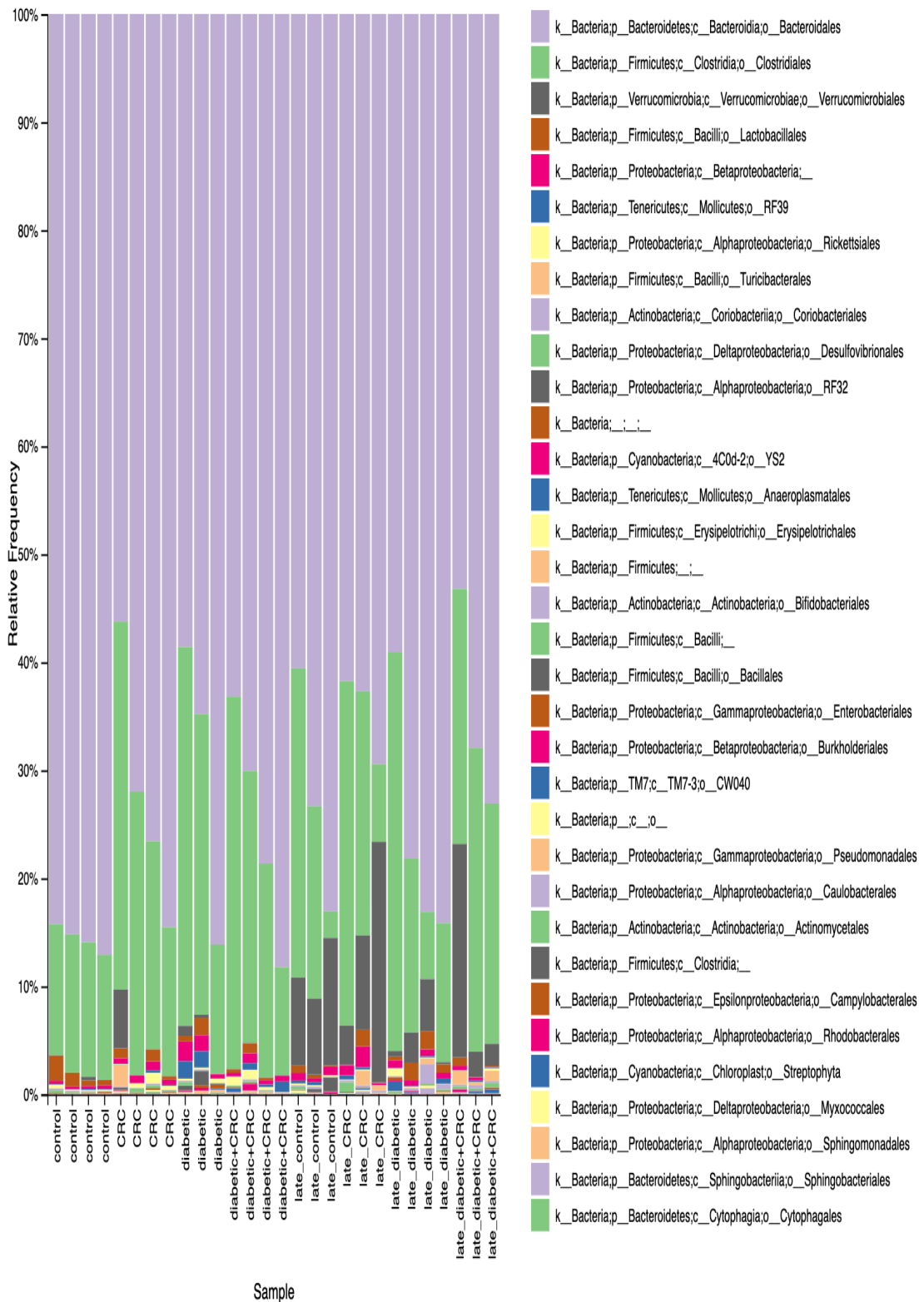


Figure 6: Different bacterial families per sample in control, diabetic and colorectal cancer mice.

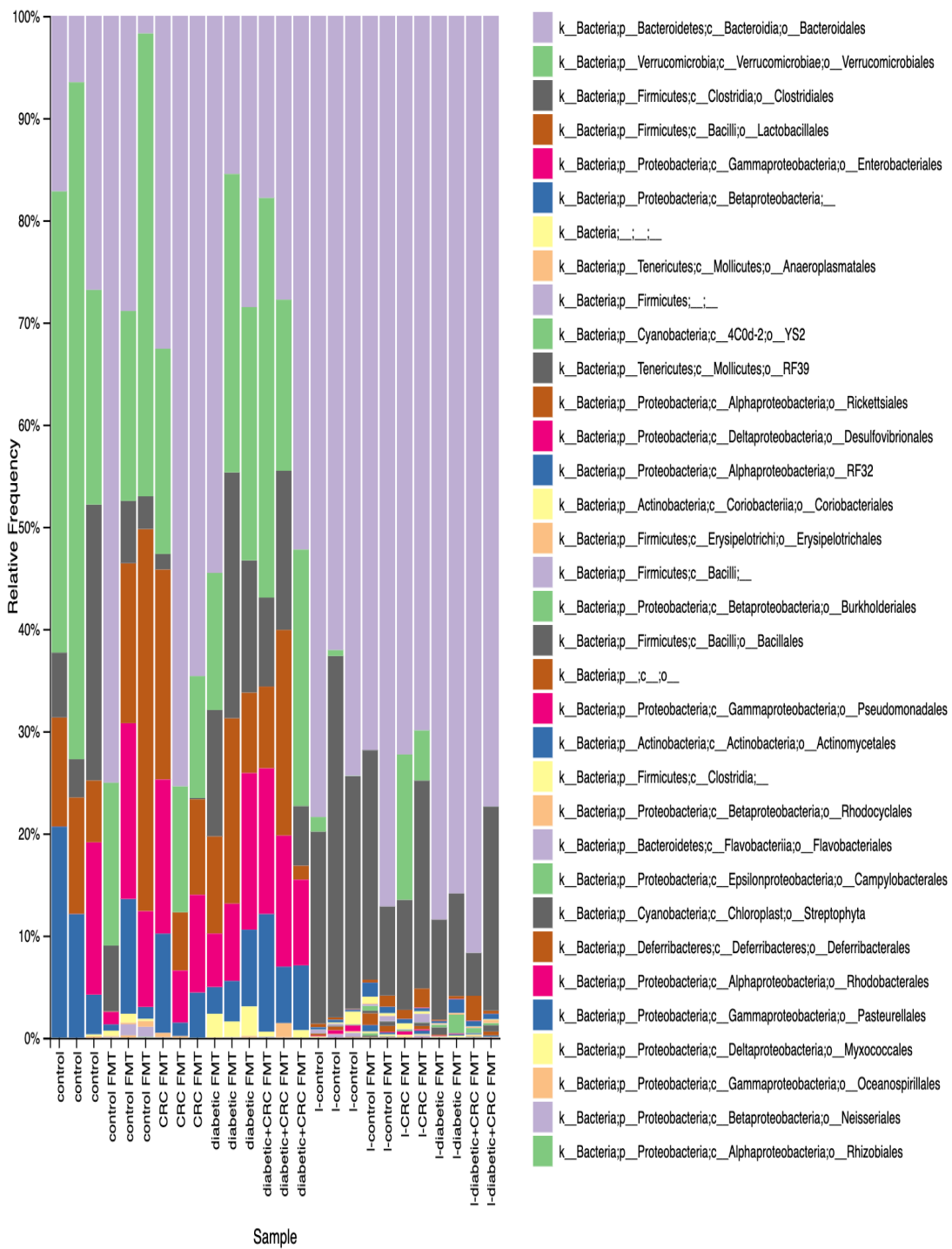


Figure 7: Different bacterial families per sample in antibiotic-treated mice.

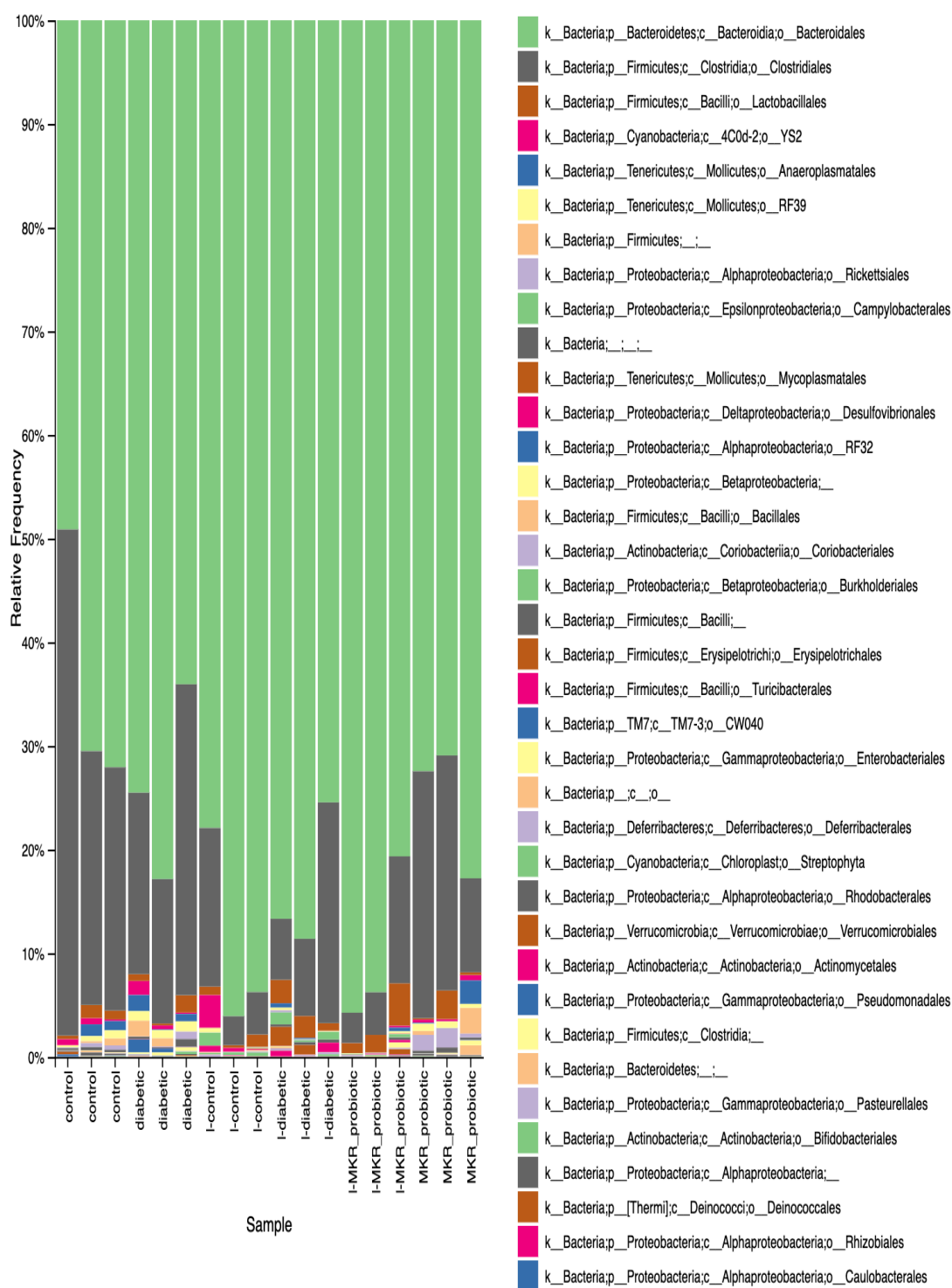


Figure 8: Different bacterial families per sample in control, diabetic and probiotics-treated diabetic mice

